T.R.
GEBZE TECHNICAL UNIVERSITY
GRADUATE SCHOOL OF NATURAL AND APPLIED SCIENCES

SYNTHESIS AND CHARACTERIZATION OF POLYHEDRAL OLIGOMERIC SILSESQUIOXANE BASED STAR POLYMERS

AHMET ÜNER
A THESIS SUBMITTED FOR THE DEGREE OF
DOCTOR OF PHILOSOPHY
DEPARTMENT OF CHEMISTRY

GEBZE
2018

T.R.

GEBZE TECHNICAL UNIVERSITY

GRADUATE SCHOOL OF NATURAL AND APPLIED SCIENCES

SYNTHESIS AND CHARACTERIZATION OF POLYHEDRAL OLIGOMERIC SILSESQUIOXANE (POSS) BASED STAR POLYMERS

AHMET ÜNER

A THESIS SUBMITTED FOR THE DEGREE OF

DOCTOR OF PHILOSOPHY

DEPARTMENT OF CHEMISTRY

THESIS SUPERVISOR

PROF. DR. AYŞE GÜL GÜREK

THESIS II. SUPERVISOR

ASSOC. PROF. DR. MEHMET ATİLLA TAŞDELEN

GEBZE

2018

T.C.
GEBZE TEKNİK ÜNİVERSİTESİ
FEN BİLİMLERİ ENSTİTÜSÜ

POLİHEDRAL OLİGOMERİK SİLSESKUİOKSAN (POSS) ESASLI YILDIZ POLİMERLERİN SENTEZİ VE KARAKTERİZASYONU

AHMET ÜNER

DOKTORA TEZİ
KİMYA ANABİLİM DALI

DANIŞMANI
PROF. DR. AYŞE GÜL GÜREK
II. DANIŞMAN
DOÇ DR. MEHMET ATİLLA TAŞDELEN

GEBZE
2018

GEBZE TEKNİK ÜNİVERSİTESİ

DOKTORA JÜRİ ONAY FORMU

GTÜ Fen Bilimleri Enstitüsü Enstitüsü Yönetim Kurulu'nun 29/11/2017 tarih ve 2017/60 sayılı kararıyla oluşturulan jüri tarafından 22/12/2017 tarihinde tez savunma sınavı yapılan Ahmet ÜNER'ın tez çalışması Kimya Anabilim Dalında DOKTORA tezi olarak kabul edilmiştir.

JÜRİ

ÜYE (TEZ DANIŞMANI)	:Prof.Dr. Ayşe Gül GÜREK
ÜYE :	Prof.Dr. Hayal BÜLBÜL SÖNMEZ
ÜYE :	Prof.Dr. Nergis ARSU
ÜYE :	Yrd.Doç.Dr. Erdinç DOĞANCI
ÜYE :	Yrd.Doç.Dr. İlke ANAÇ

ONAY

Gebze Teknik Üniversitesi ..... Enstitüsü Yönetim Kurulu'nun

...../...../..... tarih ve ...../..... sayılı kararı.

SUMMARY

In this thesis, we report the synthesis of star-shaped polymers based on a polyhedral oligomeric silsesquioxane (POSS) core as a building block. Different polymeric arms were chosen to synthesize octafunctional star polymers to be employed in three distinct applications. (1) hydrophilic arms with different chain length poly(ethylene glycol) PEG synthesized by copper(I) catalyzed azide-alkyne cycloaddition (CuAAC) click reaction, (2) pyrene end-labelled star poly(ε-caprolactone)s (PCL) with POSS (polyhedral oligomeric silsesquioxane) core prepared by combination of copper(I)-catalyzed azide alkyne cycloaddition (CuAAC) click chemistry and ring-opening polymerization techniques, (3) polymethylmetachrylate (PMMA), and polysytreyene (PS) polymers, containing a polyhedral oligomeric silsesquioxane (POSS) core via the combination of atom transfer radical polymerization (ATRP) and click chemistry techniques were synthesized and their chemical structures and molecular characteristics were clearly confirmed by FT-IR, ^{1}H-NMR and GPC analyses. Further analyses investigated their performances by AFM, TEM, DLS, UV-Vis, Raman, dielectric spectroscopy and semiconductor characterization sytem.

Key Words: Star Polymer, Click Chemistry, Polyhedral Oligomeric Silsesquioxane (POSS), Polymeric Surfactants, Non-covalent Interaction, Organic Field Effect Transistor (OFET).

ÖZET

Bu tez çalışmasında merkezi polihedral oligomerik silseskuioksan (POSS) olan yıldız polimerler sentezlenmiştir. Polimerik kollar, değişik uygulama tipleri için farklı olarak seçildi. (1) farklı zincir uzunluklarını sahip polietilen glikol (PEG) içeren polimerler bakır(I) katalizörlüğünde azid-alkin halka-katılma (CuAAC) klik reaksiyonuyla (2) piren uçlu yıldız poli(ε-kaprolakton) (PCL) içeren with POSS merkezli polimerler halka açılma ve bakır(I) katalizörlüğünde azid-alkin halka-katılma (CuAAC) klik reaksiyonu kombinasyonuyla (3) polimetilmetakrilat (PMMA), ve polistiren (PS) polimerler içeren (POSS) merkezli yıldız polimerler atom transfer radikal polimerizasyonu (ATRP) ve klik kimyası tekniklerinin kombinasyonuyla sentezlendi. Polimerlerin kimyasal yapıları ve moleküler karakteristikleri FT-IR, ^{1}H-NMR ve GPC analizleriyle incelendi. Polimerlerin performansları ve diğer özellikleri AFM, TEM, DLS, UV-Vis, Raman, dielektrik spektroskopisi ve yarı iletken karakterizasyon sistemiyle analiz edildi.

Anahtar Kelimeler: Yıldız Polimer, Klik Kimyası, Polihedral Oligomerik Silseskuioksan (POSS), Polimerik Surfaktant, Kovalent Olmayan Etkileşim, Organik Alan Etki Transistörü (OFET).

ACKNOWLEDGEMENTS

First of all, I would like to express fully respect to my advisors, Dr. Ayşe Gül Gürek and Dr. M. Atilla Taşdelen, for giving me an opportunity to study and work with them, and for their kind help and tremendous support. Their confidence, passion and dedication to science really inspired me a lot and urge me to be a good researcher. I would like to highlight my special thanks to Dr. M. Atilla Taşdelen for advices, encouragement, and friendship. I was very lucky to have such a good mentor.

I would like to give my sincere thanks to my reader Dr. Erdinç Doğancı, who also has taken care of me a lot. I am very honored to have a such dedicated research partner to support me in all steps of my lab works. Although, I am not his student, he often asked me about my research progress and gave me a lot of encouragements.

Moreover, I am very much thankful to Dr. H. Bülbül Sönmez and Dr. Nergis Arsu who took part in making this thesis real.

I would like to take this opportunity to say warm thanks to all my beloved friends, who have been so supportive along the way of doing my thesis.

I also owe a deep debt of gratitude to our university for giving us an opportunity to complete this work.

Last but not least, I would like to express my wholehearted thanks to my precious wife and my lovely daughter. I am most appreciative of their deep love and strong support. Without this, I would never be able to go so far.

This thesis is dedicated to my family.

TABLE of CONTENTS

LIST of ABBREVIATIONS and ACRONYMS

Abbreviations and Acronyms		**Explanations**
h	**:**	Hour
mmol	**:**	Milimol
min	**:**	Minute
j/g	**:**	Joule/gram
A°	**:**	Angstrom
Hz	**:**	Hertz
mL	**:**	Mililiter
nm	**:**	Nanometer
ppm	**:**	Parts per million
M_n	**:**	Number average molecular weight
w/v	**:**	Weight/volume
D_H	**:**	Hydrodinamic diameter
Eq	**:**	Equation
CuAAC	**:**	Copper-Catalyzed Azide-Alkyne Cycloaddition
DCM	**:**	Dichloromethane
DMF	**:**	Dimethyl formamide
DSC	**:**	Differential Scanning Calorimetry
DLS	**:**	Dynamic Light Scattering
FTIR	**:**	Fourier-Transform Infrared Spectroscopy
GPC	**:**	Gel Permeation Chromatography
GTU	**:**	Gebze Technical University
AFM	**:**	Atomic Force Microscope
MWNT	**:**	Multi-walled carbon nanotube
CNM	**:**	Carbon Nanomaterial
SWNT	**:**	Single-walled carbon nanotube
ATRP	**:**	Atom Transfer Radical Polymerization
^{1}H-NMR	**:**	Proton Nuclear Magnetic Resonance Spectroscopy
PDI	**:**	Polydispersity Index
mPEG	**:**	Methoxy Poly(ethylene glycol)

PMDETA	**:**	N,N,N′,N″,N″-Pentamethyldiethylenetriamine
PS	:	Polystyrene
PMMA	:	Polymethylmethacrylate
PCL	:	Polycaprolactone
Pyr	:	Pyrene
RMS	:	Root Mean Square
TEM	:	Transmission Electron Microscopy
Tg	:	Glass transition temperature
TGA	:	Thermal Gravimetric Analysis
ROP	:	Ring Opening Polymerization
ε-CL	:	Epsilon Caprolactone
PBIB	:	Propargyl 2-bromoisobutyrate
CuPc	:	Copper(II) phthalocyanine
P3HT	:	poly(3-hexylthiophene-2,5-diyl)
OFET	:	Organic Field Effect Transistor
PCBM	:	phenyl-C61-butyric acid methyl ester
UV-vis	:	Ultraviolet–visible
MIM	:	Metal Insulator Metal
V_{TH}	:	Threshold Voltage
V_{GG}	:	Given Gate Voltage
μ	:	Mobility
Gs	:	Gate source
V_{DS}	:	Drain source voltage

LIST of FIGURES

LIST of TABLES

1. INTRODUCTION

Hybrid materials have attracted interest due to the combination of superior properties coming from both inorganic and organic building blocks since last decades [1]. Polyhedral oligomeric silsesquioxanes (POSS) as an important class of organic/inorganic hybrid materials with a general chemical formula of $(RSiO_{1.5})n$ (n= 6, 8, 12, etc.) have been considerably studied because of their significant properties such as thermal and oxidation resistance and reduction in flammability [2-4]. In addition, the POSS nanocages can enhance the mechanical properties and affect the viscoelastic properties of the product [5]. Organic groups (R) at each of the eight corners have been comprehensively studied to obtain valuable different hybrid polymers with excellent properties [6-11]. POSS nanobuilding block is a strongly hydrophobic core, and its use in design of amphiphilic hybrid macromolecules has been an exciting academic and industrial research area since recent years [8-12]. As high efficiency method, controlled/living radical polymerization technique is used to obtain broad range of amphiphilic hybrid polymers containing POSS either end- or side- or core- positions. For example, atom transfer radical polymerization (ATRP) was used to synthesize POSS-containing amphiphilic copolymer, such as star-shaped POSS-poly(2-(N,N-dimethylamino) ethyl methacrylate) hybrid polymer [13]. Furthermore, reversible addition fragmentation chain transfer polymerization is also used to synthesize the telechelic hybrid poly(acrylic acid) containing POSS [14]. More recently, click chemistry has been proved to be a fast, efficient and useful method to prepare well defined tailor-made polymers [15, 16]. In particular Cu(I) catalyzed 1,3-dipolar Huisgen cycloaddition (CuAAC) reaction between azide-alkyne functional groups has gained remarkable attention due to the high yield and applicability under the mild reaction conditions [17, 18]. This reaction has been widely used for the fabrication of various organic and hybrid complex macromolecular structures [19-24].

The study presented here indicates the synthesis of star-shaped polymers with POSS core via CuAAC click chemistry. The chemical structures of the obtained polymers were analyzed by FT-IR and ^{1}H-NMR spectroscopies. In addition, their thermal properties were investigated by differential scanning calorimeter and thermogravimetric analysis. The number average molecular weight and polydispersity index of polymers were also determined by gel permeation chromatography. Moreover, the surface and micelle properties of them were examined by transmission

electron microscopy (TEM), atomic-force microscopy (AFM), dynamic light scattering (DLS) and contact angle techniques and the dielectric properties of the star-shaped polymers were acquired by using impedance spectroscopy.

2. THEORETICAL PART

2.1. Polymeric Surfactants

Amphiphilic macromolecular systems which are having both hydrophilic and lipophilic groups in the structure commonly named as polymeric surfactants. They have the same approach and chemical structure design comparing to their small conventional surfactant counterparts. In the literature for these macromolecular systems there are also other descriptions such as surface active polymers, amphiphilic polymers, micellar polymers, associative polymers, water soluble polymers and other related terms. Based on hydrophilic part charge (in many cases hydrophilic group contains negative and positive charges), they can be classified in polyelectrolytes. By considering the much higher comlex molecular structure (different topology of the molecule, functional groups on backbone of the polymer) of polymeric surfactants comparing to low molecular weight convenient surfactants, they can have very different properties for the various application fields.

It is interesting that polymeric surfactants have important roles in our daily life as natural polymers [13, 25]. Polysaccharides and proteins are the mostly found classes and examples of naturally occuring polymeric surfactants. Casein works as an emulsion stabilizer polymeric surfactant in milk and chitosan is the notable example for polysccharides class [26]. Isolation of polymeric surfactants from natural sources are usually very difficult and costly. For this reason, there are many studies on synthetic polymeric surfactants to meet needs. As they have different properties and possible to design tialor-made macromolecules, they have gained notable attention since last decades to be used in possible potential application fields including coatings, cosmetics, agro chemistry, water treatment, biotechnology, eletronic, medicine and emulsion polymerization [18, 20, 27-31]

.

2.1.1. Classification of Polymeric Surfactants

From a chemical structure point of view, polymeric surfactants are generally divided into two classes depending on their hydrophilic and hydrophobic groups distribution. (Figure 2.1) Macromolecules formed by amphiphilic monomers and oligomers as a repeating unit are commonly called as polysoaps, though polymers in which there is a straigt and clear splitting between two parts are defined as

macrosurfactants [22, 26]. By using existing synthetic polymerization methods, its possible and encouraging to obtain complex architectures [32, 33]. Therefore, interest on amphiphilic polymers is increasing and complex architectures can be considered as a different, new and promising class of polymeric surfactants (Figure 2.2).

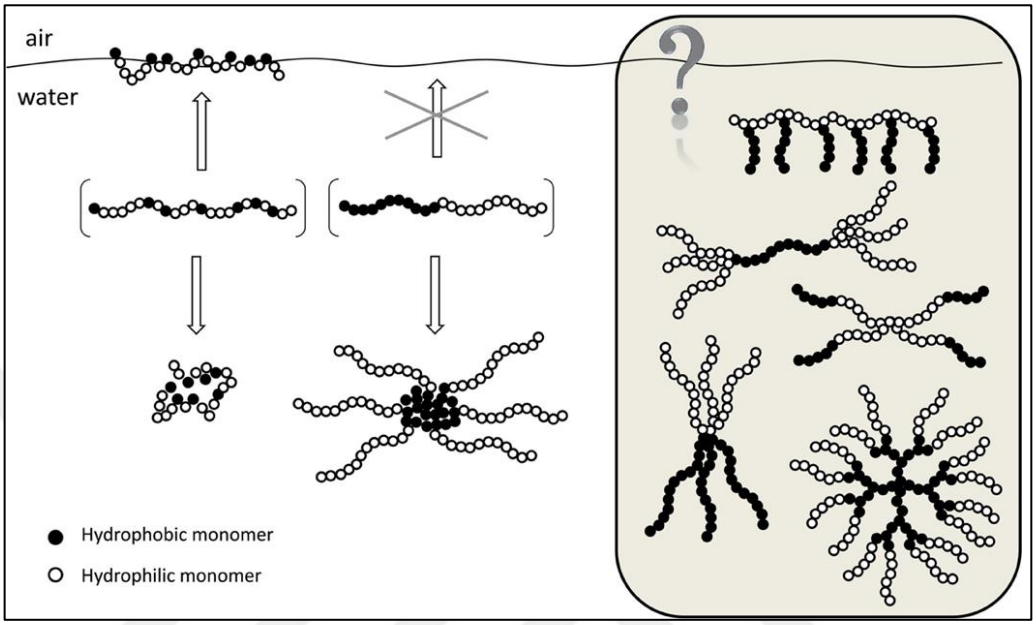

Figure 2.1: Schematic representation of the different behavior displayed in solution and at the air/water interface by polysoaps (left) and macrosurfactants (center). Very few data points are available about complex architectures (right).

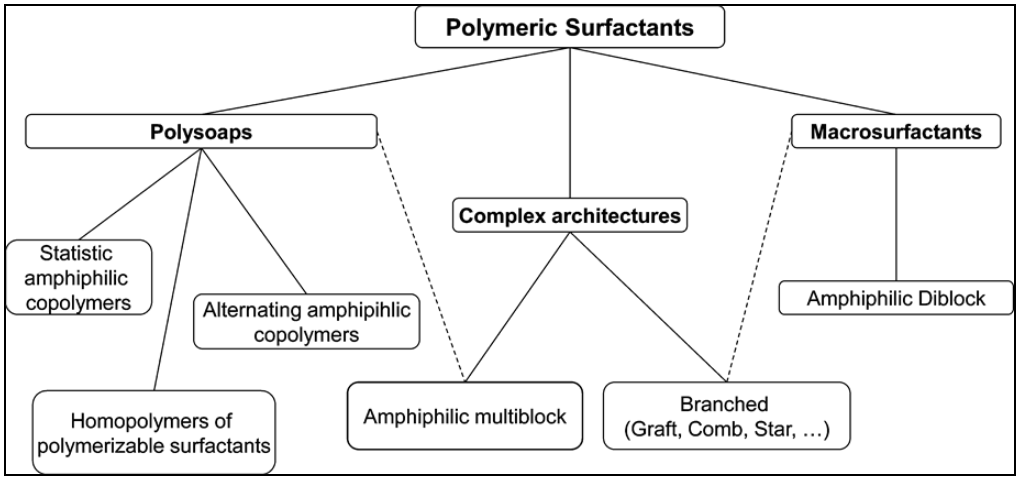

Figure 2.2: Classification of Polymeric Surfactants

2.1.1.1 Polysoaps

In this section of polymeric surfactants, hydrophobic and hydrophilic parts of the polymers are distributed all over the polymer backbone disorderly. Strauss, who worked on the research on their aggregation properties in the 1950s gave the name "polysoap" for these type of polymeric surfactants [34, 35]. Polymers designed and used for EOR (Enhanced Oil Recovery) can be groupped into this class. The most common and very well known systems are hydrophobically modified polyacrylates, polyacylamides and polysaccharides. Review by Laschewsky [26] gives a comprehensive overview of polysoaps and the details on molecular structures that can be found in the literature. Altough they are polymeric surfactants and surface activity property is the most important parameter, its not easily found in the studies.

2.1.1.2 Macrosurfactants

In the macrosurfactant class, there are also interesting and well-known polymeric structures are included. The most important structure is an amphiphilic diblock copolymers in this class. Their abilities are allowing them to gain an interest on different applications such as preparing smart materials for different purposes. There are several reviews available in the literature regarding the micellization, used as an emulsifier in the emulsions (mainly for oil in water emulsions), synthesis and stimuli-responsive behaviors in aqueous media published in the recent literature. A number of reviews concerning synthesis, micellization, emulsions stabilization, and stimuli-responsive behavior of amphiphilic block copolymers appeared in recent [36-39].

Its easy to understand the designing of these polymers. In principle, every polymer structure established by a hydropobic back bone (block) and a water-soluble (charged or neutral) group can be also classified in this section. Beside their chemical structures, configurable hydrophilic groups of the blocks are very interesting for this polymeric surfactant class. These tunable systems can show different micelliziation and surface active properties when the pH, temperature or electrolyte content of the media is changed. These kind of modifiable hydrophilicity containing polymers called as "schizophrenic" been appearing in the literature. These systems usually show pH- or temperature-dependent micellization and surface activity. When both blocks present switchable hydrophilicity, these polymers are often referred to as "schizophrenic" [40-42].

2.1.1.3 Complex Architectures

Today, its much easier then before to synthesize tailor-made molecules. Availability of the synthetic methods, chemicals and resources make different polymers synthesis possible. Vision of the researchers can be the starting point of obtaining new polymeric surfactants with complex architectures and would be endless until the creative imagination continues. Complex architectures of the polymeric surfactants very well explained by Riess in 2003 [36].

Table 2.1**:** List of Amphiphilic Block Copolymers Based on PAA and PMAA

Amphiphilic polymer	precursor	Synthetic method
PAA diblock		
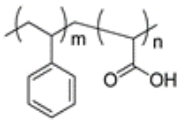 PS-b-PAA **1**	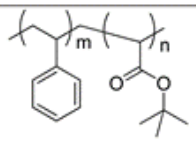 PS-b-PtBA **1a**	ATRP anionic NMP
	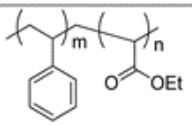 PS-b-PEA **1b**	RAFT
	-	NMP
	-	RAFT
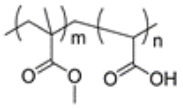 PMMA-b-PAA **2**	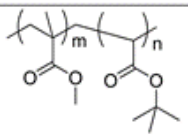 PMMA-b-PtBA **2a**	ATRP anionic
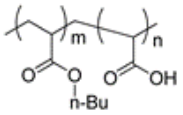 PBA-b-PAA **3**	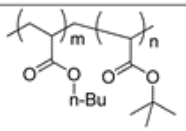 PBA-b-PtBA **3a**	ATRP
	-	RAFT
	-	NMP
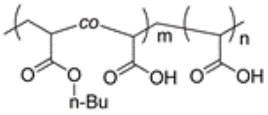 P(BA-co-AA)-b-PAA **4**	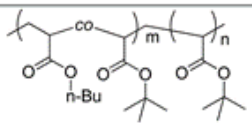 P(BA-co-tBA)-b-PtBA **4a**	ATRP
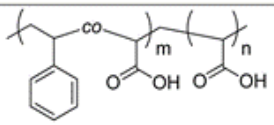 P(S-co-AA)-b-PAA **5**	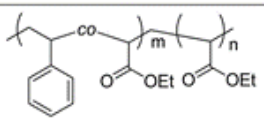 P(S-co-EA)-b-PEA **5a**	RAFT
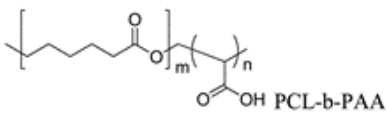 PCL-b-PAA **6**	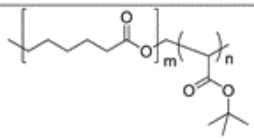 PCL-b-PtBA **6a**	ATRP

Table 2.2: List of Amphiphilic Block Copolymers Based on PAA and PMAA

Amphiphilic polymer	precursor	Synthetic method
PAA triblock		
PAA-PS-PAA **14**	PtBA-PS-PtBA **14a**	ATRP NMP
PS-PAA-PS **15**	PS-PtBMA-PS **15a**	anionic
PS-PAA-PBA **16**	PS-PtBMA-PBA **16a**	anionic
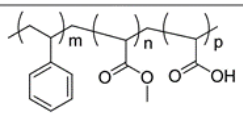 PS-b-PMA-b-PAA **17**	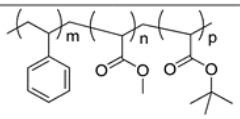 PS-b-PMA-b-PtBA **17a**	ATRP
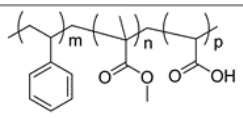 PS-b-PMMA-b-PAA **18**	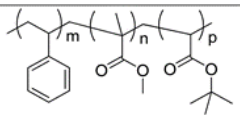 PS-b-PMMA-b-PtBA **18a**	ATRP
PMAA diblock		
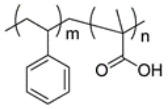 PS-b-PMAA **19**	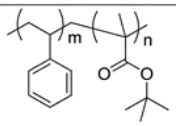 PS-PtBMA **19a**	ATRP anionic
	-	RAFT
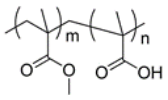 PMMA-b-PMAA **20**	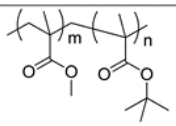 PMMA-b-PtBMA **20a**	ATRP GTP
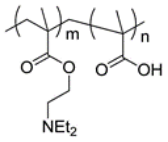 PDEAEMA-b-PMAA **21**	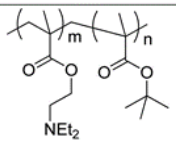 PDEAEMA-b-PtBMA **21a**	ATRP anionic
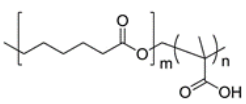 PCL-b-PMAA **22**	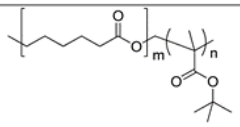 PCL-b-PtMBA **22a**	ATRP
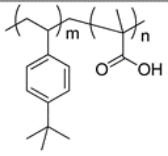 PtBS-b-PMAA **23**	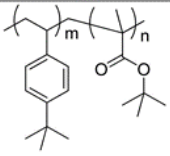 PtBS-b-PtBMA **23a**	anionic

2.1.2. Synthesis of Polymeric Surfactants

To prepare amphiphilic polymers who has surface activity to be determined by surface tension, contact angle and critical micelle concentration (CMC) measurements there are effective and different synthetic methods.

Polystyrene, polyacrylates, polyolefin, or nonwater-soluble polyethers are the widely used hydrophobic blocks. Depending on a different electrical charge or neutral character of hydrophilic blocks, different monomers are used such as vinylic or acrylic monomers bearing sulfonated, carboxylic, or amino groups, poly(ethylene glycol) (PEG) moieties or hydrosoluble acrylates such as 2-hydroxyethyl methacrylate (HEMA) or PEGylated acrylic monomers.

By having an advantage of producing amphiphilic copolymers with controlled molecular weight distribution and well defined molecular structure, controlled living polymerization methods such as atom transfer radical polymerization (ATRP) [43], reversible addition-fragmentation chain transfer polymerization (RAFT) [44], and nitroxide-mediated polymerization (NMP) [45, 46], are becoming the synthetic approach. Nevertheless, points to take into consideration about functional group tolerance still bringing some limitations or question marks to use these methods in some cases but very rarely. Another good point of using these methods is suppressing side reactions such as chain termination.

In comparison with controlled living polymerization, conventional free-radical polymerization methods are not preferred due to the lack of narrow molecular weight distribution and poor control over structure of synthesized polymers. There are limited number of examples for syntesis of amphiphilic block polymers by free radical polymerization method found in the recent literature.

2.1.2.1 Poly(acrylic acid) and Poly(methacrylic acid) Blocks

Polycarboxylates are commonly used, studied and found a broad application fields commercially as well. Amphiphilic polymers of polycarboxylate blocks are also gaining high interest with their properties. Basically, polyacid blocks are giving hydrophilicity to the amphiphilic polymer and this hydrophilic character depends on a degree og protonation of the carboxylic group types. In addition to this, altough they are generally a hydrophilic part of the polymers, their hydrophobic character in water has also been studied. They are more frequently found as hydrophilic partners, but

their ability to form micelles in acidic conditions acting as hydrophobic block in water has been also demonstrated [47].

Beside its features and common use in amphiphilic polymers, the synthesis of block copolymers containing acrylic or methacrylic acid is tough due to difficulty of handling the free carboxylic acid group with most of the controlled polymerization techniques [48, 49]. The main strategy in those cases is utilizing the acid which is not easily polimerizable to the better performing related ter-butyl ester as a monomer. This approach also surpass the issue of finding a suitable solvent for both the hydrophilic and the hydrophobic blocks, which is normally not critical point of synthesis. A list of relevant examples of block copolymers containing PAA or PMAA is given in Table 2.1 and Table 2.2.

Atom transfer radical polymerization (ATRP) is increasingly used method for the synthesis of amphiphilic polymer containing a carboxylic acid as the repeating unit in the hydrophilic block. ATRP of sodium acrylate in water was successfully applied by Ashford and co-workers as a first example via using an oligomeric PEO initiator and the CuBr/2,2-bipyridine system. Obtained polymers having low molecular weight and low polydispersities [50]. This success brought attention on those studies and to modify poly(acrylic acid) surfaces seems to be restricted [51].

Starting from the relevant ter-butyl ester approach to prepare amphiphilic block copolymers was first reported by Matyjaszewski's group, utilizing either tert-butyl acrylate (tBA) [52] or tert-butyl methacrylate (tBMA) [53]. In these polymerization series, poly(tert-butyl acrylate) was also used as a macroinitiator and obtained a good blocking efficiency. Solvents and metal ligands are bringing different results on polymerization rate. Using polar solvents and corporating a small amount of Cu(II) decrease the reaction rate and giving polymers with narrower molecular weight distribution.

In the list of examples given in Table 2.1, amphiphilic polymers prepared via ATRP technique. Diblock, triblock, and three-arm star 1a polymers have been prepared via ATRP with a standard CuBr/PMDETA catalytic system. To come to this optimum conditions, several studies were performed to succeed low dispersities, high molecular weights and feasible rates. All these trials and works showed that the CuBr/PMDETA combination is better for the synthesis of PtBA macroinitiator in a polar solvent (dibenzylether) and in the presence of small amounts of $Cu(Br)_2$ reducing the rate as a deactivator [54].

Before using the living radical polymerization methods, which take place under milder conditions, anionic polymerization was the most commonly used technique to obtain well-defined polymers with low polydispersities. Living anionic polymerization has also been comprehensively used to prepare amphiphilic block copolymers before the development of radical polymerization techniques [38]. Relevant examples are listed in Table 2.1.

McCormick and co-workers also worked with reversible addition-fragmentation chain transfer (RAFT) radical polymerization techniques for the synthesis of water-soluble and responsive amphiphilic polymers. Obtained polymers were mainly targetted to be used in stimuli-responsive systems application [44].

Nitroxide-mediated polymerization (NMP) is one of the firstly used and comprehensibly simplest controlled radical polymerization techniques. Polymerizations are carried out through with a nitroxide generated stable radical. This stable radical comprise the deactivation of growing polymer chains in propagation step [45]. Altough it is the simplest technique, ATRP and RAFT methods are widely used. But in any case, NMP still is attractive method due to it has more possibility to apply on broad range of reactions and less complexity of used chemicals [55].

Table 2.3: Amphiphilic Block Copolymers Containing an Aromatic Sulfonate Block

Amphiphilic polymer	precursor	Synthetic method	Amphiphilic polymer	precursor	Synthetic method
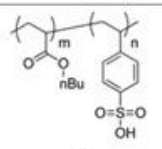 **34**	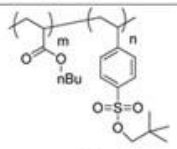 **34a**	ATRP	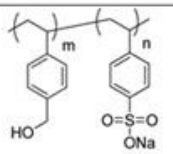 **40**	-	NMP
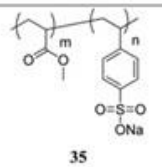 **35**	-	ATRP	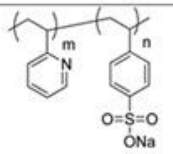 **41**	-	
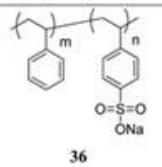 **36**	-	NMP + emulsion	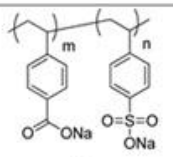 **42**	-	RAFT
	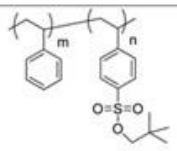 **36a**	NMP	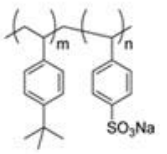 **43**	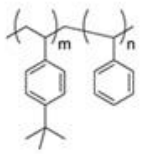 **43a**	Anionic
	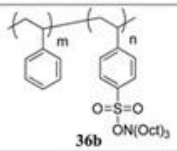 **36b**	RAFT	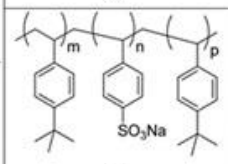 **44**	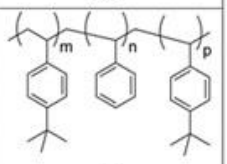 **44a**	
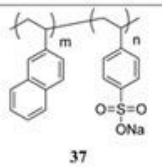 **37**	-	NMP	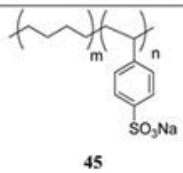 **45**	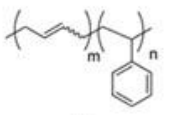 **45a**	anionic
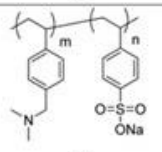 **38**	-	NMP	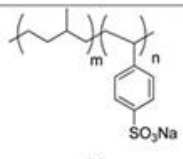 **46**	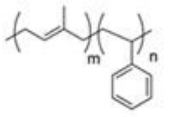 **46a**	anionic
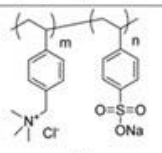 **39**	-				

2.1.2.2 Aromatic Sulfonate Blocks

Preparation of sulfonated polystyrene blocks by post polymerization is the oldest method and difficult to succeed with a high yield of sulfonation. Sulfone linkages could ocur due to side reactions during the postpolymerization. Regarding that, polymerization of sulfonated styrene blocks are more studied with other preferred procedures.

ATRP is used very commonly to prepare poly(styrene sulfonate) (PSS) blocks by protecting sulfonate group via ethyl etster approach together with hydrolysis or thermolysis reactions. In Table 1, molecule with the number of 34 was recently prepared by using ATRP of the relevant neopentyl ester, followed by thermolysis process at 150°C. Styrene sulfonic acid brushes have also been studied by ATRP. Ethyl and dodecyl esters are already found in the literatüre [56]. In addition to this, sodşum styrene sulfonate synthesis by direct ATRP has also been published [57] and number 35 in Table 2 was also prepared successfully by having different hydrophilic lipophilic balance values [58].

NMP and RAFT are also used for the synthesis of amphiphilic block copolymers which are containing PSS. Mitsukami et al. Studied and reported the synthesis of a tunable hydrophilic copolymer of PSS by using RAFT [26].

2.1.2.3 Poly(vinyl pyridine) and Quarternized Arylamines Blocks

In this class, there are polymerized vinyl pyridine and styrene derivatives which contain amino groups attached to the phenyl ring and poly(vinyl pyrrolidone) (PVP) based block copolymers. Surface properties of these systems are very rare in the literature but there are some articles regarding the micelle formation and particle stability in water solution. As its seen in Tables 2.5 and 2.6, there are also several studies with PVP blocks including various hydropobic groups.

Table 2.4: P2VP and P4VP based Amphiphilic Block Copolymers

Polymer	Synthetic method	Polymer	Synthetic method
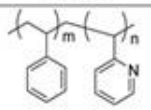 PS-b-P2VP **47**	anionic	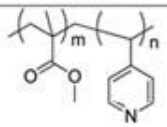 PMMA-P4VP **52**	anionic ATRP
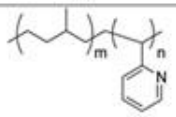 P-hIP-P2VP **48** 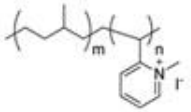 P-hIP-P2VPMeI **48a**	anionic + quaternization	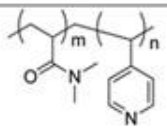 PDMA-b-P4VP **53** PDMA-b-P4VPC$_{16}$Br **53a**	NMP
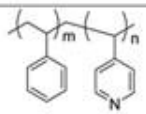 PS-b-P4VP **49**	ATRP RAFT NMP	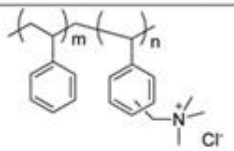 **54a**	
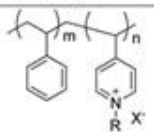 RX = MeI **49a** RX = C_4I **49b** RX = C_6I **49c** RX = C_{10}I **49d** RX = C_{10}Br **49e** RX = C_{18}I **49f**	anionic + quaternization	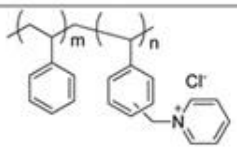 **54b** 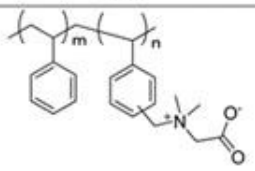 **54c** 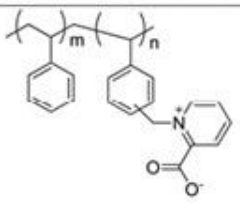 **54d**	
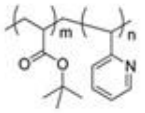 PtBMA-P2VP **50**	anionic		
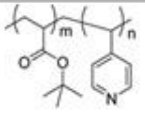 PtBMA-P4VP **51**	anionic	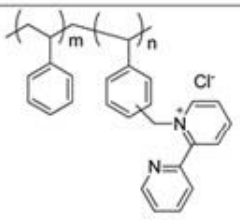 **54e**	

2.1.2.4 Poly(ethylene glycol)/Poly(ethylene oxide) Blocks

Poly(ethylene oxide) based amphiphilic copolymers can be found as the most studied class of polymeric surfactant field. They are also the first designed structures as a big surfactant molecule due to the solubility of hydrophilic group. These studies were not limited only in scientific field but also found a big market in the commercial surfactants. Since a long time, with a different molecular weight and various topologies based on PEO and poly(propylene oxide) (PPO) block polymers are very well known. (e.g., Pluronic types from BASF)

As they are also produced commercially, concerning the properties of PEO and PPO block copolymers there are several reviews in the last years [29, 59, 60]. These PEG/PEO based polymers are generally synthesized by 2 main ways: ring opening polymerization of ethylene oxide and condensation of ethylene glycol. Preparation and even large scale production of PEG (or PEO) is very well managed and utilized. Today, not only the basic block polymers are available but also a broad range of molecular weight, different functional groups of he relevant block copolymers are commercially available.

Because of this convenience, to prepare PEG including polymeric surfactants is just designing and combining hydrophobic blocks with commercially available PEG macroinitiator. In Table 2.7, it can be seen as examples of polymeric surfactants synthesized via starting from a PEG macroinitiator.

Some polymerization methods can also require a small modifications on PEG moiety to be able to make synthesis possible of the second block. For example, PEG with hydroxyl terminal groups has been used directly in anionic polymerization of acrylic monomers [61] and ring-opening polymerization of preparation of PEG-b-PLA [71] Further modifications of terminal hydroxyl group may lead a favorable initiator for different polymerization techniques and to obtain a tailor made polymers. By preparing 4-Cyanopentanoic acid dithiobenzoate containing PEG macroinitiator, N-acryloyl-2,2-dimethyl-1,3-oxazolidine was polymerized [62], ATRP technique was also used to prepare amphiphilic copolymers by modifying PEG with halogen moities on terminal groups such as halogen-termi-nated PEG has been used as number 56,57,58,59,60 in the Table 2.7 and can also be found in the literature [63-65].

Table 2.5: PEG Containing Macrosurfactants

Polymer	Synthetic method	Polymer	Synthetic method
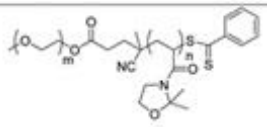 55	RAFT	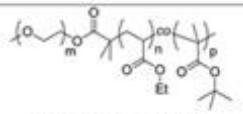 PEO-b-P(EA-co-tBMA) 68	
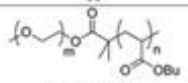 PEO-b-PnBA 56	ATRP	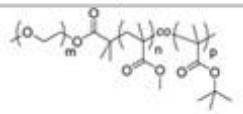 PEO-b-P(MMA-co-tBMA) 69	
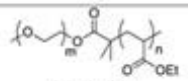 PEO-b-PEA 57		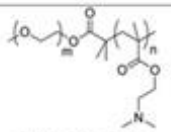 PEO-b-PDMAEMA 70	
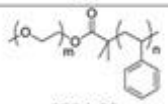 PEO-b-PS 58		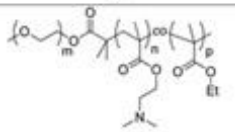 PEO-b-P(DMAEMA-co-EMA) 71	
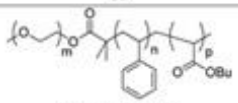 PEO-b-PS-b-PnBA 59		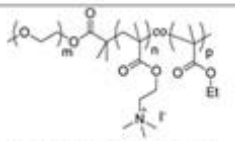 PEO-b-P(TMAEMA-co-EMA) 71a	
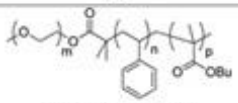 PEO-b-PS-b-PnBMA 60		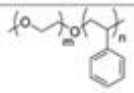 58a	anionic
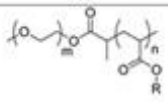 PEO-b-P(FluoroctylMA) R = $CH_2CH_2(CF_2)_6F$ 61 R = $CH_2(CF_2)_7F$ 62		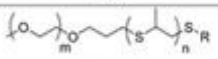 PEO-b-PPS 72	
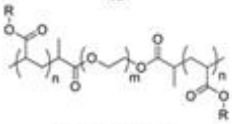 R = $CH_2CH_2(CF_2)_6F$ 63 R = $CH_2(CF_2)_7F$ 64		 PEO-b-PSS-b-PEO 73	
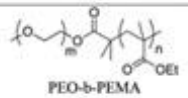 PEO-b-PEMA 65		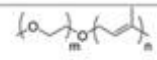 PEO-b-PI 74	
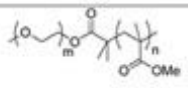 PEO-b-PMMA 66		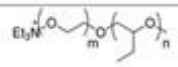 Me_3N^+-PEO-b-PBO 75	
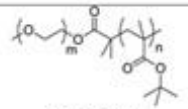 PEO-b-PtBMA 67		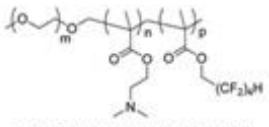 MePEO-b-PDMAEMA-b-POFPMA 76	

2.1.2.5 Alkylaminoacrylate Blocks

Acrylic acid based amphiphilic block copolymers with amino modifications are also studied and several publications can be found in the literature. This class of block copolymers have gained much interest since last decades due to their easily modifiable amino groups and their pH sensitive hydrophilic nature. After preparing an aminoacrylate polymer, its easy to obtain a quarternized derivative which gives permanent positively charged amphihilic blocks.

2-(Dimethylamino) ethyl methacrylate (DMAEMA) and N,N-Diethylaminoethyl methacrylate (DEAEMA) are the mostly studied types of amphiphilic alkylaminoacrylate based polymers. These block polymers were firstly started to work by Armes' group and they mainly used ATRP technique for the synthesis [66-68].

2.1.2.6 Other Water Soluble Acrylate Blocks

Different type of acrylic monomers have been incorporated for various hydrophilic polymer synthesis as a hydrophilic part of the molecule. These synthesis were mostly run via living cotrolled radicalic reactions. However, in recent years, ATRP technique was preferred to prepare tailor made polymeric surfactants based on acrylate blocks.

Beside choosing the polymerization method, choosing proper solvent is also an important point of the reactions. Common solvents dpeneding on different hydrophilic and hydrophobic monomers can be found as DMF, THF, DMA and dioxane, aither alone or a combination with water [69, 70].

2.1.2.7 Synthesis of Polysoaps

Most of the studies on polysoaps for which surface properties have been researched based on different moieties of acrylamide or acrylic acid and modified polysaccharides. On the synthesis of these polysoap types, main approaches are free radical polymerization or polycondensation methods. Due to their long time use and well known details, synthesis of polysoaps is not challenging and no need a significant developments on synthesis methods.

2.1.2.8 Synthesis of Complex Polymeric Surfactants

Complex structures of polymeric surfactants are also gaining high interest since last few years. Altough there are many studies on these polymeric surfactant class, surface properties of these systems have not been investigated within synthesis studies. Focus on the synthesis of this group is much higher then the researching on surface properties [32, 71, 72]. Polymeric surfactants whose surface properties in water have been studied are mostly represented by comb-like, hyperbranched, star-shaped, miktoarm or dendrimeric copolymers. By increasing and developing of new synthesis methods, preparation of amphiphilic copolymers can be succeeded easier. Controlled radical polymerization method, ATRP, sing-opening polymerization and "click chemistry" are the mostly used methods which make high possibility on synthesis of polymeric surfactants [73-76].

2.2 Non-Covalent Functionalization of Carbon Nanomaterials

Carbon nanomaterials (CNMs) are exciting candidates for a broad range of application fields due to their extraordinary physical, chemical, thermal, and mechanical properties [77, 78]. However, their insoluble character in solvents doesnt allow them to be used in those attractive applications.

Consequently, making CNMs possible soluble in different proper solvents is essential. There has been many approaches developed and applied for repeatable dispersions of carbon nanotubes. Mechanical dispersion preparation techniques such as high speed mixing or ball milling method is tried but causing the loose of aspect ratio [79]. Chemical methods which are basically based on surface functionalization of CNMs are used to enhance their compatibility with the demanded solvent, by reducing agglomeration possibility [80]. On the other hand, other chemical methods which are aggressive chemical processes such as use of strong acids at high temperatures might cause decomposition on chemical structure.

So that, treating CNMs by possible non-covalent interaction is preferred due to the possibility of functionalization on CNM's surface without any defect on the structure of the system [81]. Different strategies of the noncovalent interactions would work depending on a structure of the used molecule. If the used molecule has both

hydrophobic and hydrophilic parts, hydrophobic part would be adsorbed with nanomaterial's sidewalls via van der Waals, π-π or C-π and other interactions and hydrophilic part provides the solubility in water media. In adition to this, if the used molecule is having an ionic character, nanomaterial surface is also charged by that ionic molecule and aggregation is prevented by coulombic forces' repulsion between CNMs. In the last decades, surfactants and polymers have been widely used to functionalize CNMs via non-covalent treatment. These preparations were both used in aqueous and solvent solutions of dispersed nanotubes.

2.2.1 Functionalization with Surfactants

Surfactants are amphiphilic molecules might be used to process stable colloidal dispersions due to their distinct structural properties. As they consist on polar head group which is hydrophilic and the hydrophobic hydrocarbon chains, surfactant molecules might adsorb at the interface between oil and water or air and water to reduce the surface tension.

Solubilizer character of surfactants specify the physical adsorbtion on CNMs to disperse nanomaterials in solvents [82]. This is an easy solubilization process can be done in the lab without any complexity. Solubilizer solution and CNM sample is just mixed and treated with a ultrasonic sonicator. Sonication step is very important to overcome van der Waals bonds n the CNMs by the mechanical energy. This at the end allows surfactant molecules to adsorb onto the surface CNMs' walls. Type and concentration of the surfactant and the quality of the CNMs are the most important and indicative parameters of the solubility. Stability of the system is driven by electrostatic interactions [83] and steric repulsions [84] between the solubilizer and CNMs' surface.

In the literature there are several dispersion studies of CNMs with both ionic and nonionic surfactant molecules such as sodium dodecelybenzene sulfonate (SDBS), sodium dodecyl sulfate (SDS), cetyltrimethlyammonium bromide (DTAB), alcohol ethoxylates and polysorbates [84-87]. Dispersion of single walled carbon nanotube (SWNT) in a SDS micelles via sonication process has been reported by Smalley and his co-workers [88]. These dispersions of CNMs with SDS occurs by the combination of steric repulsion forces and high negatively charged surface. Nevertheless, simple alky chains of those convenient surfactants such as SDS and DTAB are known to create basic hydrophobic interactions with CNMs [88, 89]. As an outcome of this

simple interaction, surfactant molecules are not providing a sufficient dispersion and they are just pasked around the nanotubes. SDS-SWNTs packs are not stable and disassociate even at low temperatures [90].

From that point of view, surfactant structure is so critical and defines the stability of the dispersion in proper solutions. Choosing a correct surfactant enhances the efficiency of the adsorbtion on CNMs walls. Surfactants with aromatic groups are much performing and capable for π-π stacking interactions. By comparison study between SDS and SDBS to demonstrate the role of aromatic groups has been reported. At the same conditions with same alkyl chain length, dispersive efficacy and stability of the dispersion of SWNT is better due to the presence of phenyl ring of SDBS molecule [91].

Beside chemical structure, alkyl chain length and the topology are also very important on surfactant-CNM interactions. Longer alkyl chain and highly branched which means more hydrophobicity provide better dispersion stability then the linear ones [91, 92].

Polymeric surfactants such as silicone based polymer surfactants show better performances compare to conventional simple surfactants. Due to super wetting effect and very low surface tension properties, MWNT might be easily dispersed in a water with this macromolecule surfactant [93].

2.2.2 Functionalization with Polymers

Instead of small molecular surfactants, polymers with amphiphilic structure is mostly used to disperse CNMs. The main advantage of these big molecules is that the polymers reduce the entropic penalty of micelle formation. In addition to this, spme polymers have considerably high interaction energy with CNMs. Polymers are also facing some problems while interacting with rigid SWNTs. This mechanically tough nanotube might push polmer structure into undesired chemical structure. To minimize this problem, some polymers may wrap carbon nanotubes as a helical shape [94].

2.2.3 Wrapping CNMs with Polymers

There are several studies on non-covalent interaction between carbon nanomaterials and polymers. SWNTs with different linear polymers such as polyvinyl

pyrrolidone (PVP) and polystyrene (PS) has been dispersed in water and reported by Smalley et al. [94].

Surfactant which means here solubilizer effect can be seen from PVP. This polymer has a hydrophobic backbone wrap around the nanomaterial and with hydrophilic part increase the solubility in water. MWNTs are also widely studied to have a stable dispersion in water by modifying with polymers [95].

MWNTs are also interacted with a water-soluble sulfonated polyaniline (SPAN). This system is very soluble in water and this feature bring many different opportunities to be used in new applications [96].

Natural polymers are also interesting molecules to be used in carbon nanotube functionalization. Proteins and polypeptides have already been studied and reported with a combination of SWNTs and provide them a solubility property in different solvents [97, 98].

2.2.4. Adsorption of Polymers on CNMs

Adsorbption on CNMs' wallside is demonstrated via high affinity of the molecule for the surface of carbon nanotube. From that perspective, pyrene which has a large aromatic group is widely used to study on noncovalent interaction of CNMs [99]. Because of it's effectiveness on nanotube functionalization, pyrene moities have been studied on biological research such as immobilization of proteins [100].

Pyrene containing molecules have also shown efficient performance for adsorption on SWNT sidewalls via noncovalent interaction and increase the solubility. By considering aromatic group containing molecules due to their affinity on nanotubes, anthracenes might be another group which can form π-π interactions.

As a result of some studies, the interaction of anthracenes on CNMs walls seems to be sufficiently strong but pyrenes can replace them due to their stronger adsorption on nanomaterials.

Other examples of polyaromatic molecules, phatalocyanines and porphyrins can be found in the literature with their effective adsorption properties on carbon nanotubes. SWNT has been dispersed by porphyrin in proper solvents such as methanol and DMF with a long stability period [101].

Comparing these heterocyclic aromatic molecules with pyrene, they are interacting with nanomaterials as same as pyrene whic is van der Waals forces.

Nevertheless, porphyrins are weaker with their interactions due to their metal ions in the molecule.

2.2.5. POSS Molecules for CNM Applications

POSS itself as a building block and POSS containing molecules have attractive properties and encourage researchers to prepare modified POSS moieties to be used in as a modifier of CNM to prepare various required nanomaterials.

It's seen in Figure 2.9 that MWNTs have been modified covalently via pyrene containing POSS molecules. This orgnic-inorganic hybrid material has been dispersed in toluene, THF and n-hexane and observed stable dispersions by Majeed et al. [102].

Other example for MWNT dispersion has been studied with aminopropylisobutyl polyhedral oligomeric silsesquioxane (POSS–NH_2). It was directly reacted with the MWNT and obtained a soluble hybrid material MWNT/POSS [103].

POSS grafted MWNT has also been prepared to investigate its nanocomposites of PLLA. MWNTs is modified with POSS via amide linkages. After the acid treatment of MWNT (MWNT-COOH), nanatoube is functionalized with acyl chloride (MWNT-COCl) by treating them with thionyl chloride (SOCl2), and then MWNT-COCl was reacted with aminopropylisooctyl-POSS to prepare POSS grafted MWNT (MWNT-g-POSS) [104].

Figure 2.3: Reaction Scheme for the Preparation of Pyrene-POSS and Functionalization of MWNTs With Pyrene-POSS

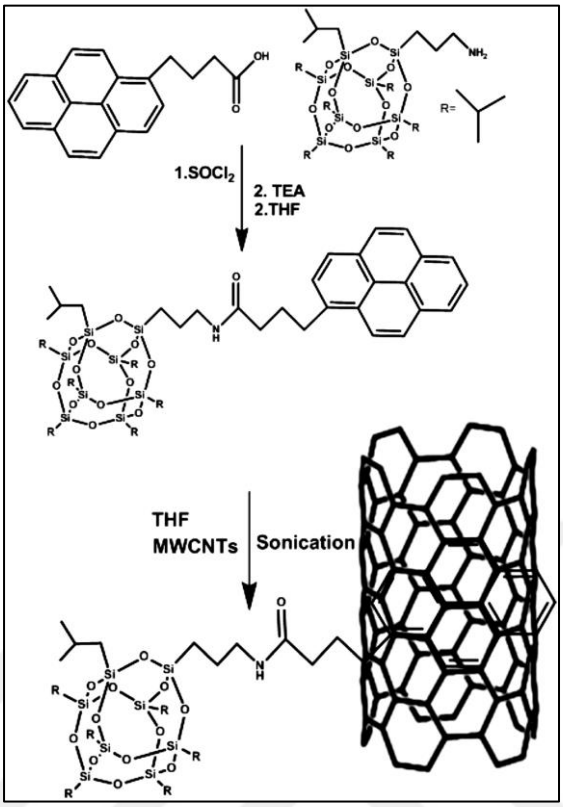

2.3 POSS Polymers for Organic-Electronics Related Materials

Inorganic materials have been used and commercialized for electronic applications as semiconductor. In recent years, organic based semiconductors also gained a high interest as they are lower cost alternative to inorganic ones [105].

Silicon transistors are widely used class of the inorganic transistors. However, these inorganic materials are having disadvantages of being costly and not flexible as organic materials. Also they are not compatible with high temperature resistant substrates. To replace these silicon transistors, organic thin film transistors (OTFTs) have been investigated. But, still these high performing OTFTs were not giving the expected low-cost benefit. Because of that, several other polymeric gate insulators such as poly(methylmethacrylate) (PMMA), polyimide, polystyrene and poly (styrene-butadiene) have been researched and used in specific applications [106, 107]. Silicon based semiconductor materials are widely preferred in electronics applications. After the studies with organic semiconductors, it seems that they might replace silicon

based ones [106]. Since POSS is an organic-inorganic hybrid material, it has been researched very broadly for organic diode materials, and related other works have been considered. POSS contaning materials brought very diversed properties for organic electronics. They are acceptable in organic electronic devices which require electrolytes and also in energy storing applications. Octa-functional POSS polymer based on imidazolium iodide groups has been already investigated on dye-sensitive solar cell application by Zhang et al. [108]. Results showed that the ionic conductivity could be significantly improved by iodine doping and long term stability makes the material highly applicable.

POSS derivatives having an insulating property have also been used for organic field-effect transistors (OFET) as a dielectric component by Kim et al. [109].

In recent studies, POSS derivative with epoxy functional groups has been synthesized and used as an insulator. While POSS materials have a good thermal, mechanical and electrical properties, showing an effective insulator performance make these materials preferable to be used in OTFTs. By functionalization with epoxy groups, more additional benefits come through this UV curable system [110].

3. POLYMERIZATION METHODS AND CLICK CHEMISTRY

3.1 Atom-Transfer Radical Polymerization

Radical polymerization method is widely used for the production of millions tons of the commercial polymers with various types of chemical structures. Though, its very well known that the control of the polymerization is not easy to produce well designed polymers. For that reason, controlled radical polymerization has given an opportunity to obtain tailor-made polymers with perfectly controlled molecular structure.

Atom Transfer Radical Polymerization (ATRP) is one of the controlled radical polymerization method which based on an equilibrium between propagating radical species and macromolecular alkyl halide molecules (PnX). The growing non-active species interact with transition metal complexes at a constant activation rate (k_{eact}) with the rate constant of activation (keact) with transition metal complexes at their lower state of oxidation level, Mtm/L, acting as mobilizer to form growing radicals (Pn •), and deactivators-transition metal complexes in their higher state of oxidation, with halide ligands X−Mtm+1/L coordination (Figure 3.1) [42].

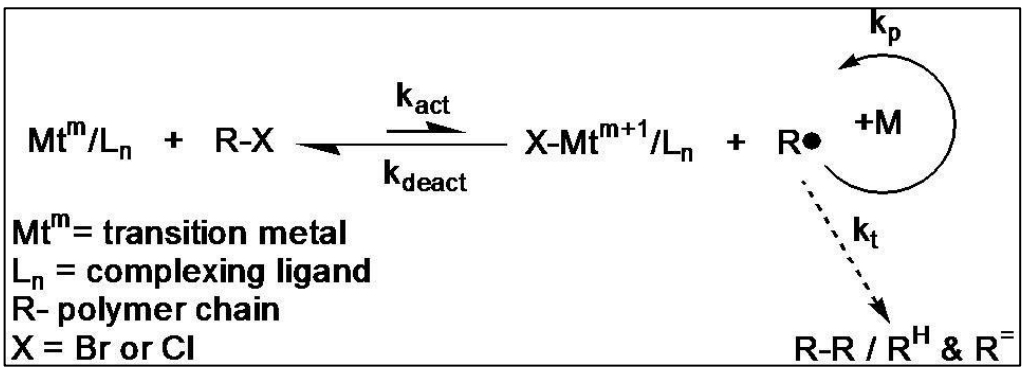

Figure 3.1: Mechanism of Metal Complex Mediated ATRP

3.2 Ring Opening Polymerization (ROP)

Ring opening polymerization (ROP) is a significant process for formation of polymers. In this type of reactions, polymerization propagates via the addition of

opened structures to the polymer chain, in the same manner as in chain-growth mechanism (Figure 3.2).

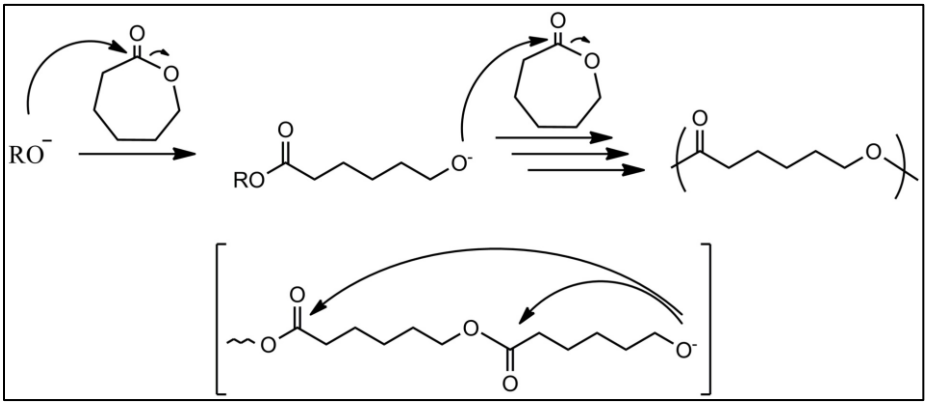

Figure 3.2: Scheme of Ring Opening Polymerization

A wide range of structures can be synthesized by ROP such as, alkanes, alkenes, ethers, acetals, lactones, lactides, carbonates, phosphates, phosphonates, phosphites, phosphines, phosphazenes, anhydrides, polysulfur, polysulfides, lactams, siloxanes, silaethers, carbosilanes, silanes, imides, N-carboxyanhydres, 1,3-oxaza derivatives[111]. ROP is known as an easy and featured method of producing macromolecules. ROP allows one to generate new polymers with tailored material properties such as high molecular weight, low polydispersity and other characteristics as required according to the specific application. ROP enables the preparation of complex structures such as stars, brushes, cyclics and crosslinked materials which need controlled synthesis conditions [112, 113].

From the point of the production of aliphatic polyesters, with these beneficial features ROP is preferable in comparison to step growth polymerization. As known, the step growth polymerization, based on the polycondensation of hydroxycarboxylic acids or of a diol with dicarboxylic acid [113], has some disadvantages such as difficulties in controlling the molecular weight and polydispersity of the polymer, necessity the removal of water from the reaction medium to increase the conversion, high temperatures and long reaction times with accompanying side reactions. Also, polycaprolactone is utilized in agricultural applications as mulch films, ropes or cups. The production of polycaprolactone and polylactic acid in large volumes is realized for using as packaging materials and commodity plastics [111].

In ROP, the nature of active species, in other words the initiator type determines the polymerization mechanism. There are three major mechanisms for the ROP as cationic, anionic and coordination-insertion [112].

3.3 Click Chemistry

"Click" chemistry is the well known chemical process to functionalize polymeric materials resulting a high yield and unique tailor-made structures with specified properties. Among the click chemistry methods, Huisgen 1,3-dipolar cycloaddition of azides and alkynes via Cu(I)-catalyzed was developed and widely used since years [114].

In the past few years, "click reactions", as termed by Sharpless et al., [1] have gained a great deal of attention due to their high specificity, quantitative yields, and near-perfect fidelity in the presence of most functional groups. The most popular click chemistry reaction is the copper-catalyzed Huisgen dipolar cycloaddition reaction between an azide and an alkyne leading to 1,2,3-triazole (Figure 3.3).

Figure 3.3: Scheme of Azide-Alkyne Cycloaddition

4. MATERIAL AND METHOD

The chemicals and their properties used in this study are listed in Table 4.1.

Table 4.1: The chemicals used in synthesis, separation and purification processes.

Name	Company	CAS Number	Assay
3-chloropropyltrimethoxysilane	Sigma-Aldrich	2530-87-2	≥ 97%
Hydrochloric acid (HCl)	Sigma-Aldrich	7647-01-0	37%
Tetrahydrofuran (THF)	Merck	109-99-9	≥ 99.8%
Poly(ethylene glycol) methyl ether (Mn1000,2000,5000g/mol)	Sigma-Aldrich	9004-74-4	
Sodium hydride (NaH)	Sigma-Aldrich	7646-69-7	95%
1-pyrene methanol	Sigma-Aldrich	24463-15-8	98%
Tin(II) 2-ethylhexanoate	Sigma-Aldrich	301-10-0	92.5-100%
ε-Caprolactone	Sigma-Aldrich	502-44-3	97%
Propargyl 2-bromoisobutyrate (PBIB)	Sigma-Aldrich	40630-86-2	≥ 97%
Propargyl alcohol	Sigma-Aldrich	107-19-7	99%
Copper(I) bromide (CuBr)	Sigma-Aldrich	7787-70-4	98%
2-bromo-2-methylpropanoyl bromide	Sigma-Aldrich	20769-85-1	98%
Anisole	Sigma-Aldrich	100-66-3	99.7%
Dichloromethane (DCM)	Merck	75-09-2	99.8%
Methyl methacrylate (MMA)	Alfa Aesar	80-62-6	99% stab.
Styrene	Sigma-Aldrich	100-42-5	≥ 99.5% stab.
Methanol	Sigma-Aldrich	67-56-1	99.8%
Magnesium sulfate ($MgSO_4$)	Sigma-Aldrich	7487-88-9	99.5%
N,N,N′,N″,N″-Pentamethyldiethylenetriamine (PMDETA)	Aldrich	3030-47-5	99%
N,N-Dimetilformamide (DMF)	Sigma-Aldrich	68-12-2	99.8%
Sodium azide (NaN_3)	Aldrich	26628-22-8	≥ 99.5%
Sodium bicarbonate ($NaHCO_3$)	Sigma-Aldrich	144-55-8	≥ 99.7%
Sodium chloride	Alfa-Aesar	7647-14-5	99%
Styrene	Aldrich	100-42-5	≥ 99%
Triethylamine (TEA)	Sigma-Aldrich	121-44-8	≥ 99%
1-ethynylpyrene	Sigma-Aldrich	34993-56-1	96%
Sodium sulfate (Na_2SO_4)	Sigma-Aldrich	7757-82-6	≥99%
Propargyl bromide	Aldrich	106-96-7	80%

The devices used in this study are listed in Table 4.2.

Table 4.2: The devices used in the characterization studies.

Name	Conditions
Differential Scanning Calorimetry (DSC)	DSC 8500 (Perkin Elmer) instrument under a nitrogen flow of 10 mL/min.
Thermal Gravimetric Analysis (TGA)	TGA/SDTA 851 (Mettler Toledo) thermogravimetric analyzer
Fourier-transform Infrared Spectroscopy (FTIR)	Perkin Elmer Spectrum Two™ spectrometer equipped with UATR accessory.
Gel Permeation Chromatography (GPC)	Agilent 1260 Infinity GPC/SEC instrument consisting of a pump, a refractive index detector and two Agilent PLgel columns (Mixed-C, 5 μm, 7.5 × 300 mm)
Dynamic Light Scattering (DLS)	Nano-ZS Zen 3600
Transmission Electron Microscope (TEM)	JEOL JEM-1400 Plus
Nuclear Magnetic Resonance Spectroscopy (NMR)	Varian UNITY INOVA 500 spectrometer
Atomic Force Microscope (AFM)	Alpha 300 A
Fluorescence Spectroscopy	Agilent Carry Eclipse Bundle A time resolved fluorescence spectrophotometer (FL-1057 TCSPC).
Dielectric Spectroscopy	HP 4194 A
Semiconductor Characterization System	Kiethly 4200 SCS
UV-Vis Spectrometer	Perkin Elmer Lambda 30
Raman Spectroscopy	Thermo DXR Raman

5. EXPERIMENTAL

5.1. General Procedure

The reactions carried out in inert atmosphere (dry argon atmosphere) in order to prevent oxidation and other possible side reactions because of oxygen and moisture in the air. The glassware used in the reactions were dried in the burner flame and treated with argon.

5.1.1. Preperation of Dry N,N-Dimetilformamide (DMF)

DMF was stirred overnight by adding CaH_2 and then distilled under vacuum. Prepared dry DMF, was kept under argon in the presence of molecular sieves (4A°).

5.1.2. Drying of the Synthesized Polymers

The synthesized polymers were precipitated in appropriate solvents, filtered through a G4 sintered filter and weighed on a precision balance. Polymers were allowed to dry at room temperature under reduced pressure by recording the weighing results. Then, weight of the polymer was checked periodically and the same value of the last three measurements showed that polymer was dry.

5.2. Experiments

5.2.1. Synthesis of Octakis (3-chloropropyl)silsesquioxane POSS(Cl)$_8$

Octa(3-chloropropyl) POSS was synthesized by minor modification of the procedure reported elsewhere [111]. 3-chloropropyltrimethoxysilane (20.0 g, 0.10 mol), methanol (450 mL), and conc. HCl (25 mL of 35% in H_2O) was placed in a one-necked, round-bottomed flask and stirred at room temperature for 5 weeks. **POSS-(Cl)$_8$** was obtained as a white powder after suction filtration and washing several times with deionized water and ethanol, respectively. The final product was dried under reduced pressure at 50 °C for 4 hours until a constant weight (Figure 5.1).

Yield: 3.85 g (29.5%). FT-IR (ATR, cm^{-1}): 2945, 2896 and 2872 (CH); 1080 (Si-O-Si); 690 (C-Cl). ^{1}H NMR (500 MHz, $CDCl_3$, δ, ppm): 0.79 (t, 16H, -SiC***H***$_2$-), 1.87

(quint, 16H,-$CH_2C\boldsymbol{H}_2CH_2$-), 3.54 (t, 16H, -$C\boldsymbol{H}_2$Cl). ^{13}C NMR (125 MHz, $CDCl_3$, δ, ppm): 9.36 (-Si$C\boldsymbol{H}_2$-), 26.27 (-$CH_2C\boldsymbol{H}_2CH_2$-), 47.04 (-$C\boldsymbol{H}_2$Cl). ^{29}Si NMR (80 MHz, $CDCl_3$, δ, ppm): -67.35 (-***Si***CH_2-).

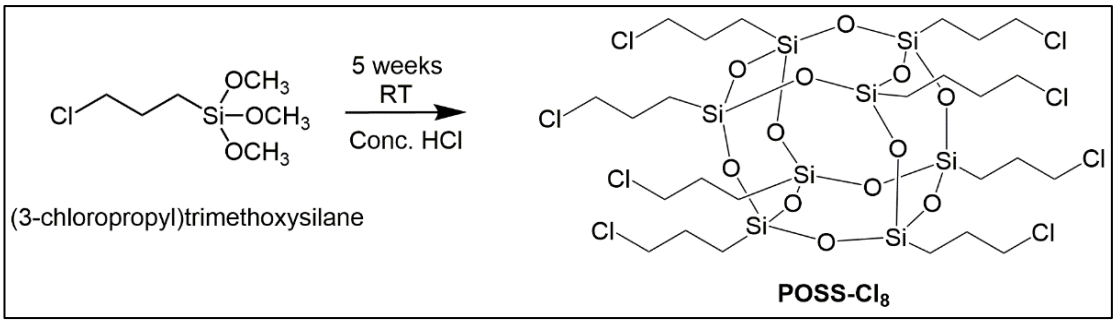

Figure 5.1: General reaction scheme for the synthesis of $POSS(Cl)_8$

5.2.2. Azidation of Octakis(3-chloropropyl)silsesquioxane $POSS(N_3)_8$

$POSS\text{-}(Cl)_8$ (3.5 g, 3.38 mmol) and sodium azide (14.04 g, 216.02 mmol) was dissolved in anhydrous DMF (40 mL) under inert argon atmosphere and immersed into an oil bath thermostated at 120 ^oC. After stirring for 72 hours, the solvents were removed at reduced pressure. The reaction mixture was diluted with THF and passed through basic alumina column to remove residual sodium salt. The solvent was evaporated under high vacuum and obtained a colorless viscous liquid (Figure 5.2). Yield: 2.98 g (81%). FT-IR (ATR, cm^{-1}): 2934 and 2866 (CH); 2093 (N_3); 1096 and 1014 (Si-O-Si). ^{1}H NMR (500 MHz, $CDCl_3$, δ, ppm): 0.69 (t, 16H, -Si$C\boldsymbol{H}_2$-), 1.64 (quint, 16H,-$CH_2C\boldsymbol{H}_2CH_2$-), 3.26 (t, 16H, -$C\boldsymbol{H}_2N_3$). ^{13}C NMR (125 MHz, $CDCl_3$, δ, ppm): 9.54 (-Si$C\boldsymbol{H}_2$-), 31.39 (-$CH_2C\boldsymbol{H}_2CH_2$-), 53.38 (-$C\boldsymbol{H}_2$Cl). ^{29}Si NMR (80 MHz, $CDCl_3$, δ, ppm): -69.07 (-*Si*CH_2-).

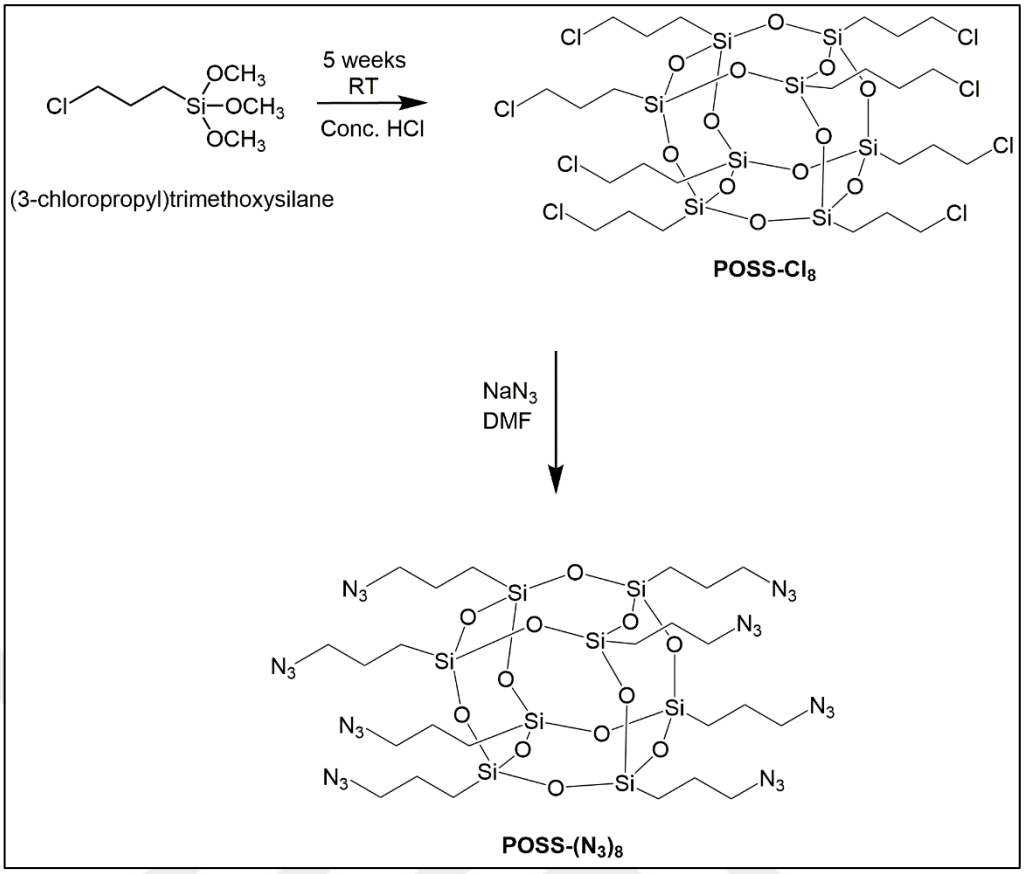

Figure 5.2: General Reaction Scheme for the Synthesis of $POSS(N_3)_8$

5.2.3. Synthesis of Alkyne-mPEG

Alkyne functionalized poly(ethylene glycol) monomethyl ether (Alkyne-mPEG) was prepared according to a published report in the literature [18, 19]. To a solution of mPEG-2000 (3.00 g, 1.50 mmol) in 20 ml of dichloromethane (DCM), NaH (60% w/w in mineral oil, 0.09 g, 3.75 mmol) was added at 0 °C under stirring. After stirring for 30 min, propargyl bromide (80% in toluene, 0.16 ml, 1.80 mmol) was added slowly, and the mixture was stirred at 0 °C for 2 h. The ice bath was removed and the reaction allowed to warm to room temperature and stirred with a magnetic stirrer for 24 h. Then the reaction mixture was dispersed in water and extracted with dichloromethane for twice. After dried with $MgSO_4$, the final product was obtained by precipitation in diethyl ether. The precipitate was filtered of and and vacuum-dried at room temperature until a constant weight (Figure 5.3).

Yield: 2.61 g (82%). FT-IR (cm^{-1}): 2922 and 2849 (C-H); 1462; 1284; 1239; 1099; 955; 837. ^{1}H NMR (500 MHz; $CDCl_3$; δ, ppm): 2.45 (t, -C≡C***H***); 3.39 (s, -$CH_2CH_2OC\boldsymbol{H}_3$); 3.65-3.72 (br, -$C\boldsymbol{H}_2C\boldsymbol{H}_2O$-); 4.21 (d, -$C\boldsymbol{H}_2$C≡CH).

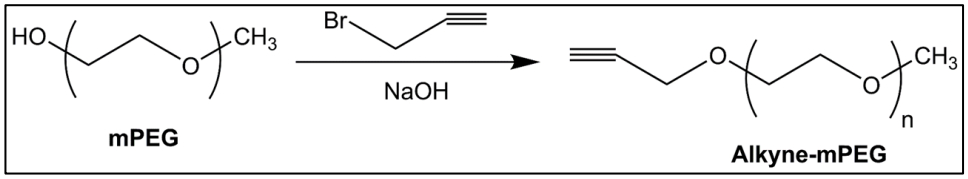

Figure 5.3: Schematic Illustiration for the Synthesis of Alkyne-mPEG

5.2.4. Synthesis of POSS-(mPEG)$_8$ Star-Shaped Polymers by CuAAC Click Chemistry

Octa-functional star-shaped polymers with POSS core and PEG arms were synthesized by using CuAAC click chemistry. **Alkyne-mPEG** (1.70 g, 0.83 mmol) and **POSS-(N_3)$_8$** (0.10 g, 0.09 mmol) were dissolved in degassed DMF (15 mL) in an round-bottom flask and stirred under argon atmosphere for 10 min. PMDETA (0.05 g, 0.28 mmol) was then added and degassed by gently purging with argon atmosphere for 5 min. Finally, copper(I) bromide (CuBr) (0.04 mg, 0.28 mmol) was added to the solution and reaction mixture was degassed again. After the mixture was stirred under nitrogen protection at room temperature for 48 h, it was diluted with DCM (100 mL) and transferred to an extraction funnel. Polymer solution then washed successively with brine (2x50 mL) and water (50 mL). Organic phase was dried with anhydrous $MgSO_4$ and concentrated to about 5 mL in vacuo. Finally, polymer was recovered by precipitation into cold hexane, and collected by vacuum filtration through a sintered glass filter (G4) and dried for 48 h under reduced pressure at 35 °C until a constant weight was obtained (Figure 5.4).

Yield: 1.48 g (92%). FT-IR (cm^{-1}): 2948 and 2884 (CH); 1096 and 1014 (Si-O-Si). ^{1}H NMR (500 MHz, $CDCl_3$, δ, ppm): 0.63 (t, 16H, -SiC***H***$_2$- in POSS); 1.98 (quint, 16H,-CH_2C***H***$_2CH_2$- in POSS); 3.44 (s, 24H -$(OCH_2CH_2)_nOC$***H***$_3$ in mPEG); 3.65 (t, 32H, -$(OC$***H***$_2C$***H***$_2)_nO$- in mPEG); 4.36 (s, 16H, triazole-C***H***$_2$O- in mPEG);.4.71 (t, 16H, -C***H***$_2N_3$ in POSS); 7.75 (s, 8H,-C_2***H***N_3- in triazole ring).

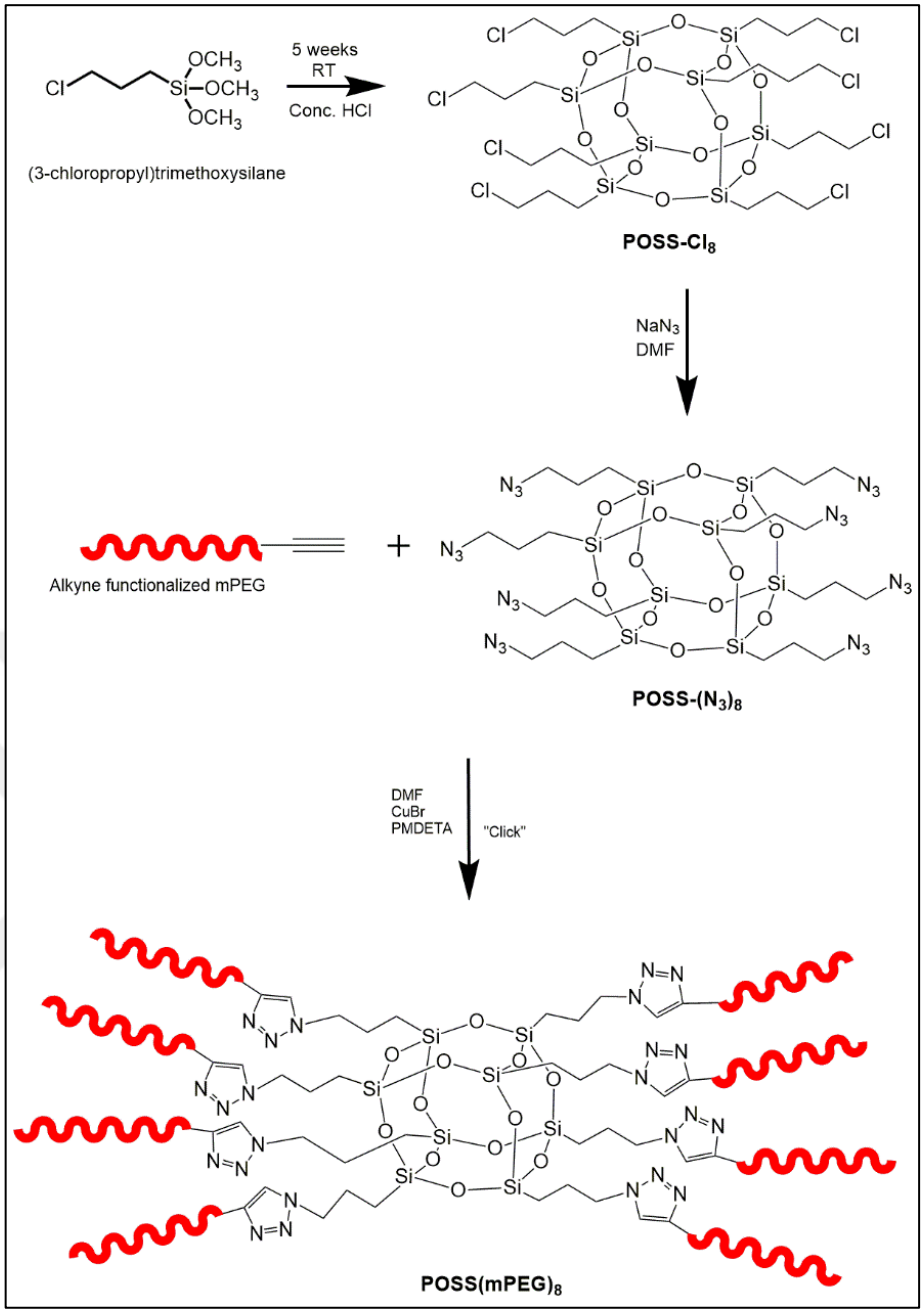

Figure 5.4: General Reaction Scheme for the Synthesis of POSS(mPEG)$_8$ Star-Shaped Polymers by CuAAC Click Chemistry.

5.2.5 Synthesis of Pyrene-Functionalized POSS POSS(Pyr)$_8$

1-ethynyl pyrene (0.66 g, 2.937 mmol) and **POSS-(N$_3$)$_8$** (2) (0.2 g, 0.184 mmol) were dissolved in nitrogen-purged 5 mL DMF. PMDETA (0.92 g, 4.406 mmol) and CuBr (0.63 g, 4.406 mmol) were added to the solution and it was again degassed with argon. Then, the solution was extracted in DCM. Finally, solvent was evaporated by yielding a dark yellow product.

Yield: 0.77 g (89%). FT-IR (ATR, cm^{-1}): 2929 and 2860 (CH); 1665 (C=C); 1085 (Si-O-Si). ^{1}H NMR ($CDCl_3$, δ): 8.72 (d, 8H, $C_2\boldsymbol{H}N_3$ (triazole ring)); 8.12-7.56 (m, 72 H, $C_{16}\boldsymbol{H}_9$ (Pyr)); 4.51 (t, 16H, -$CH_2CH_2C\boldsymbol{H}_2$–triazole ring); 2.27 (quint, 16H,-$CH_2C\boldsymbol{H}_2CH_2$-); 0.89 (t, 16H, -Si$C\boldsymbol{H}_2$-). ^{13}C NMR ($CDCl_3$, δ): 9.54 (-Si$C\boldsymbol{H}_2$-), 31.39 (-$CH_2C\boldsymbol{H}_2CH_2$-), 53.38 (-$C\boldsymbol{H}_2$Cl). ^{29}Si NMR ($CDCl_3$, δ): -69.07 (-*Si*$CH_2$-).

5.2.6 Synthesis of α-Pyrene Functionalized Linear PCL Polymer

1-pyrene methanol (0.51 g, 2.190 mmol), $Sn(Oct)_2$ (0.09 g, 0.219 mmol), and ε-CL (5.0 g, 43.806 mmol) were added into a Schlenk tube and degassed by argon for 10 min and stirred 24 h at 115 °C. The obtained polymer was diluted in DCM and precipitared in cold methanol. The solution was dried under a pressure at room temperature.

Yield: 5.12 (93%). $M_{n,NMR}$: 2400 g/mol; $M_{n,GPC}$: 1585 g/mol; M_w/M_n: 1.31. FT-IR (cm^{-1}): 2940 and 2862 (C-H); 1722 (C=O); 1472 (C-H); 1240 ((C=O)-O); ^{1}H NMR ($CDCl_3$, δ): 8.28-7.99 (m, $C_{16}\boldsymbol{H}_9$ (Pyr)); 4.06 (m, $C\boldsymbol{H}_2$O(C=O) in PCL); 3.65 (t, terminal $C\boldsymbol{H}_2$OH in PCL); 2.30 (m, O(C=O)$C\boldsymbol{H}_2$ in PCL); 1.64 (m, O(C=O)$CH_2C\boldsymbol{H}_2CH_2C\boldsymbol{H}_2CH_2$O(C=O) in PCL); 1.37 (m, O(C=O)$CH_2CH_2C\boldsymbol{H}_2CH_2CH_2$O(C=O) in PCL)

5.2.7 Synthesis of α-Pyrene and ω-Alkyne Functionalized PCL Polymers

α-pyrene functonalized PCL (4.0 g, 1.590 mmol) was dissolved in 50 mL THF in a two-necked reaction flask After a homogenous mixture, TEA (0.48 g, 4.771 mmol) was added into a solution and cooled down to -15 ^{o}C. Propargyl chloroformate (0.94 g, 7.952 mmol) solution was prepared in 20mL THF and dropped into the mixture slowly. After 48 h at room temperature, solvent was evaporated and product was

extracted with 100 mL DCM with addition of $NaHCO_3$ and distilled water. Obtained product was precipitated in cold methanol and dried under a vacuum at room temperature.

Yield: 3.76 (91%). $M_{n,NMR}$: 2482 g/mol; $M_{n,GPC}$: 2255 g/mol; M_w/M_n: 1.45. FT-IR (cm^{-1}): 2945 (C-H); 2865 (C-H); 2098 (-C≡C-); 1722 (C=O); ^{1}H NMR ($CDCl_3$, δ): 8.29-7.98 (m, $C_{16}\boldsymbol{H}_9$ (Pyr)); 4.08 (m, $C\boldsymbol{H}_2O(C=O)$ in PCL); 4.74 (s, -$C\boldsymbol{H}_2$-C≡CH); 2.42 (s, -CH_2-C≡$C\boldsymbol{H}$); 2.31 (m, O(C=O)$C\boldsymbol{H}_2$ in PCL); 1.65 (m, O(C=O)$CH_2C\boldsymbol{H}_2CH_2C\boldsymbol{H}_2CH_2O$(C=O) in PCL); 1.39 (m, O(C=O)$CH_2CH_2C\boldsymbol{H}_2CH_2CH_2O$(C=O) in PCL).

5.2.8 Synthesis of Pyrene End-Capped Star-Shaped PCL Polymers with POSS Core

$POSS(N_3)_8$ (0.1 g, 0.092 mmol) and **α-pyrene containing ω-alkyne functionalized PCL polymers** (2.29 g, 0.881 mmol) were dissolved in 40 mL DMF. CuBr (0.32 g, 2.203 mmol) and PMDETA (0.38 g, 2.203) were added to the reaction mixture and stirred at room temperature for 48 h. The neutral alümina column was used to remove copper catalyst and subsequent precipitation was performed in cold methanol. The product was dried at room temperature under a pressure vacuum (Figure 5.5).

Yield: 1.89 (94%). $Mn,_{NMR}$: 11670 g/mol; $Mn,_{GPC}$: 8100 g/mol; Mw/Mn: 1.99. FT-IR (cm-1): 2940 and 2860 (C-H); 1722 (C=O); ^{1}H NMR ($CDCl_3$, δ): 8.34-8.00 (m, $C_{16}\boldsymbol{H}_9$ (Pyr)); 4.08 (m, $C\boldsymbol{H}_2O(C=O)$ in PCL) and (t, 16H, -$C\boldsymbol{H}_2$-triazole ring); 2.32 (m, O(C=O)$C\boldsymbol{H}_2$ in PCL); 1.85 (quint, 16H,-$CH_2C\boldsymbol{H}_2CH_2$-); 1.65 (m, O(C=O)$CH_2C\boldsymbol{H}_2CH_2C\boldsymbol{H}_2CH_2O$(C=O) in PCL); 1.39 (m, O(C=O)$CH_2CH_2C\boldsymbol{H}_2CH_2CH_2O$(C=O) in PCL); 0.86 (t, 16H, -Si$C\boldsymbol{H}_2$-).

5.2.9 Noncovalent Grafting of Carbon Nanomaterials

Functionalization of carbon nanomaterials (Fullerene, single-walled carbon nanotube, multi-walled carbon nanotube, and graphene) was accomplished according to the literature method by mixing. 2 mg of Carbon Nanomaterials with 30 mg of pyrene-ended POSS molecules and POSS-cored star polymer were mixed in separate vials in 10 mL of THF at room temperature for 24 h [115]. The functionalized Carbon Nanomaterials were filtered through a filter paper (Whatman Schleicher and Schuell,

blue ribbon, 2 lm) and washed with THF. The collected functionalized carbon nanomaterials were ultrasonicated in THF for 10 min, filtered, and washed with THF again to remove any unbound polymers. The obtained carbon nanomaterial complexes were dried under reduced pressure at room temperature. Pyrene functional macromolecule contents of the carbon nanomaterials complexes were evaluated via TGA analysis.

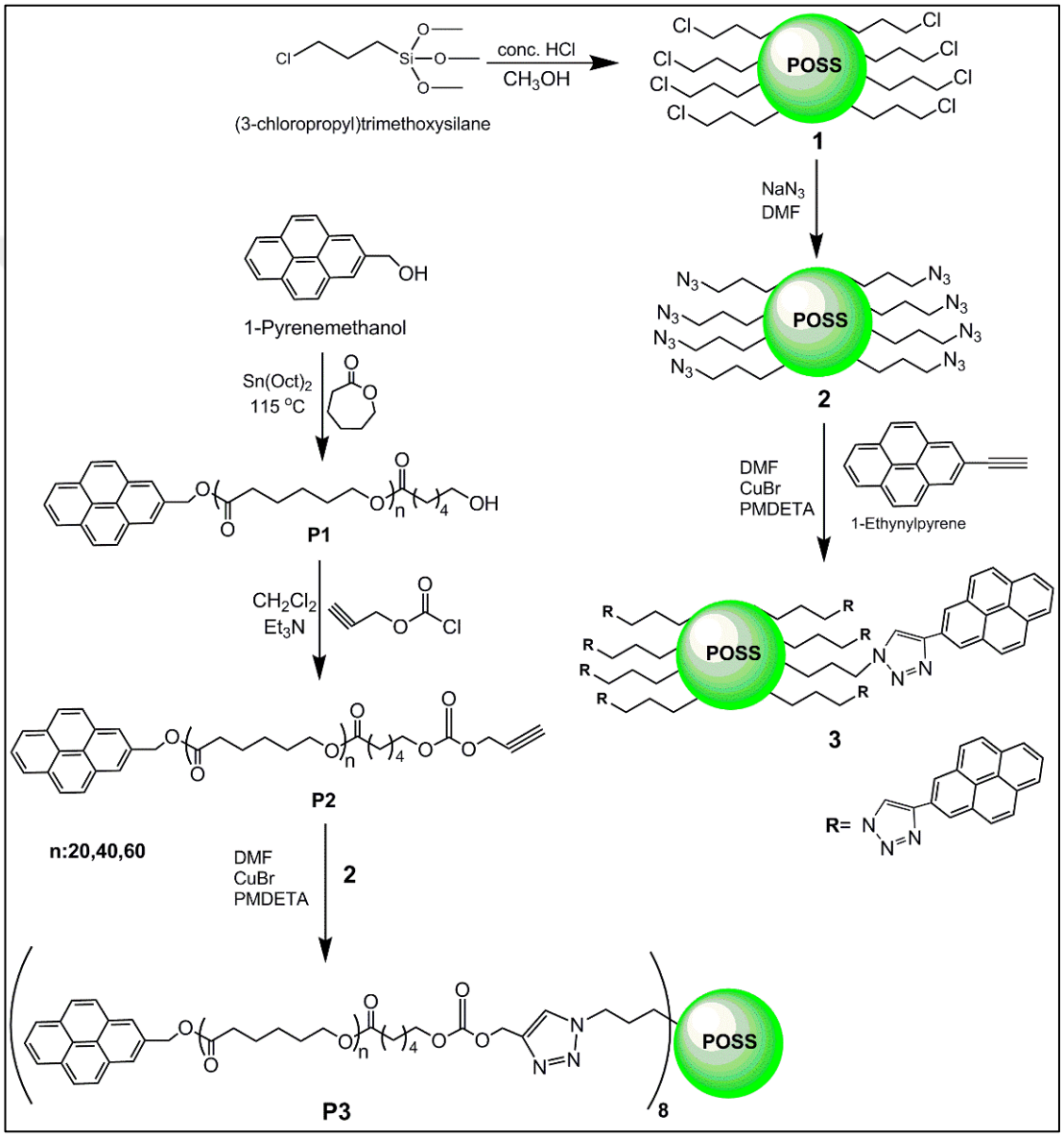

Figure 5.5: Reaction Scheme for the Synthesis of Pyrene End-Capped Star Shaped PCL Polymers with POSS Core.

5.2.10 Synthesis of Propargyl 2-Bromoisobutyrate (PBIB)

The ATRP initiator for alkyne functionalized PMMA and PS, propargyl 2-bromoisobutyrate (PBIB), was prepared by the esterification reaction between propargyl alcohol and 2-bromoisobutyryl bromide according to the literature method with the minor modifications [112, 113]. A two-necked flask equipped with a magnetic stirrer and a dropping funnel was charged with propargyl alcohol (3.0 g, 0.054 mol), TEA (16.25 g, 0.161 mol), and anhydrous THF (50 mL) under argon atmosphere. The mixture was then cooled to -15 ^{o}C by using ice-salt mixture and 2-bromo-2-methylpropanoyl bromide (18.454 g, 0.080 mol) in THF solution (30 mL) was slowly introduced dropwise to the solution while stirring. After the precipitated insoluble salts was removed by suction filtration, the filtrate was concentrated and then further purified by silica gel column chromatography using DCM as the eluent. The solvent was removed on a rotary evaporator and the crude product was distilled under reduced pressure to obtain a colorless liquid.

Yield: 8.89 g (81%). FT-IR (ATR, cm^{-1}): 3299 (≡C-H); 2125 (-C≡C-); 2982 and 2935 (C-H); 1738 (C=O); 1466, 1390, 1371, 1270, 1153, 1106, 1011, 987. ^{1}H NMR (500 MHz, $CDCl_3$, δ, ppm): 4.76 (s, 2H, -C***H***$_2$OC(O)-); 2.51 (s, 1H, C≡C***H***);1.95 (s, 6H, -C(C***H***$_3$)$_2$).

5.2.11 Synthesis of Alkyne-PMMA

Alkyne-functionalized PMMA was prepared via ATRP method according to a published report in the literature method with the minor modifications [116]. PBIB (0.21 g, 0.99 mmol), MMA (3.0 g, 29.96 mmol), and anisole (3 mL) were added to a single-necked flask under oxygen-free argon atmosphere, followed by PMDETA (0.35 g, 1.998 mmol). CuBr (0.14 g, 0.99 mmol) was then added and mixture was degassed by flushing with O_2-free argon for 10 min. The reaction mixture was immersed in oil bath at 90 °C for 5 h, then the flask taken from the oil bath, and rapidly cooled to room temperature to stop the polymerization. The product was diluted with THF and passed through a short column of neutral alumina (activated, basic, Brockmann I) to remove copper salts. After removing THF by a rotary evaporator, the concentrated solution was precipitated into a large amount of cold methanol. The precipitate was collected by filtration through a sintered glass filter (G4) and dried under reduced pressure at room temperature until a constant weight.

Yield: 1.39 g (93%). FT-IR (ATR, cm^{-1}): 3442 (O-H); 2997 and 2949 (C-H); 1738 (C=O); 1434, 1386, 1241, 1141, 992. ^{1}H NMR (500 MHz, $CDCl_3$, δ, ppm): 3.59 (s, C***H***$_3$O(C=O)); 2.08-1.74 (m, -(C***H***$_2$C(CH_3)(C=O))-); 1.11-0.69 (s, C***H***$_3$C-).

5.2.12 Synthesis of Alkyne-PS

Alkyne-functionalized PS was prepared via ATRP method according to a published report in the literature method with the minor modifications [117]. PBIB (0.2 g, 0.98 mmol), styrene (3.05 g, 29.27 mmol), and anisole (3 mL) was added first to a reaction flask equipped with a magnetic stirrer, followed by PMDETA (0.34 g, 1.95 mmol) and CuBr (0.14 g, 0.98 mmol), respectively. The reaction mixture as deoxygenated by bubbling with argon for 10 min. and placed in an oil bath at 90 ^{o}C. After 6 hour, the flask was rapidly cooled to room temperature in an ice bath. After that time dark-green polymerization mixture was first passed through a short column of neutral alumina column (activated, Brockmann I), using THF as an eluent to remove the catalyst and precipitated into a large amount of cold methanol. Then, the precipitate was isolated by filtration and dried under reduced pressure at ambient temperature until a constant weight.

Yield: 1.39 g (93%).FT-IR (cm^{-1}): 3027 (C-H, aromatics); 2921 and 2849 (C-H, alkyl); 1734; 1597; 1497; 1456. ^{1}H NMR (500 MHz, $CDCl_3$, δ, ppm): 7.37-6.20 (s, Ar-***H***), 2.13-1.70 (m, C***H*** of PSt backbone), 1.70-1.14 (m, C***H$_2$*** of PS backbone).

5.2.13 Synthesis of Star-shaped Polymers POSS(PS)$_8$ and POSS(PMMA)$_8$ by CuAAC Click Chemistry

The POSS-$(N_3)_8$ (0,015g, 0.013 mmol), with a small excess amount of alkyne-PS (0.52 g, 0.16 mmol) or alkyne-PMMA in the presence of DMF (5 mL) were added in a round-bottom flask and purged with argon for 10 min. Then, copper(I) bromide (CuBr) (0.006g, 0.04 mmol) and PMDETA (0.007 g, 0.04 mmol) were added to the mixture and kept under a positive pressure of inert gas. The reaction mixture was stirred at room temperature for 48 h. After given time, it was diluted with dichloromethane (100 mL) and then washed successively with brine (2x50 mL) and water (50 mL). The organic phase was concentrated to about 5 mL in vacuum and dried with anhydrous $MgSO_4$. The remaining solution was precipitated into cold

hexane, filtered through a sintered glass filter (G4) and dried under vacuum oven at 40°C to a constant weight. (Figure 5.6.)

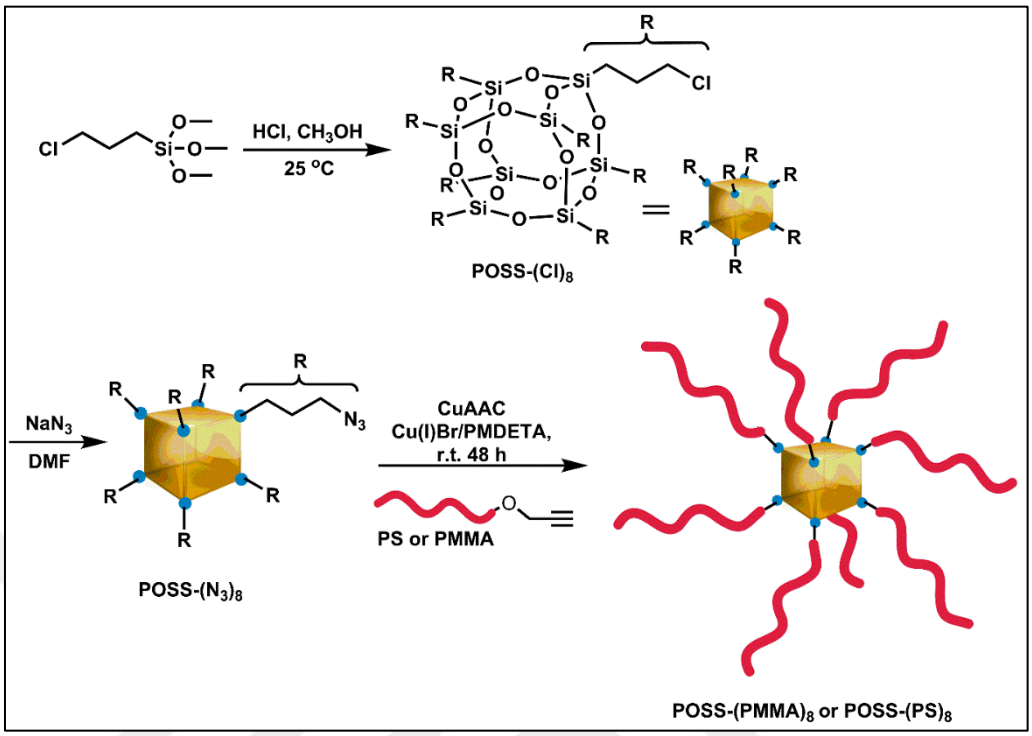

Figure 5.6: General Synthesis Procedure of POSS(PMMA)$_8$ and POSS(PS)$_8$

POSS(PMMA)$_8$ Yield: 1.48 g (92%). FT-IR (cm^{-1}): 2948 and 2884 (CH); 1096 and 1014 (Si-O-Si). ^{1}H NMR (500 MHz, $CDCl_3$, ppm): 0.63 (t, 16H, -SiC***H***$_2$- in POSS); 1.98 (quint, 16H,-CH_2C***H***$_2CH_2$- in POSS); 3.44 (s, 24H -$(OCH_2CH_2)_nOC$***H***$_3$ in *m*PEG); 3.65 (t, 32H, -$(OC$***H***$_2C$***H***$_2)_nO$- in *m*PEG); 4.36 (s, 16H, triazole-C***H***$_2$O- in *m*PEG);.4.71 (t, 16H, -C***H***$_2N_3$ in POSS); 7.75 (s, 8H,-C_2***H***N_3- triazole ring). ^{13}C NMR (125 MHz, $CDCl_3$, δ, ppm):18.85(-Si***C***H_2-); 29.12 (-CH_2***C***H_2CH_2-); 58.75 (-***C***H_2-N-); 70.10 (-***C***H_2-O-). ^{29}Si NMR (79.49 MHz, $CDCl_3$, δ, ppm): -69.36 (-***Si***-CH_2-).POSS(PS)$_8$ Yield: 1.48 g (92%). FT-IR (cm^{-1}): 2948 and 2884 (CH); 1096 and 1014 (Si-O-Si). ^{1}H NMR (500 MHz, $CDCl_3$, δ, ppm): 0.63 (t, 16H, -SiC***H***$_2$- in POSS); 1.98 (quint, 16H,-CH_2C***H***$_2CH_2$- in POSS); 3.44 (s, 24H -$(OCH_2CH_2)_nOC$***H***$_3$ in *m*PEG); 3.65 (t, 32H, -$(OC$***H***$_2C$***H***$_2)_nO$- in *m*PEG); 4.36 (s, 16H, triazole-C***H***$_2$O-in *m*PEG);.4.71 (t, 16H, -C***H***$_2N_3$ in POSS); 7.75 (s, 8H,-C_2***H***N_3- in triazole ring). ^{13}C NMR (125 MHz, $CDCl_3$, δ, ppm): 18.85 (-Si***C***H_2-); 29.12 (-CH_2***C***H_2CH_2-); 58.75 (-***C***H_2-N-); 70.10 (-***C***H_2-O-). ^{29}Si NMR (79.49 MHz, $CDCl_3$, δ, ppm): -69.36 (-***Si***-CH_2-).

5.2.14 Fabrication and Characterization of OFET Based on POSS-$(PMMA)_8$ and POSS-$(PS)_8$

We fabricated MIM devices on ITO-patterned glass substrates to compare the insulating property of the POSS-$(PS)_8$ and POSS-$(PMMA)_8$. The Ag top electrode with an area of 4 mm^2 was evaporated through a shadow mask. POSS-PMMA and POSS-PS (60 mg), were dissolved in 1.0 mL of butylacectate, and the solution was prepared by spin coating method on substrate at 1500 rpm for 30 sec. Then CuPc was evaporated on dielectric layer. The coated films were annealed in an oven at 90 ºC for 30 min. The OFET devices were also fabricated using interdigitated Au source-drain electrodes on glass substrates. The source-drain electrodes were photo lithographically produced. Source-drain electrodes are configured as interdigitated fingers with a channel length of 50 µm. Figure 1 shows that schematic illustration of produced OFET devices.

The capacitances of MIM devices were measured using an HP 4194A Impedance Analyzer. The electrical characteristics of the OFETs were measured in ambient atmosphere with Kiethly 4200 semiconductor parameter analyzer. The surface morphologies were characterized by using an atomic force microscopy (AFM).

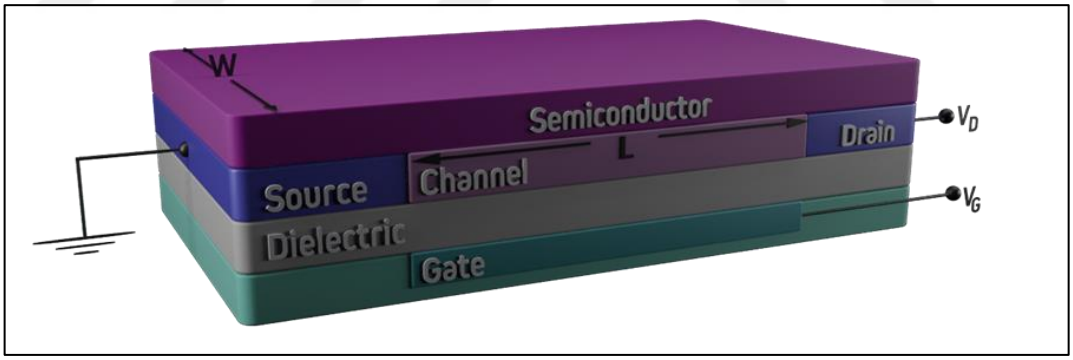

Figure 5.7: Shematic Organic Field Effect Transistors (OFET) Structure

6. RESULTS AND DISCUSSION

6.1. Characterization of POSS-(mPEG)$_8$ Star-Shaped Polymers

The click chemistry reactions were successfully applied for the synthesis of star-shaped polymers containing POSS core with different types of polymeric arms in the literature [117, 118]. Star-shaped surface active polymers were simply prepared by CuAAC click chemistry. For this purpose, clickable POSS(N_3)$_8$ and mPEG-alkyne were independently prepared by well-known procedures (Figure 5.4). The azidation of the (POSS-(Cl)$_8$ was followed by FTIR and ^{1}H-NMR analyses. The appearance of the azide band at 2096 cm^{-1} was a clear proof of the successful functionalization (Figure 6.1).

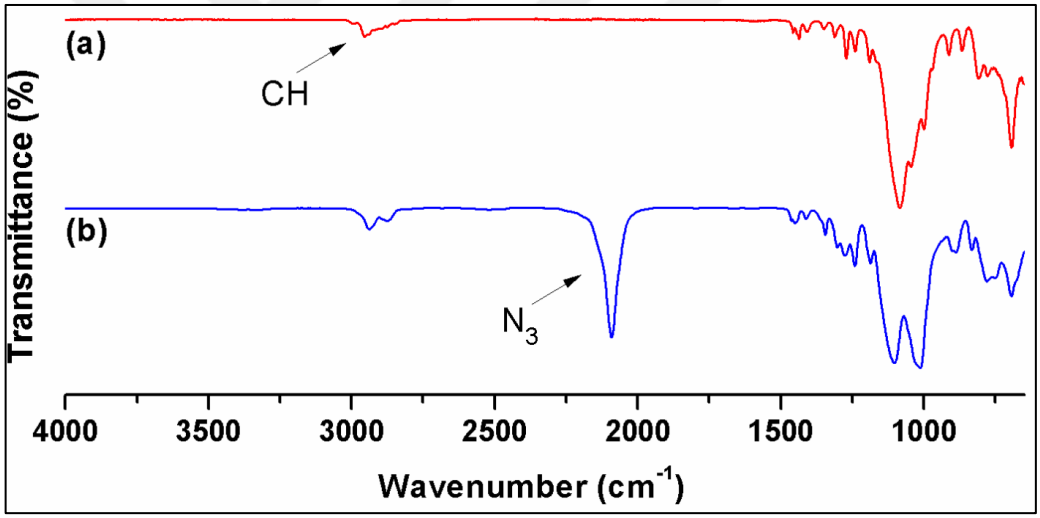

Figure 6.1: FT-IR transmittance spectra of a) POSS-(Cl)$_8$, b) POSS-(N_3)$_8$.

In the ^{1}H NMR spectra of the copolymers (Figure 6.2), the backbone protons (Ha) gave signals between 1.42 and 2.04 ppm, while aromatic CH protons (Hc) in As it is displayed in Figure 6.2a, the methylene proton signals of the POSS(Cl)$_8$ molecule were observed at 3.54 (H_c), 1.87 (H_b), and 0.79 (H_a) ppm. Through the azidification, these signals quantitatively shifted to the higher magnetic fields [H_a = 0.69, H_b = 1.64, H_c =3.26] in Figure 6.2b, providing a further support for the complete conversion. The CuAAC click reaction between azide functional groups of POSS-(N_3)$_8$ and mPEG-alkyne molecules in deaerated DMF by using Cu(I)Br/PMDETA catalyst/ligand system gave octa-functionalized star-shaped POSS polymers in very high yields at

room temperature. The methylene peak (H_c) depicted at 3.26 ppm in the ^{1}H NMR spectrum drifted to downfield by 4.71 ppm after star-shaped polymer formation. Moreover, the new peak belonging to triazole ring (H_d) was appeared at 7.75 ppm in the ^{1}H NMR spectrum of POSS-$(PEG)_8$. Furthermore, the characteristic methylene (H_f) and methyl end-group (H_g) peaks of PEG blocks were observed at 4.36 and 3.44 ppm, respectively. The comparison of the ^{1}H NMR spectra of POSS-$(PEG)_8$ (Figure 6.2c) and POSS$(N_3)_8$ (Figure 6.2b) clearly supported this conclusion.

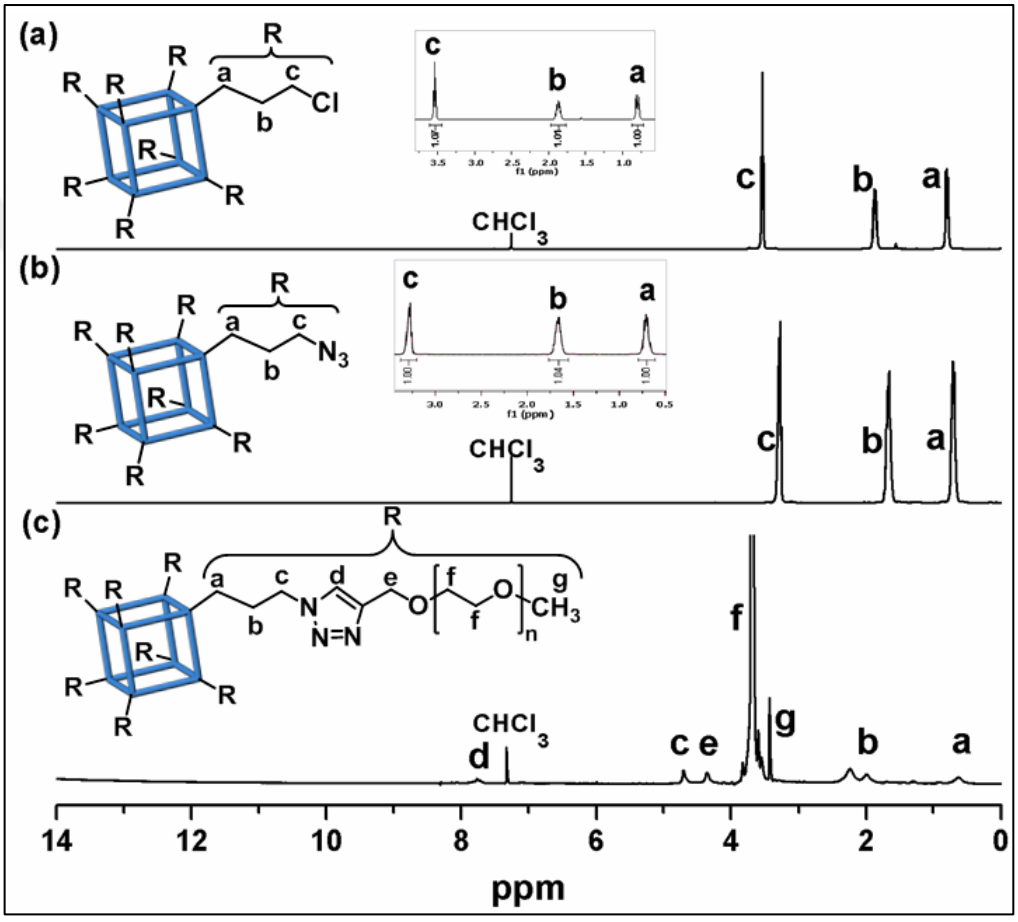

Figure 6.2: ^{1}H NMR Spectra of a) POSS-$(Cl)_8$, b) POSS-$(N_3)_8$, c) POSS-$(PEG2000)_8$

The molecular weights ($M_{n,GPC}$) and molecular weight distributions of the polymers were estimated by GPC and summarized in Table 6.1. As can be seen in Figure 6.3, all polymers had unimodal and narrow curves implying that no homopolymer contamination observed after the click reactions. Moreover, the molecular weights of star polymers were gradually increased and their molecular weight distributions were found as 1.14, 1.22, and 1.38, which were also a proof for

the efficient click reactions. Calculation of molecular weights ($M_{n,NMR}$) was done by using the peak area ratios of end methylene groups (H_c) of propyl chain on POSS core to methylene groups (H_f) of PEG block. This calculation method gave $M_{n,NMR}$ = 6550 g mol^{-1}, 8100 g mol^{-1}, and 13800 g mol^{-1} for PEG750, 1000, and 2000, respectively. The $M_{n,\ NMR}$ values of star-shaped amphiphilic polymers were slightly lower than the experimental ($M_{n,\ GPC}$) results. This error could be aroused from our GPC system, which was calibrated with linear polystyrene standards. The GPC results did not reflect the actual values of more globular-like star polymers. However, it was necessary to have a look at the GPC plot of all obtained star-shaped amphiphilic polymers to confirm their real shifts to higher molar mass and unreacted mPEG-alkyne homopolymers.

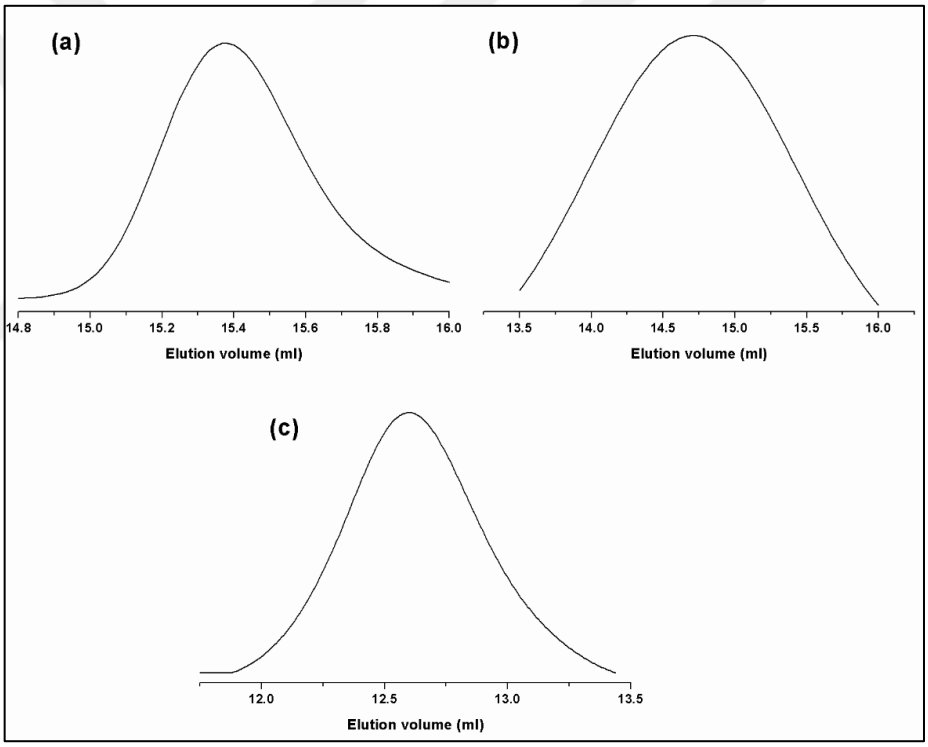

Figure 6.3: GPC Traces of the Star Shaped Polymeric Surfactants a) POSS-(PEG750)$_8$, b) POSS-(PEG1000)$_8$, c) POSS-(PEG2000)$_8$.

Thermal analyses of the star-shaped polymers were investigated by using DSC and TGA. DSC thermograms are illustrated in Table 6.1, Figure 6.4. Comparing the melting points of linear mPEGs (mPEG$_{750}$, T_m= 30°C; mPEG$_{1000}$, T_m=36°C and mPEG$_{2000}$, T_m= 51.2°C) to those of star-shaped polymers, their melting points (POSS(PEG$_{750}$)$_8$, T_m= 43.71°C; POSS(PEG$_{1000}$)$_8$, T_m=46.43°C and POSS(PEG$_{2000}$)$_8$,

T_m= 57.30°C) were dramatically increased. These increases were observed much higher for low molecular weight sample POSS(PEG_{750})$_8$ due to the high POSS concentration in the final product.

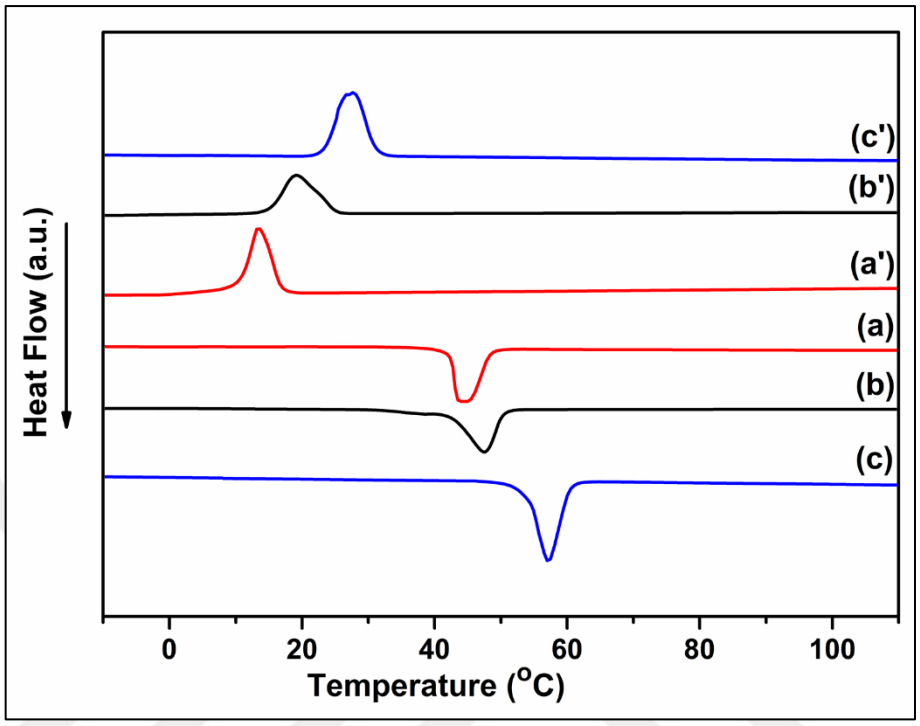

Figure 6.4. DSC Curves of the Star Shaped Polymeric Surfactants: a) POSS-(PEG750)$_8$, b) POSS-(PEG1000)$_8$, c) POSS-(PEG2000)$_8$.

From TGA analysis of star-shaped polymers, their weight losses versus temperature curves were presented in Figure 6.5 and the results of T_{onset}, T_{max} and char yield were given in Table 6.1. It can be obviously observed that while T_{max} values didn't change among these three star- shaped polymers, char yield considerably decreased by increasing molecular weight of mPEG in star-shaped polymer. These results implied that the increase in concentration of POSS molecule in the star-shaped polymers provided more thermal stability.

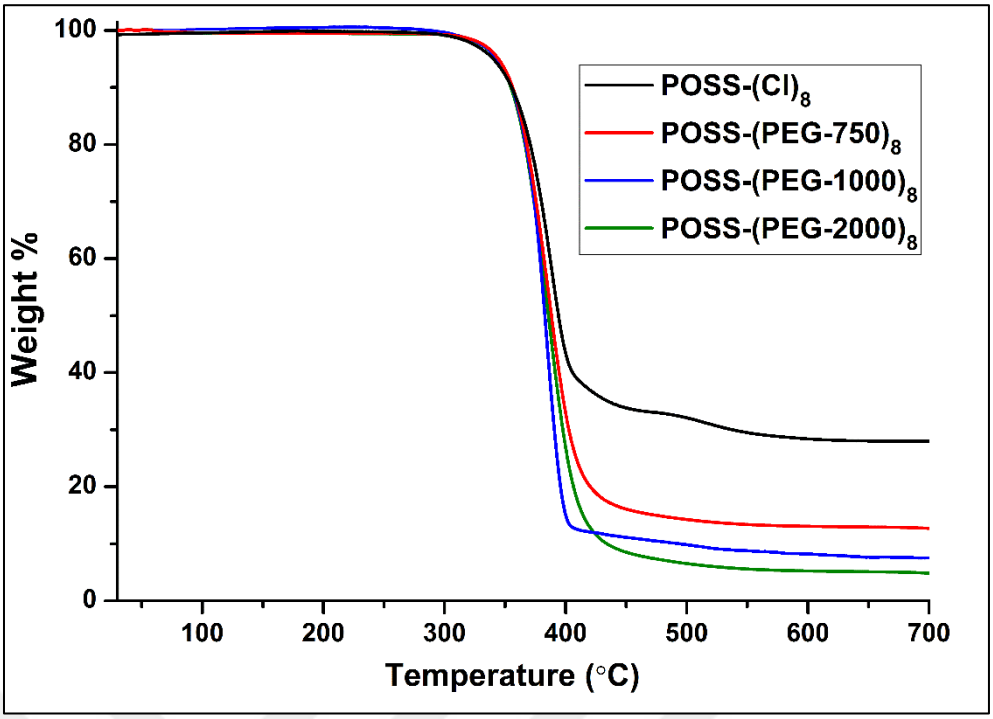

Figure 6.5: TGA Thermographs of the Star Shaped Polymeric Surfactants.

Table 6.1: Molecular weight data and thermal properties of the POSS(Cl)$_8$ and resulting star polymers

Entry	$M_{n,NMR}$[a]	$M_{n,GPC}$[b]	PDI[b]	T_m (°C)[c]	T_{onset} (°C)[d]	T_{max} (°C)[e]	Char Yield (%)[f]
POSS-(Cl)$_8$	n.a.	n.a.	n.a.	n.a.	344.09	387.13	28.97
POSS-(PEG750)$_8$	6550	7300	1.38	43.71	344.31	394.30	12.69
POSS-(PEG1000)$_8$	8100	11900	1.14	46.43	308.53	389.89	8.84
POSS (PEG2000)$_8$	13800	15200	1.22	57.30	322.13	392.83	5.53

[a]$M_{n,NMR}$ was calculated according to the ^{1}H-NMR analysis; [b]$M_{n,GPC}$ and PDI = M_w/M_n were obtained via GPC analysis using linear polystyrenes with narrow molecular weight distributions as calibration standards. THF was used as the mobile phase; [c]T_m donated the melting point of the polymers in the second heating run of the DSC experiments; [d]T_{onset} was the onset decomposition temperature of the polymers in TGA experiments; [e]T_{max} was the temperature corresponding to the maximum rate of weight loss in TGA experiments; [f]The percent of char yield at 700 °C in TGA experiments; n.a. not available

6.1.1. Self-Assembly and Surface Properties of POSS-Star Polymer in Aqueous Solution

The sizes of POSS-based star polymers were investigated by TEM, AFM, DLS and contact angle techniques (Table 6.2). According to DLS results, these star polymers exhibited well-defined assemblies with relatively narrow polydispersities in aqueous solution. A good agreement between length of PEG arms and mean hydrodynamic diameters (D_H) was observed, as the mean D_H values were calculated as 7.6, 12.7 and 34.1 nm for POSS-$(PEG750)_8$, POSS-$(PEG1000)_8$, and POSS-$(PEG2000)_8$, respectively (Figure 6.6). A similar trend was also reported by previously published studies. Overall, for the POSS-based star polymers reported here, longer PEG arms led to higher D_H while the micellar structures in aqueous solution were maintained.

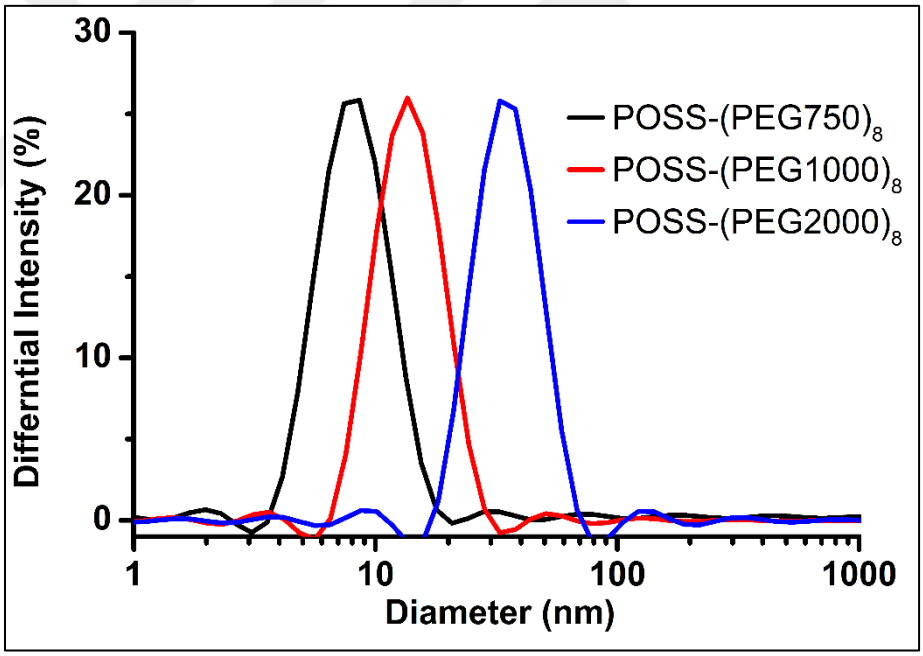

Figure 6.6: Comparison of Hydrodynamic Diameter (D_H) of POSS-$(PEG750)_8$, POSS-$(PEG1000)_8$ and POSS-$(PEG2000)_8$ in Aqueous Solution.

In order to further characterize the surface properties and self-assemble behaviors of star-shaped polymers, the TEM and AFM analyses were performed and their results were displayed in Figure 6.7 and Table 6.2. It was seen that all POSS-based star polymers displayed spherical shape micelles with the average radius of 35 nm for

POSS-$(PEG750)_8$, 38 nm for POSS-$(PEG1000)_8$, 40 nm for POSS-$(PEG2000)_8$. This shape regularity and the differences were attributed to the well-defined three-dimensional framework structure of the POSS and lengths of the hydrophilic arms. The hydrophilic PEG arms were mainly in the corona of the micelles, whereas the hydrophobic POSS cores were located on the center of the micelles. In addition, the AFM results also confirmed the formation of well-defined star-shaped amphiphilic polymers. Noticeably, the root mean square (RMS) roughness of these polymers (10, 23 and 76 nm for POSS-$(PEG750)_8$, POSS-$(PEG1000)_8$, and POSS-$(PEG2000)_8$ were clearly increased by increasing the length of PEG arms. On the other hand, the AFM images clearly presented the porosity differences of resulting star polymers that were also increased by increasing the chain length.

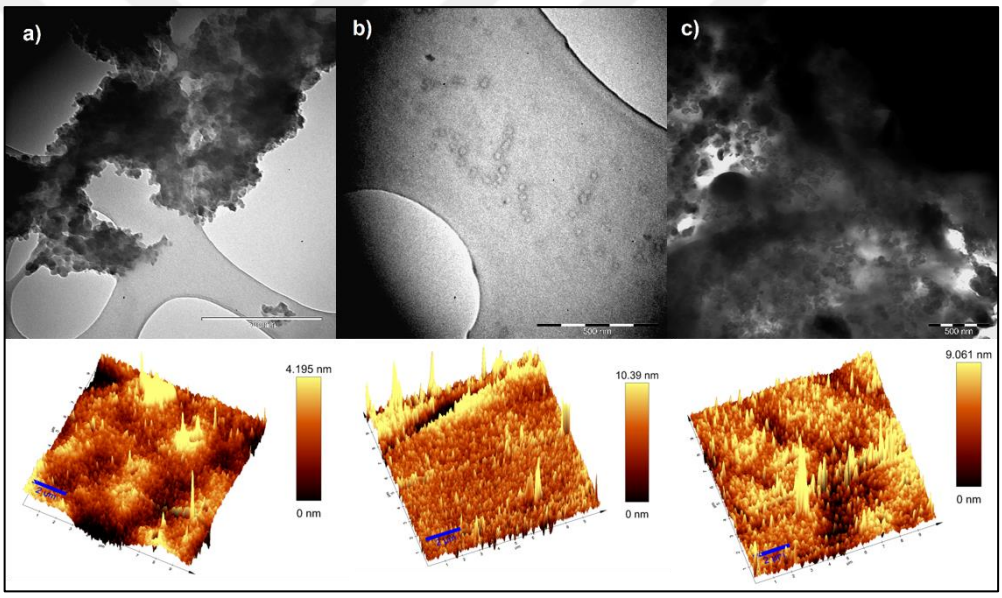

Figure 6.7: AFM and micelle images of a)POSS-$(PEG750)_8$, b)POSS-$(PEG1000)_8$, c)POSS-$(PEG2000)_8$ in aqueous solution.

The wettability properties of POSS-based star polymers were performed by contact angle measurements implying the degree of wetting when polymer sample and water were in interactions. It was evidently seen that all samples displayed very small contact angles (<<90°) corresponding to high wettability properties. Due to its higher hydrophilic PEG content in the amphiphilic star polymer structure, the POSS-$(PEG2000)_8$ had the highest wettability properties (lowest contact angle) that were readily depressed by water. In addition, the longer PEG chains also led to increase in

the RMS value of obtained star-shaped polymers from 10.5 to 76 nm. In other words, the hydrophilicity of PEG chains enabled to include more water molecules in the star-shaped polymers. Thus the longer polymer chains became entangled around the POSS core through hydrophilic interactions and concurrently formed hydrogen bonds with the surrounding water molecules.

Table 6.2: Results of the AFM, contact angle and surface tension measurements

Sample	**DHa (nm)**	**<r>b (nm)**	**RMSc (nm)**	**(qe)d (o)**
POSS-(PEG750)$_8$	**7.6**	**35**	**10.5**	**41**
POSS-(PEG1000)$_8$	**12.7**	**38**	**23**	**32**
POSS-(PEG2000)$_8$	**34.1**	**40**	**76**	**10**

[a]Hydrodynamic diameter was determined by dynamic light scattering;
[b]Average radius was determined by transmission electron microscopy;
[c]Root mean square roughness was determined by atomic force microscopy;
[d]Contact angle was determined by contact angle meter.

6.2. Characterization of Pyrene End-Capped Star-Shaped PCL Polymers with POSS Core

The synthesis of eight-armed and α-pyrene, ω-alkyne functionalized star-shaped PCL polymers carried through via three series of reactions. In the first step, α-pyrene functionalized linear PCL polymer was successfully prepared via the ring opening polymerization (ROP) of ε-caprolactone (ε-CL) with a hydroxyl functionalized pyrene as an initiator. Within these reaction series, arm-first approach was considered to prepare star-shaped PCL polymer with POSS-core.

In the second step of these series, α-pyrene functionalized linear PCL polymer reacted with propargyl chloroformate via estherification reaction, yielding α-pyrene and ω-alkyne functionalized PCL polymer. In the final step, pyrene end-capped PCL polymer with POSS core was synthesized using click chemistry reaction between α-pyrene and ω-alkyne functionalized PCL polymer and azide functionalized POSS under ambient conditions.

The structural characterizations of the star polymers were investigated by FTIR and ^{1}H NMR spectroscopic methods. The absence of azide peak at 2100 cm^{-1} in the

FTIR spectrum of POSS-(Pyr) (Figure 6.8) obviously confirmed the success of the click reaction.

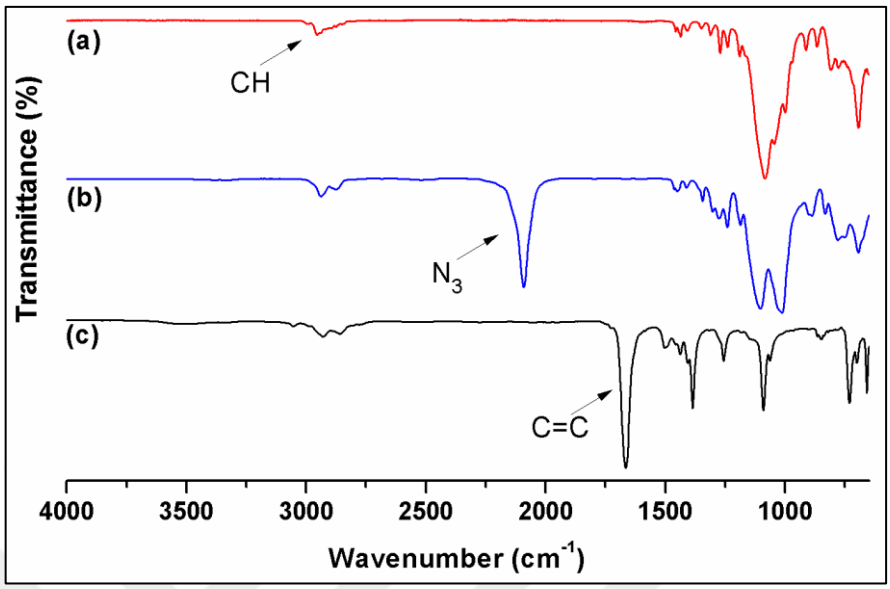

Figure 6.8: FT-IR Transmittance Spectra of a) $POSS(Cl)_8$, b) $POSS(N_3)_8$, c) $POSS(Pyr)_8$.

Regarding the ^1H NMR analysis, the methylene proton signals of the POSS molecule (**1**) were observed at 3.54 (Hc), 1.87 (Hb), and 0.79 (Ha) ppm in Figure 6.8a. Upon azidification, the signals of the methylene protons of POSS quantitatively shifted to the higher magnetic field [Ha = 0.69, Hb = 1.64, Hc =3.26] (Fig. 6.8b), providing a further support for the complete conversion via the azidification reaction. Cu(I)-catalyzed 1,3-dipolar cycloaddition reaction between azide functional groups of $POSS(N_3)_8$ and 1-ethynyl pyrene in deoxygenated DMF by using Cu(I)Br/PMDETA catalyst/ligand system gave pyrene functionalized POSS molecules ($POSS\text{-}(Pyr)_8$) in a very high yield at room temperature. The methylene peak (H_c) depicted at 3.26 ppm in the ^1H NMR spectrum of the precursor compound $POSS(N_3)_8$ drifted to downfield by 1.25 ppm upon Cu(I)-catalyzed 1,3-dipolar cycloaddition reaction. Moreover, the new peaks appeared in the ^1H NMR spectrum of $POSS\text{-}(Pyr)_8$ (Figure 6.8c) as a result of the ‘‘click’’ reaction. The new peaks belonging to aromatic pyrene and triazole methyne protons of 4 are presented at 8.12–7.56 and 8.72, respectively (Figure 6.8c).

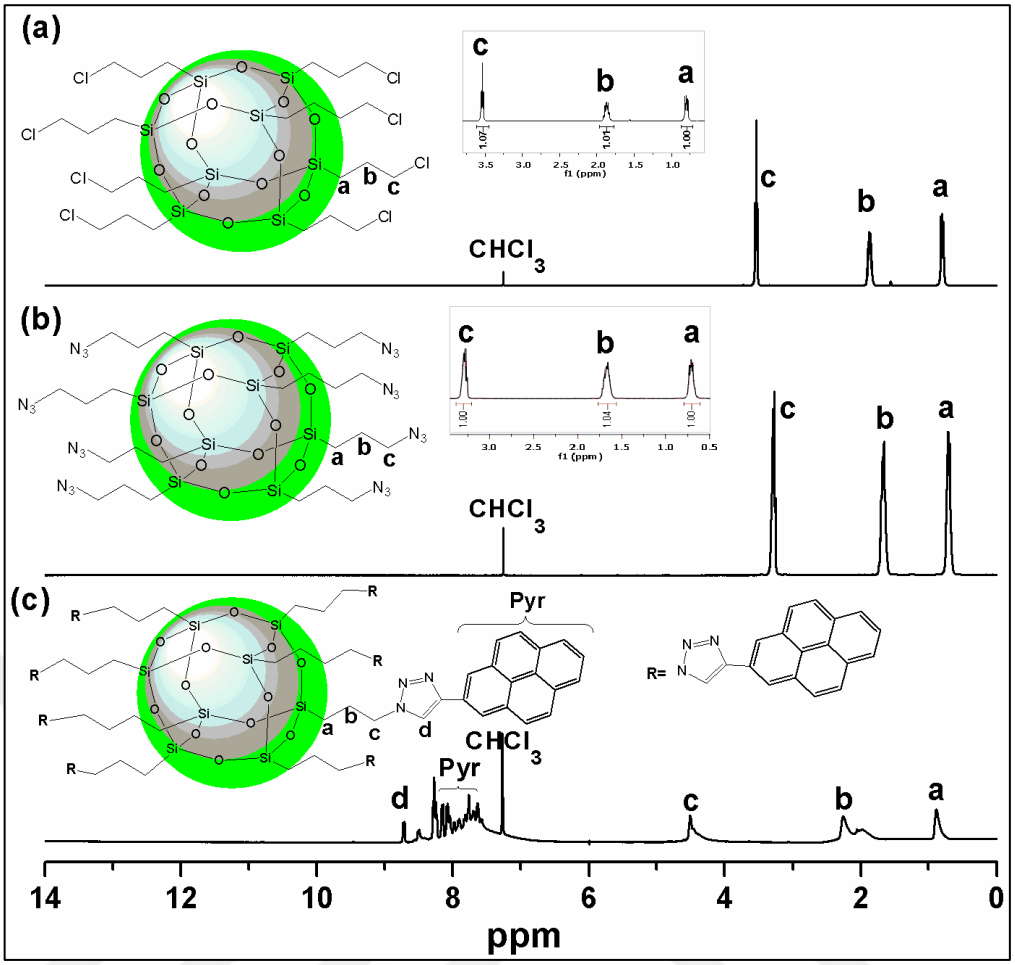

Figure 6.9: ^{1}H NMR spectra of a) POSS(Cl)$_8$, b) POSS(N$_3$)$_8$, c) POSS(Pyr)$_8$.

FT-IR and ^{1}H NMR spectroscopic methods confirm the successful synthesis of PCL star-shaped polymers and POSS derivatives. In addition to that, GPC measurements were also run for PCL polymers to obtain molecular weight distribution and average molecular weight datas. In the FTIR spectra, after the azidification of **P1-20** (Figure 6.10a), the peak at 2110 cm^{-1} indicating the presence of azide functional group in polymer **P2-20** (Figure 6.10b). The disappearing of azide peak at 2110 cm^{-1} in the FTIR spectrum of **P3-20** (Figure 6.10c) clearly confirmed the successful click reaction.

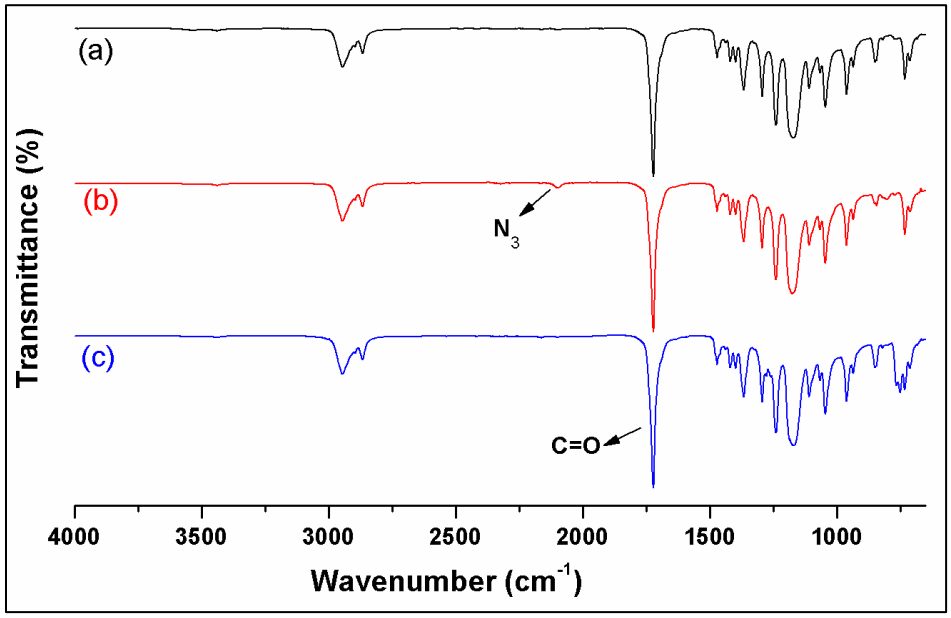

Figure 6.10: FT-IR Transmittance Spectra of a) P1-20, b) P2-20, c) P3-20.

The ^{1}H NMR spectra of P3-10, P3-20 and P3-30 were given as representative examples relating to the synthesis of star polymers. In Figure 6.11a, the peaks at 2.31, 1.62, 1.38 and 4.07 ppm were assigned to the repeating unit protons (Ha, Hb, Hc and Hd) of P1-20. The peak belonging to terminal methylene proton (He at 3.65 ppm, multiple) confirmed that the P1-20 was terminated by hydroxyl end groups thereby determining the molecular weight. By comparing the integral areas from repeating units to the end groups, the molecular weight of P1-20 could be calculated. There was a good relationship between calculated and theoretical molecular weights (Hd/He, measured = 19.00, the theoretical value is 20.00). After esterification reaction, the new peaks belonging to aromatic, methylene (Hf) and methyne (Hg) groups of pyrene and alkyne moieties were clearly detected at 8.28-7.99, 4.71 and 2.40 ppm (Figure 6.11b). Upon the CuAAC click reaction, the resonances of the methylene protons (Hj, Hi and Hh at 0.78, 1.86 and 4.08 ppm) in POSS core were obviously proved the presence of POSS core in the P3-20 star polymers (Figure 6.11c). Moreover, the integral ratio of Ha and Hj protons belonging to repeating PCL and POSS core could be utilized for the determination of the molecular weights as well as the number of arms of star polymers. In order to support these data, the GPC measurements of linear and star polymers were performed. The good correlations between determined Mn,GPC with the calculated Mn,NMR, as well as the narrow polydispersity indexes below than 1.57 confirmed the synthesis of star polymers with well-defined properties (Table 6.3).

According to the ^{1}H-NMR calculations, the number of arms were determined as 7.1, 6.8 and 6.4 for of P3-20, P3-40 and P3-60.

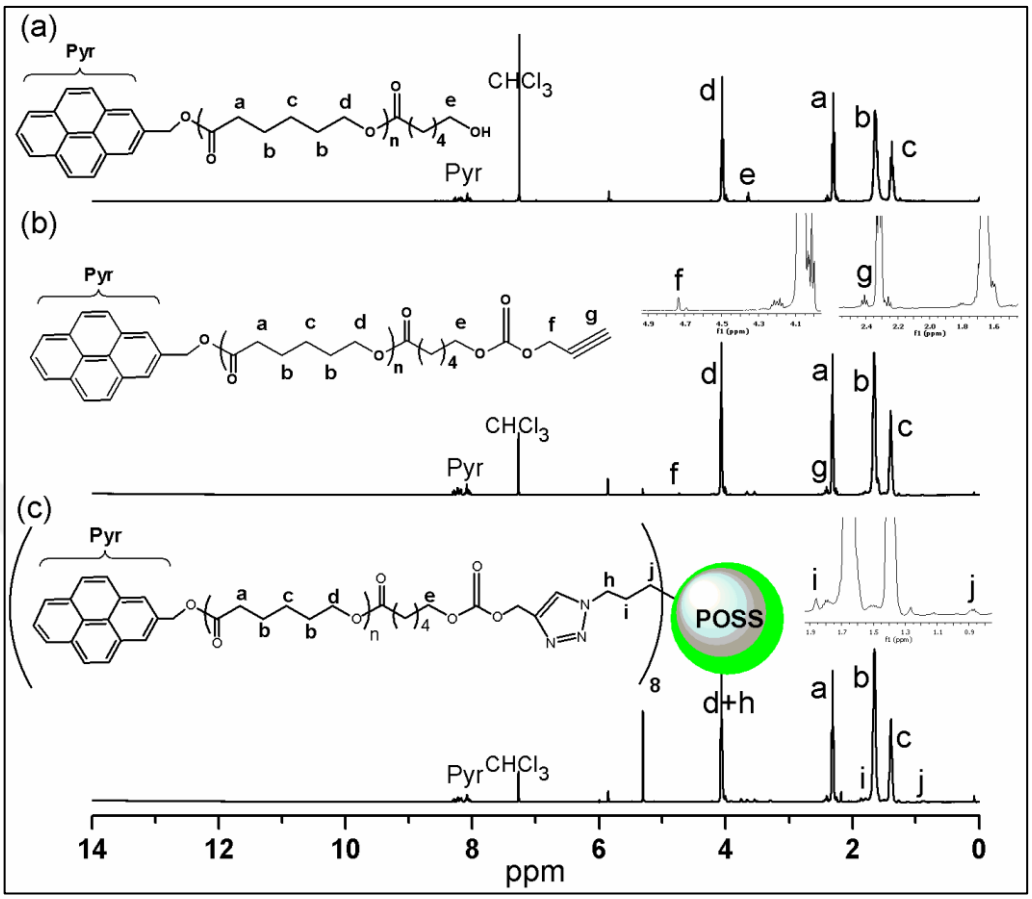

Figure 6.11: ^{1}H NMR Spectra of a) P1-20, b) P2-20, c) P3-20 in $CDCl_3$.

The thermal analyses of the polymers were carried out with both DSC and TGA. The degree of crystallinity (Xc) values of star polymers (P3 series) were lower linear polymers (P1 and P2 series). This could be mainly attributed to the imperfect crystallinity in the branched polymers compared to the linear ones. In our case, the chain movements of PCL units were inhibited and their crystallinity was diminished. Furthermore, the conformations on the star polymer chains arised less intermolecular interaction which caused the decrease of the enthalpy of fusion. Due to the imperfection of the crystallinity of star shaped polymer, there was not perfect single melting curve in DSC thermograms (Figure 6.12). In contrast, the the melting points of star polymers did not exhibit significant changes compared to linear polymers. According to TGA experiments, the char yields, Tonset, and Tmax of the star polymers (P3 series) and ω-alkyne functionalized linear polymers (P2 series) were higher than

that of precursors (P1 series), because of containing POSS core and acetylene increased thermal stability of polymers (Figure 6.13).

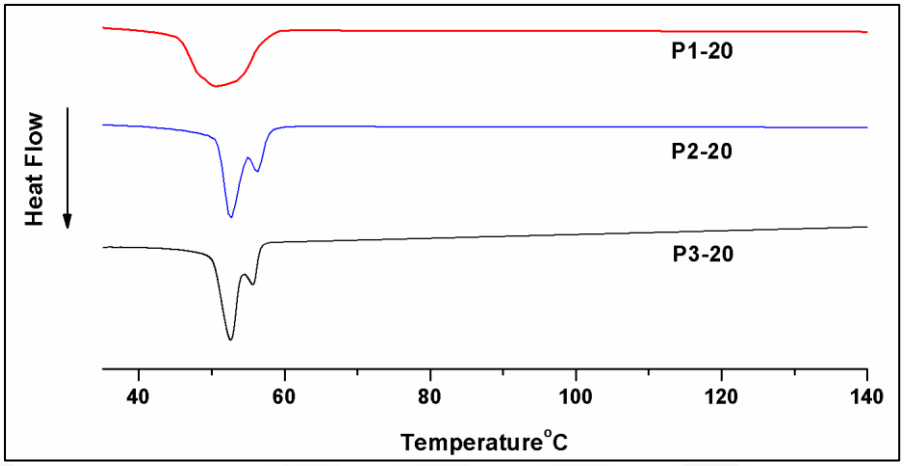

Figure 6.12: The Second Heating DSC Thermograms of P1-20, P2-20, and P3-20 at the rate of 10°C min^{-1}.

Table 6.3. Conditions and characterization data of precursor polymers together with star polymers

Entry	$M_{n,NMR}$ (g/mol) [a]	$M_{n,GPC}$ (g/mol) [b]	M_w/M_n	f_{NMR}	$T_{m,onset}$ (°C)[e]	ΔH_{m1} (J/g)[f]	X_c (%)[g]	T_{onset} (°C)[h]	T_{max} (°C)[i]	*Char Yield* (%)[j]
P1-20	2400	2600	1.31	n.d.[c]	45.30	85.61	61.32	275.26	356.43	1.53
P2-20	2500	2700	1.45	n.d.[c]	50.62	85.21	61.03	311.82	396.32	1.41
P3-20	21700	22400	1.57	7.1[d]	49.38	79.09	56.65	365.47	410.72	11.23
P1-40	4600	4700	1.38	n.d[c]	53.17	85.83	61.48	283.91	354.04	0.04
P2-40	4700	4850	1.41	n.d.[c]	53.41	86.2	61.97	346.26	405.33	0.03
P3-40	42100	43500	1.51	6.8[d]	53.54	82.09	58.80	374.88	407.61	11.80
P1-60	6900	7150	1.40	n.d.[c]	54.31	80.32	57.53	296.74	364.51	0.95
P2-60	7100	7300	1.46	n.d.[c]	54.05	84.95	60.85	349.46	408.63	0.36
P3-60	55700	56300	1.54	6.4[d]	54.07	67.28	48.19	373.27	410.88	6.54

[a]Calculated according to the ^{1}H-NMR analysis; [b]Determined by GPC with linear polystyrene standards; [d]Determined by DSC with a heating rate of 10 °C/min under nitrogen flow (10 mL/min); [c]Not determined; [d]f = functionality, the number of arms in the star polymer, calculated by ^{1}H-NMR analysis: f = 1H (pyrene group)/1H (POSS core); [e]T_m denotes the melting point of the polymers in the second heating run of the DSC experiments; [f]ΔH_{m1} denotes the fusion enthalpy of the polymers in the first heatingrun of the DSC experiments; [g]$X_{c1} = \Delta H_{m1} / \Delta H^0_m$, ΔH^0_m is the enthalpy of fusion for perfectly crystalline PCL. ΔH^0_m = 139.6 J/g[27]; [h]T_{onset} is the onset decomposition temperature; [i]T_{max} is the temperature corresponding to the maximum rate of weight loss in TGA experiments; [j]The percent of char yield at 700 °C in TGA experiments

The introduction of pyrene into star polymers was also proven by UV-vis and fluorescence spectroscopies (Figure 6.14). All star-shaped polymers had a typical pyrene absorption with strong and broadened peaks above 300 nm, which clearly confirmed the ground state pyrene-pyrene association [29]. Notably, the intensity of absorption bands were reduced by increasing the chain lengths of the star polymers. In addition, the strong pyrene-pyrene ground state association in 3 was stronger than the star-polymers due to its higher mobility. The excimer emissions peaks were seen at 400 nm, in which indicated the interaction of excited pyrene molecules. Comparing to the star polymers, their emissions were also decreased by increasing chain lengths.

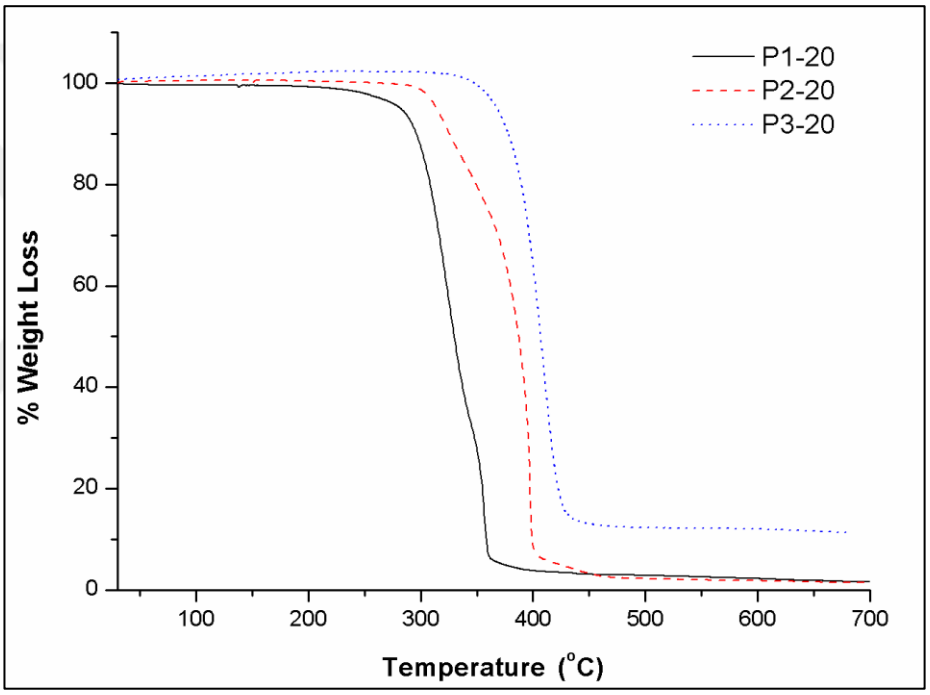

Figure 6.13: TGA Curves of the P1-20, P2-20, and P3-20.

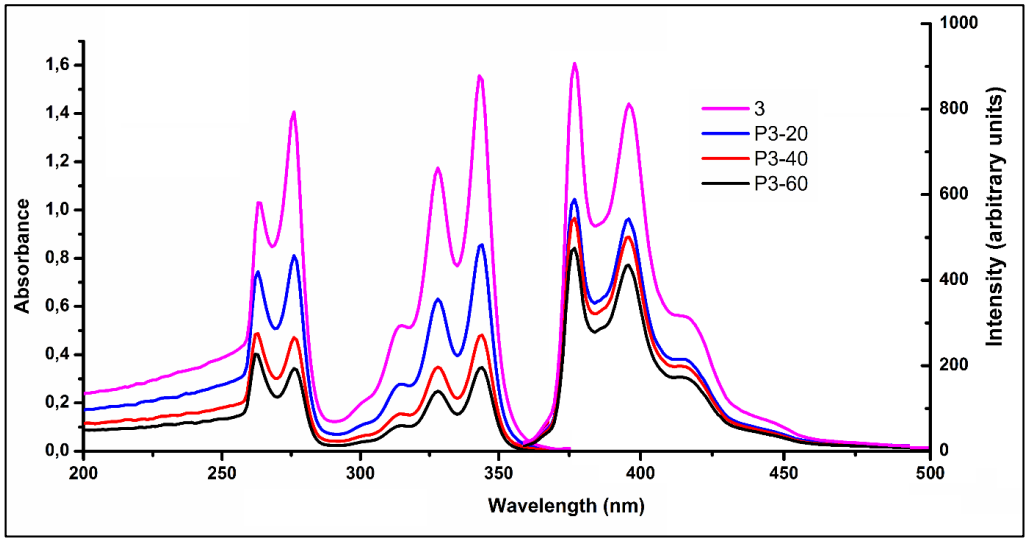

Figure 6.14: Absorption and Emission Spectra of P3-20 (3.658 x 10-5 mol L-1), P3-40 (1.789 x 10-5 mol L-1), P3-60 (1.033 x 10-5 mol L-1) and 3 (2.759 x 10-5 mol L-1) in DMF at room temperature.

6.2.1 Dispersion Stability Performance of CNMs

The dispersion stability performances of star polymers (P3-20, P3-40 and P3-60) were also investigated visually as seen in Figure 6.16. The fullerene molecule was ultrasonicated with 2.00 mg of polymer sample in THF and their images were recorded after 1 week. The best dispersion result was obtained P3-20 with fullerene.

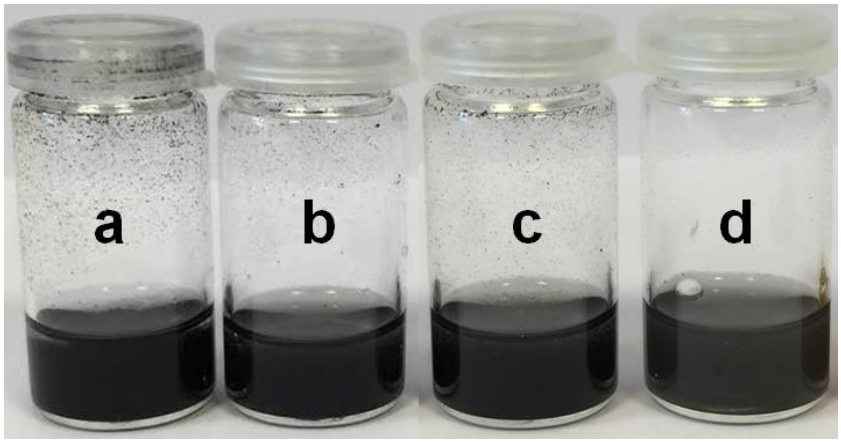

Figure 6.15: Dispersion Stabilities of the Star Polymers a) 3, b) P3-20, c) P3-40 and d) P3-60 with fullerene.

The non-covalent attachments of the pyrene end-capped POSS molecules onto fullerene were firstly investigated by TGA (Figure 6.17). The samples treated with

fullerene were denoted as fullerene-3, fullerene-P3-20, fullerene-P3-40, and fullerene-P3-60, respectively. All samples were heated from room temperature to 700 ºC with a heating rate of 10 ºC min-1. The fullerene-polymer complexes demonstrated greater weight loss (average 23 %) than the fullerene-3 (16.2 %), whereas the pristine fullerene lost only 3.5 % of its initial weight. It was concluded that the 3 sample showed more efficient attachment on the surface of fullerene than polymers by mole. The increase of molecular weights of pyrene functionalized polymers observed slightly reduced thermal stability of the fullerene-polymer complexes.

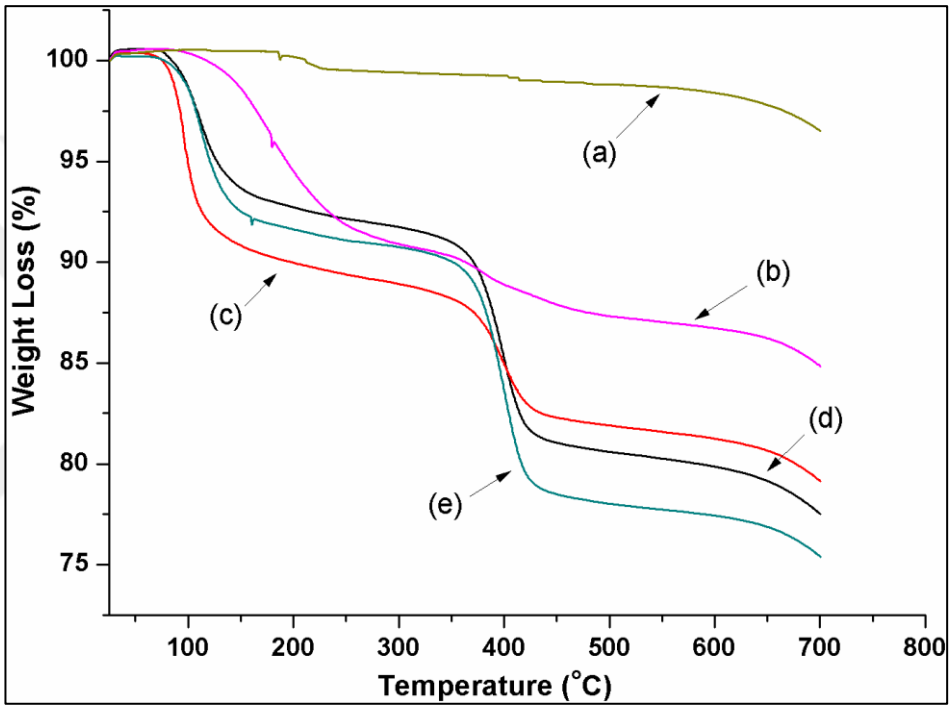

Figure 6.16: TGA thermographs of a) pristine fullerene, b) fullerene-3, c) fullerene-P3-20, d) fullerene-P3-40, and e) fullerene-P3-60 complexes.

The Raman spectroscopy was a key experimental technique to explore non-covalent interactions between polymers and carbon nanomaterial. The Raman spectra of pristine fullerene, fullerene-3 and fullerene-P3-20 dispersions were recorded at room temperature by using laser excitation at 780 nm (Figure 6.18). It was clearly seen that all dispersions gave characteristic signals including Ag(1) “breathing” mode at 500 cm-1 and Ag(2) “pentagonal pinch” mode at 1447cm-1.34 According to the Raman spectroscopy, any noticeable differences between star polymer (fullerene-P3-20) and fullerene/fullerene-3 samples did not detected.

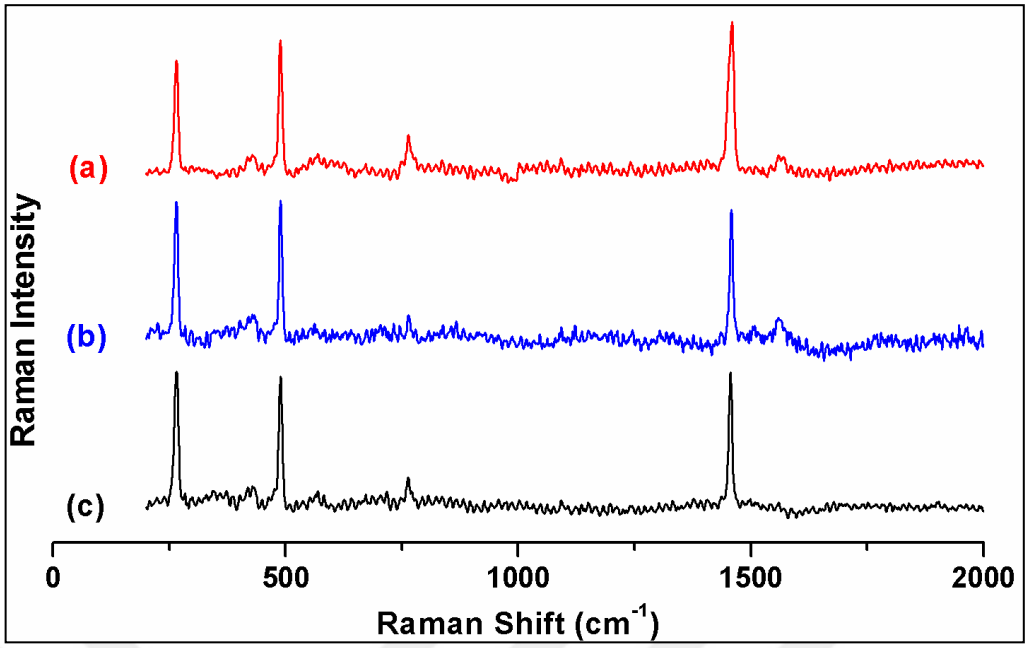

Figure 6.17: Raman spectra of a) pristine fullerene, b) fullerene-3, c) fullerene-P3-20 taken using laser excitation at 780 nm.

6.3. Characterization of POSS-$(PMMA)_8$ and POSS-$(PS)_8$ Star-Shaped Polymers

The click chemistry and controlled polymerization techniques were successfully applied for the synthesis of various star-shaped polymers such as POSS-$(PEG)_8$ [118, 119]. As a part of our continuing interest to develop novel organic-inorganic hybrid polymers, star-shaped polymers with POSS core were simply fabricated by combination of CuAAC click chemistry and ATRP technique starting from clickable POSS$(N_3)_8$, PMMA-alkyne, and PS-alkyne that were independently prepared by well-known procedures [116, 118, 120]. The azidation of the POSS$(Cl)_8$ was followed by FTIR and ^{1}H-NMR analyses. The disappearance of the azide band at 2096 cm^{-1} was a clear proof of the successful functionalization [119].

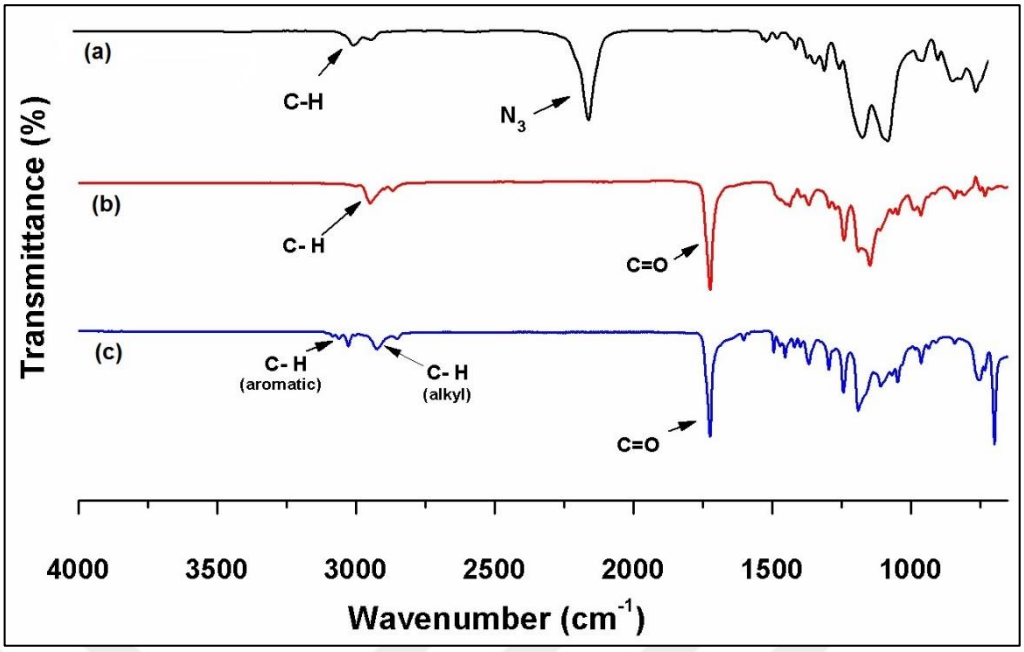

Figure 6.18: FT-IR Transmittance Spectra of a) POSS$(N_3)_8$, b) POSS-$(PMMA)_8$, c) POSS-$(PS)_8$.

After the click reaction between POSS$(N_3)_8$ and methyl metachrylate, the FT-IR spectrum in Figure 6.19b shows the appearance of the two new peaks at 1730 cm^{-1} and 2990 cm^{-1} which are consistent with stretching vibration of C=O and C-H bonds in the PMMA chain [121]. The characteristic absorption bands of PS can be clearly seen in Fig. 6.19c. Aromatic stretching bands at 3026cm^{-1} and stretching vibration of C=O bonds at 1731cm^{-1} obviously indicate the existence of PS in star-shaped polymer [122]. The CuAAC click reaction between azide functional groups of POSS$(N_3)_8$, alkyne-PMMA, and alkyne-PS molecules in deaerated DMF by using Cu(I)Br/PMDETA catalyst/ligand system gave octa-functionalized star-shaped POSS polymers in very high yields at room temperature. As its displayed in Figure 6.20a the methylene peak (H_c) depicted at 3.26 ppm in the ^1H NMR spectrum drifted to downfield by 4.71 ppm after star-shaped polymer formation. Moreover, the new peak belonging to triazole ring (H_d) was appeared at 7.75 ppm in the ^1H NMR spectrum of POSS-$(PS)_8$ and POSS-$(PMMA)_8$. Furthermore, the signals at d 0.80, 2.11 and 3.56 ppm were assigned to the characteristic protons of PMMA [136]. The phenyl protons of PS are observed at 6.2, 7.3 ppm indicating that click reaction occurred successfully [123]. The comparison of the ^1H NMR spectra of POSS-$(PMMA)_8$ and POSS-$(PS)_8$ and POSS-$(N_3)_8$ clearly supported this conclusion.

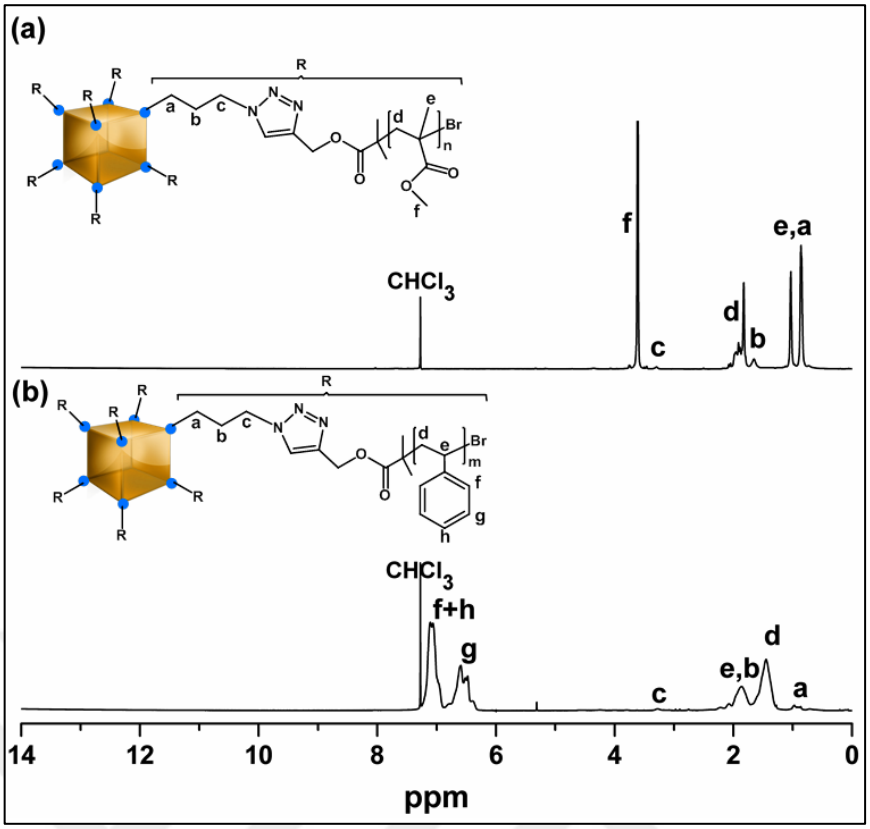

Figure 6.19: ^{1}H NMR Spectra of a) POSS-$(PS)_8$, b) POSS-$(PMMA)_8$.

Table 6.4. Conditions and Characterization Data of Precursor Polymers Together with Star-Shaped Polymers

Entry	$M_{n,\,theo}$[a] (g/mol)	$M_{n,NMR}$[b] (g/mol)	$M_{n,GPC}$[c] (g/mol)	M_w/M_n	f_{NMR}	T_g[d] (°C)	T_{onset}[e] (°C)	T_{max}[e] (°C)	Char Yield[e] (%)
Alkyne-PMMA[f]	4500	4600	4800	1.25	n.d.[g]	113.8	273.9	324.2	3.71
Alkyne-PS[f]	3300	3400	3600	1.32	n.d.[g]	98.9	391.9	432.4	3.8
POSS-$(PMMA)_6$	31400[h]	31200	33700	1.39	6.4[i]	n.d.[g]	297.2	389.5	5.5
POSS-$(PS)_7$	25800[h]	22800	26400	1.36	7.1[i]	n.d.[g]	347.6	414.7	6.9

[a]$M_{n,\,theo} = m_{monomer}$ x $[M]_0/[I]_0$ x conversion;. [b]Calculated according to the ^{1}H-NMR analysis; [c]Determined by GPC with linear polystyrene standards; [d]Determined by DSC with a heating rate of 10 °C/min under nitrogen flow (10 mL/min); [e]Determined by TGA with a heating rate of 10 °C/min from room temperature to 700 °C under a nitrogen atmosphere; [f]Prepared by ATRP of MMA (43% yield) or St (25% yield) in bulk using propargyl 2-bromoisobutyrate as an initiator and the molar ratio of [Monomer]:[PBIB] = 30:1; [g]Not determined; [h]Sum of $M_{n,NMR}$ of the precursor polymers. [i]f = functionality, the number of arms in the star polymer, calculated by ^{1}H-NMR analysis: f = 1H (end group)/1H (initiator).

The number-average molar masses (M_n) of precursors and homoarm star-shaped polymers POSS-$(PMMA)_8$ and POSS-$(PS)_8$ determined by GPC (RI) are rather well in accordance with the theoretical ones and the apparent molecular weight distributions (M_w / M_n) are relatively low below 1.40. Related data are given in Table 6.4.

The calculations gave *f* NMR = 6.4 and 7.1 arms for POSS-$(PMMA)_8$ and POSS-$(PS)_8$ respectively, and confirm the formation of star-shaped topology of the polymers. The $M_{n,NMR}$ values of the homoarm polymers are not significantly different than both theoretical ($M_{n,theo}$) and experimental ($M_{n,GPC}$) molar masses. The f_{NMR} values of the homoarm polymers are also lower than the theoretical values as well. These results may possibly be explained by the slow diffusion of high molecular weight polymer arms, being responsible for incomplete inclusion of the CuAAC click reactions.

Thermal phase transition temperatures (T_g) and thermal stability of the star-shaped polymers were investigated via DSC and TGA experiments, respectively. The related data are summarized in Table 6.4.

Thermal stability of the star-shaped polymers was investigated by TGA under nitrogen atmosphere. The temperatures of T_{onset} and T_{max} values, and the char yield are listed in Table 6.4.

In view of the results given in Table 6.4, the presence of POSS molecule in the structure of POSS-$(PMMA)_8$ significantly increased Tonset and Tmax values as compared with those of alkyne-PMMA. On the other hand, these values decreased for POSS-$(PS)_8$ comparing to alkyne-PS. According to the TGA results, char yields of star-shaped polymers are higher than that of pristine polymers under nitrogen atmosphere. A reasonable explanation for these results is that incorporation of inorganic POSS cores not only increases the inorganic content in the networks but also provides thermal stability of the star polymers. These results further confirm the star-shaped formation containing inorganic POSS core.

6.3.1 Dielectric Properties of the Star Polymers

As shown in Figure 6.22, static dielectric constants measured at 100 Hz increase with POSS-$(PMMA)_8$. The obtained dielectric constant value of 3.6 for linear PMMA films are in very good agreement with the literature [124].

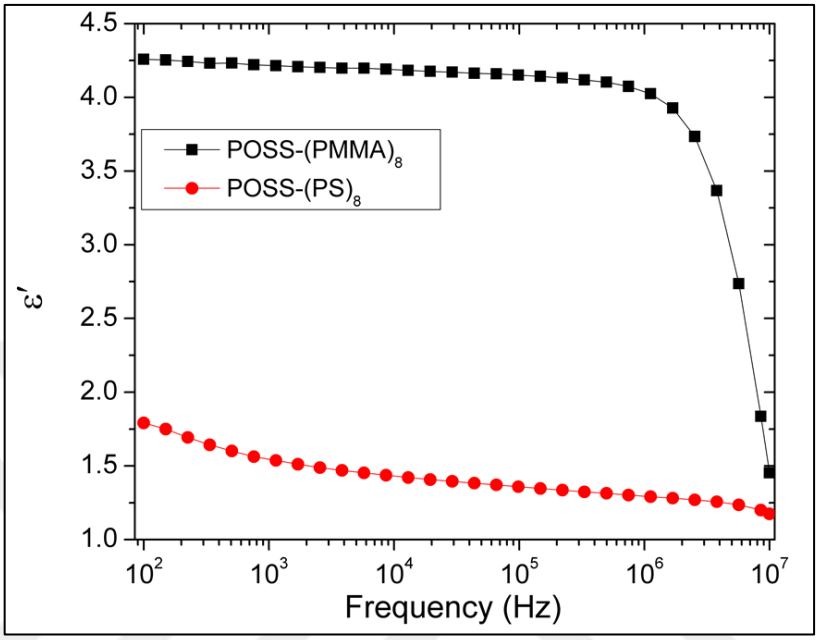

Figure 6.21: Frequency-Dependent Reel Part of Permittivity Plots for POSS-$(PMMA)_8$ and POSS-$(PS)_8$.

The dielectric constant was calculated using the following equation:

$$C = \varepsilon_0 \frac{A}{d} \qquad \text{(Eq. 6.1)}$$

where C is the measured capacitance, $\mathcal{E}_0$ is the dielectric constant in a vacuum, A is the area of the MIM capacitor, and d is the thickness of the insulating layer. The dielectric constant was calculated to be about 4.25 and 1.70 for POSS-$(PMMA)_8$ and POSS-$(PS)_8$ film, respectively. The dielectric constants of the POSS-$(PMMA)_8$ films are comparable to or slightly higher than the reported values for linear PMMA. Capacitance of the POSS-$(PMMA)_8$ and POSS- $(PS)_8$ films were more stable in the 1 kHz–1 MHz range (Figure 6.23). The measured capacitances per unit area at 100 Hz were 0.05 and 0.12 nF/cm^2 for the POSS-$(PMMA)_8$ and POSS-$(PS)_8$ films, respectively.

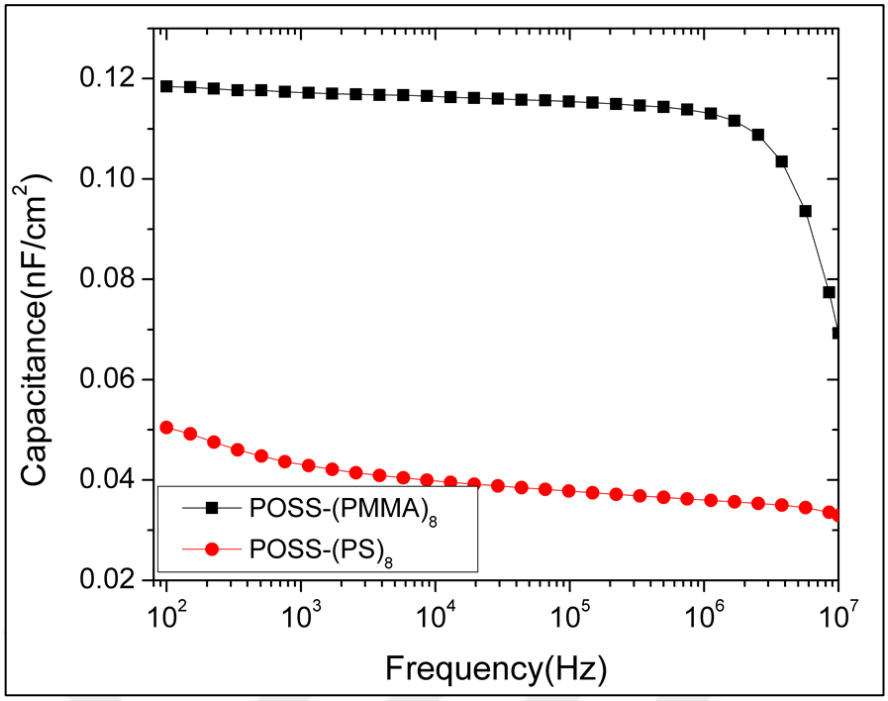

Figure 6.22: Frequency-Dependent Capacitance Plots of POSS-(PMMA)$_8$ and POSS-(PS)$_8$.

The output (Figure 6.24) and transfer characteristics (Figure 6.25) of the devices with POSS-(PMMA)$_8$ and POSS(PS)$_8$ dielectrics were investigated. The field-effect mobility (μ) and threshold voltage (V_{Th}) was obtained at the saturation regime using the following equation:

$$I_{DS} = \frac{WC_i\mu}{2L} x\ (V_{GS} - V_{Th})^2 \qquad \text{(Eq. 6.2)}$$

where W is the channel width, C_i is the gate insulator capacitance per unit area, L is the channel length, μ is the charge carrier mobility, V_{Th} is the threshold voltage, and V_{GS} is the gate voltage

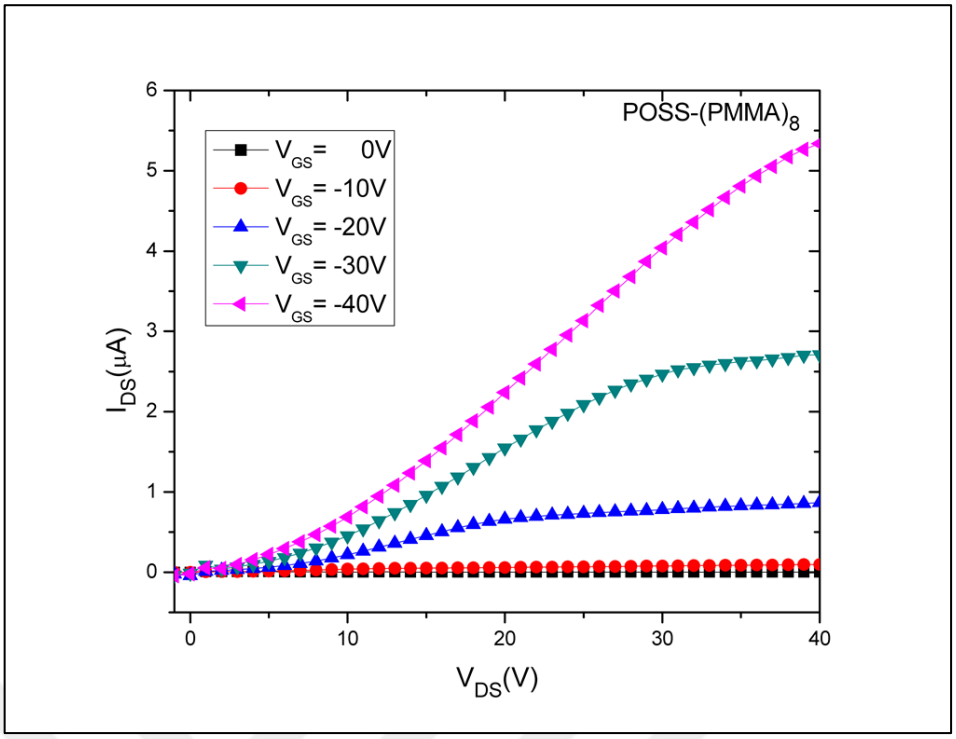

Figure 6.23: Output I-V characteristics of OFETs having semiconducting layer of CuPc and dielectric films of POSS-$(PMMA)_8$.

The μ, V_{Th} and I_{on}/I_{off} values of the OTFT fabricated using POSS-$(PMMA)_8$ were about $3.9x10^{-4}$ cm^2/Vs, -7 V, and 10^3, respectively. At a given negative gate voltage (V_{GS}), the device which is fabricated using POSS-$(PMMA)_8$ linearly increasing drain current (I_{DS}) with positive V_{DS} (Figure 6.23).

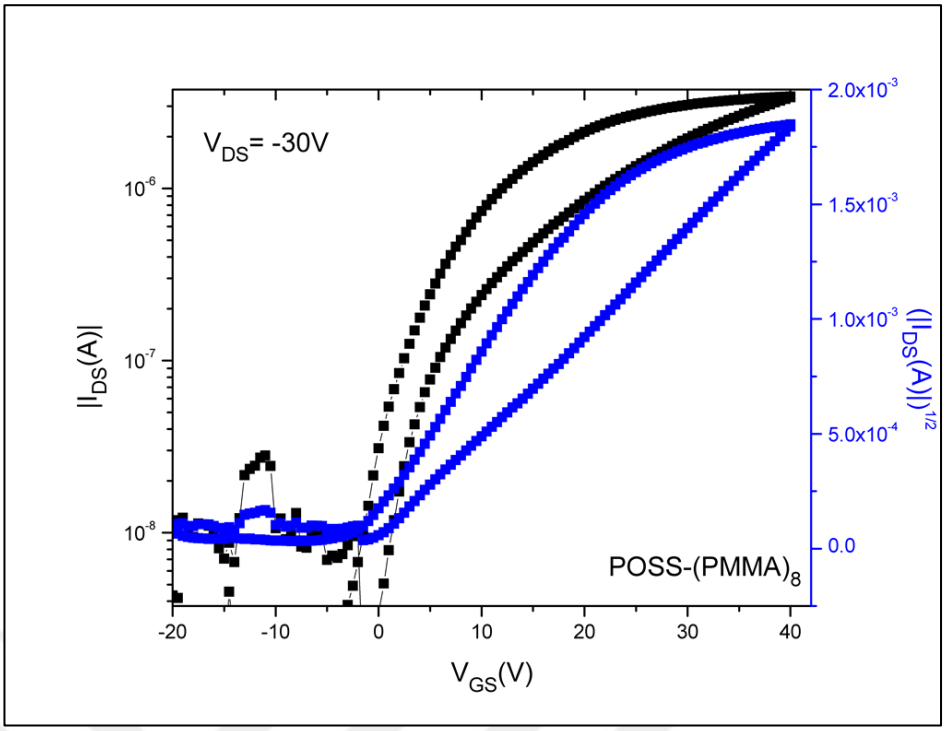

Figure 6.24: Transfer I-V characteristics of OFETs having semiconducting layer of P3HT:PCBM and dielectric films of POSS-$(PMMA)_8$.

Figure 6.25 shows AFM images of POSS-$(PMMA)_8$ and POSS-$(PS)_8$ dielectric films. Atomic force microscopy (AFM) was used to investigate the surface morphology of the POSS-$(PMMA)_8$ and POSS-$(PS)_8$ insulator layers. The images of POSS-$(PMMA)_8$ and POSS-$(PS)_8$ dielectric films show a homogeneous dispersion.

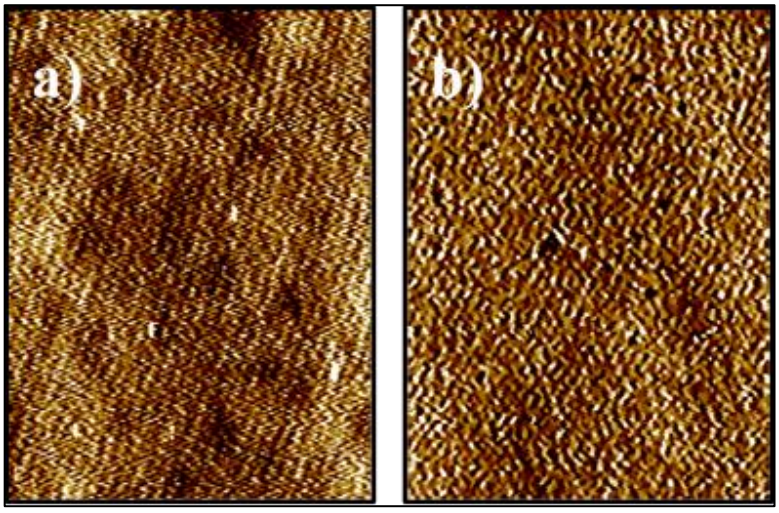

Figure 6.25: AFM images taken from the surface of a) POSS-$(PS)_8$, b) POSS-$(PMMA)_8$ based dielectric films.

7. CONCLUSION

In this thesis, POSS based star polymers with different polymeric arms were synthesized and employed in three distinct applications. Polymers were chosen on purpose to be used in appropriate application depending on their characteristics. POSS was our important building block because of its promising features and easily modifiable structure.

Our first focus application was surface active polymers and star-shaped polymeric surfactants were successfully synthesized via CuAAC click reaction using clickable POSS(N_3)$_8$ and mPEG-alkyne having three different chain lengths. The chemical structures and molecular characteristics of amphiphilic star-shaped polymers were clearly confirmed by FT-IR, ^{1}H-NMR and GPC analysis. All resulting star-shaped amphiphilic polymers displayed real shift to high molar mass and no homopolymer formation after CuAAC click reactions. Polymeric surfactants with hydrophobic head and hydrophilic tails could self-assemble into micelles in water and these micelles were observed by AFM, TEM and DLS studies and it was found that the size of the micelles was changed with the length of PEG arms. The longer PEG chains not only led to increase in the hydrodynamic diameter and RMS values, but also reduced the contact angle values of obtained star-shaped polymers. Moreover, the melting points and root mean square roughness values of them were slightly increased by increasing chain length of PEG arms, whereas their thermal stabilities were noticeably decreased. Secondly we focused on carbon nanomaterial dispersion via non-covalent interactions with polymer adsorbtion. For that purpose, we synthesized pyrene end-labelled star poly(ε-caprolactone) (PCL) with POSS (polyhedral oligomeric silsesquioxane) core prepared by combination of copper(I)-catalyzed azide alkyne cycloaddition (CuAAC) click chemistry and ring-opening polymerization techniques. ε-caprolactone was polymerized by using 1-pyrene methanol and stannous octoate as initator to obtain α-pyrene-ω-hydroxyl telechelic PCL. Then, its hydroxyl group was converted to acetylene functionality by esterification reaction with propargyl chloroformate. Finally, the CuAAC click reaction of α-pyrene-ω-acetylene telechelic PCL with POSS-(N_3)$_8$ leads to corresponding pyrene end-labeled star-shaped PCL. Furthermore, non-covalent interactions of obtained polymers with multi-walled and single-walled carbon nanotubes, fullerene and graphene were investigated in fluid media.

As we targetted on POSS star polymers and their different applications, we synthesized POSS-$(PMMA)_8$ and POSS-$(PS)_8$ by click reaction between inorganic-orgnic hybrid core POSS-$(N_3)_8$ and alkyne functionalized PMMA and PS arms. Their chemical structures and molecular characteristics are clearly confirmed by FT-IR, 1H-NMR and GPC analyses. These star shaped polymers were prepared as the insulators for organic thin film transistors (OTFTs) using CuPc as an active p-type organic semiconductor. The POSS cored star-shaped polymer layers used in transistor assemblies and they have demonstrated promising transistor characteristics.

REFERENCES

[1] Kolb H. C., Finn M., Sharpless K. B., (2001), "Click chemistry: diverse chemical function from a few good reactions", Angewandte Chemie International Edition, 40 (11), 2004-2021.

[2] Meldal M., (2008), "Polymer “clicking” by CuAAC reactions", Macromolecular Rapid Communications, 29 (1213), 1016-1051.

[3] Lutz J. F., (2007), "1, 3-Dipolar cycloadditions of azides and alkynes: a universal ligation tool in polymer and materials science", Angewandte Chemie International Edition, 46 (7), 1018-1025.

[4] Demirci G., Tasdelen M. A., (2015), "Synthesis and characterization of graft copolymers by photoinduced CuAAC click chemistry", European Polymer Journal, 66 282-289.

[5] Tasdelen M. A., (2011), "Poly (epsilon-caprolactone)/clay nanocomposites via “click” chemistry", European Polymer Journal, 47 (5), 937-941.

[6] Tasdelen M. A., Taskin O. S., Celik C., (2016), "Orthogonal Synthesis of Block Copolymer via Photoinduced CuAAC and Ketene Chemistries", Macromolecular rapid communications, 37 (6), 521-526.

[7] Dizman C., Altinkok C., Tasdelen M. A., (2017), "Synthesis of self-curable polysulfone containing pendant benzoxazine units via CuAAC click chemistry", Designed Monomers and Polymers, 20 (1), 293-299.

[8] Zana R., (2002), "Dimeric and oligomeric surfactants. Behavior at interfaces and in aqueous solution: a review", Advances in colloid and interface science, 97 (1), 205-253.

[9] Raffa P., Broekhuis A. A., Picchioni F., (2016), "Polymeric surfactants for enhanced oil recovery: A review", Journal of Petroleum Science and Engineering, 145 723-733.

[10] Raffa P., Wever D. A. Z., Picchioni F., Broekhuis A. A., (2015), "Polymeric surfactants: synthesis, properties, and links to applications", Chemical reviews, 115 (16), 8504-8563.

[11] Liu S., Armes S. P., (2001), "Recent advances in the synthesis of polymeric surfactants", Current opinion in colloid & interface science, 6 (3), 249-256.

[12] Wang Z., Li Y., Dong X.-H., Yu X., Guo K., Su H., Yue K., Wesdemiotis C., Cheng S. Z., Zhang W.-B., (2013), "Giant gemini surfactants based on polystyrene–hydrophilic polyhedral oligomeric silsesquioxane shape amphiphiles: sequential “click” chemistry and solution self-assembly", Chemical Science, 4 (3), 1345-1352.

[13] Holmberg K., (2001), "Natural surfactants", Current Opinion in Colloid & Interface Science, 6 (2), 148-159.

[14] Kosaric N., (1993), CRC Press: New York, 48, 504.

[15] Elsabee M. Z., Morsi R. E., Al-Sabagh A., (2009), "Surface active properties of chitosan and its derivatives", Colloids and Surfaces B: Biointerfaces, 74 (1), 1-16.

[16] Popot J.-L., Berry E., Charvolin D., Creuzenet C., Ebel C., Engelman D., Flötenmeyer M., Giusti F., Gohon Y., Hervé P., (2003), "Amphipols: polymeric surfactants for membrane biology research", Cellular and molecular life sciences, 60 (8), 1559-1574.

[17] York A. W., Kirkland S. E., McCormick C. L., (2008), "Advances in the synthesis of amphiphilic block copolymers via RAFT polymerization: stimuli-responsive drug and gene delivery", Advanced drug delivery reviews, 60 (9), 1018-1036.

[18] Blanazs A., Armes S. P., Ryan A. J., (2009), "Self- assembled block copolymer aggregates: from micelles to vesicles and their biological applications", Macromolecular rapid communications, 30 (4- 5), 267-277.

[19] Kwon G. S., Kataoka K., (2012), "Block copolymer micelles as long-circulating drug vehicles", Advanced drug delivery reviews, 64, 237-245.

[20] Jiang H., Taranekar P., Reynolds J. R., Schanze K. S., (2009), "Conjugated polyelectrolytes: synthesis, photophysics, and applications", Angewandte Chemie International Edition, 48 (24), 4300-4316.

[21] Zhou J., Wang L., Ma J., (2009), "Recent research progress in the synthesis and properties of amphiphilic block co-polymers and their applications in emulsion polymerization", Designed Monomers and Polymers, 12 (1), 19-41.

[22] Zhou Y., Yan D., (2009), "Supramolecular self-assembly of amphiphilic hyperbranched polymers at all scales and dimensions: progress, characteristics and perspectives", Chemical Communications, (10), 1172-1188.

[23] Durand A., Marie E., (2009), "Macromolecular surfactants for miniemulsion polymerization", Advances in colloid and interface science, 150 (2), 90-105.

[24] Harada A., Kataoka K., (2006), "Supramolecular assemblies of block copolymers in aqueous media as nanocontainers relevant to biological applications", Progress in polymer science, 31 (11), 949-982.

[25] Laschewsky A. in Molecular concepts, self-organisation and properties of polysoaps, Vol. Springer, 1995, 1-86.

[26] Kwon G. S., Kataoka K., (1995), "Block copolymer micelles as long-circulating drug vehicles", Advanced drug delivery reviews, 16 (2), 295-309.

[27] Alexandridis P., (1996), "Amphiphilic copolymers and their applications", Current Opinion in Colloid & Interface Science, 1 (4), 490-501.

[28] Winnik M. A., Yekta A., (1997), "Associative polymers in aqueous solution", Current opinion in colloid & interface science, 2 (4), 424-436.

[29] Torchilin V. P., (2001), "Structure and design of polymeric surfactant-based drug delivery systems", Journal of controlled release, 73 (2), 137-172.

[30] Garnier S., Laschewsky A., Storsberg J., (2006), "Polymeric surfactants: Novel agents with exceptional properties", Tenside Surfactants Detergents, 43 (2), 88-102.

[31] Charalambopoulou A., Bokias G., Staikos G., (2002), "Template copolymerization of N-isopropylacrylamide with a cationic monomer: influence of the template on the solution properties of the product", Polymer, 43 (9), 2637-2643.

[32] Blencowe A., Tan J. F., Goh T. K., Qiao G. G., (2009), "Core cross-linked star polymers via controlled radical polymerisation", Polymer, 50 (1), 5-32.

[33] Strauss U. P., Gershfeld N. L., (1954), "The transition from typical polyelectrolyte to polysoap. I. Viscosity and solubilization studies on copolymers of 4-vinyl-N-ethylpyridinium bromide and 4-vinyl-Nn-dodecylpyridinium bromide", The Journal of Physical Chemistry, 58 (9), 747-753.

[34] Strauss U. P., Gershfeld N. L., Crook E. H., (1956), "The Transition from Typical Polyelectrolyte to Polysoap. II. Viscosity Studies of Poly-4-vinylpyridine Derivatives in Aqueous KBr Solutions", The Journal of Physical Chemistry, 60 (5), 577-584.

[35] Riess G., (2003), "Micellization of block copolymers", Progress in Polymer Science, 28 (7), 1107-1170.

[36] Riess G., Labbe C., (2004), "Block copolymers in emulsion and dispersion polymerization", Macromolecular rapid communications, 25 (2), 401-435.

[37] Hadjichristidis N., Pitsikalis M., Iatrou H., (2005), "Synthesis of block copolymers", Block Copolymers I, 1-124.

[38] Gohy J.-F. in Block copolymer micelles, Vol. Springer, 2005, 65-136.

[39] Liu S., Billingham N. C., Armes S. P., (2001), "A schizophrenic water-soluble diblock copolymer", Angewandte Chemie, 113 (12), 2390-2393.

[40] Weaver J., Armes S., Bütün V., (2002), "Synthesis and aqueous solution properties of a well-defined thermo-responsive schizophrenic diblock copolymer", Chemical Communications, (18), 2122-2123.

[41] Liu S., Armes S. P., (2002), "Polymeric surfactants for the new millennium: A pH- responsive, zwitterionic, schizophrenic diblock copolymer", Angewandte Chemie International Edition, 41 (8), 1413-1416.

[42] Matyjaszewski K., (2012), "Atom transfer radical polymerization (ATRP): current status and future perspectives", Macromolecules, 45 (10), 4015-4039.

[43] Moad G., Rizzardo E., Thang S. H., (2006), "Living radical polymerization by the RAFT process—a first update", Australian Journal of Chemistry, 59 (10), 669-692.

[44] Hawker C. J., Bosman A. W., Harth E., (2001), "New polymer synthesis by nitroxide mediated living radical polymerizations", Chemical reviews, 101 (12), 3661-3688.

[45] Grubbs R. B., (2011), "Nitroxide-mediated radical polymerization: limitations and versatility", Polymer Reviews, 51 (2), 104-137.

[46] Dai S., Ravi P., Tam K. C., Mao B., Gan L., (2003), "Novel pH-responsive amphiphilic diblock copolymers with reversible micellization properties", Langmuir, 19 (12), 5175-5177.

[47] Chong Y., Le T. P., Moad G., Rizzardo E., Thang S. H., (1999), "A more versatile route to block copolymers and other polymers of complex architecture by living radical polymerization: the RAFT process", Macromolecules, 32 (6), 2071-2074.

[48] Chaduc I., Lansalot M., D'Agosto F., Charleux B., (2012), "RAFT polymerization of methacrylic acid in water", Macromolecules, 45 (3), 1241-1247.

[49] áO'Dell R., áP Armes S., (1999), "First example of the atom transfer radical polymerisation of an acidic monomer: direct synthesis of methacrylic acid copolymers in aqueous media", Chemical Communications, (14), 1285-1286.

[50] Jain P., Dai J., Baker G. L., Bruening M. L., (2008), "Rapid synthesis of functional polymer brushes by surface-initiated atom transfer radical polymerization of an acidic monomer", Macromolecules, 41 (22), 8413-8417.

[51] Davis K. A., Matyjaszewski K., (2001), "ABC triblock copolymers prepared using atom transfer radical polymerization techniques", Macromolecules, 34 (7), 2101-2107.

[52] Beers K. L., Caynor S. G., Matyjaszewski K., Sheiko S. S., Prokhorova S. A., Möller M., (1999), "Poly (at-butyl acrylate) brush macromolecules by ATRP: Determination of contour length from fractionation and AFM studies", 40 (2), 446-447.

[53] Davis K. A., Matyjaszewski K., (2000), "Atom transfer radical polymerization of tert-butyl acrylate and preparation of block copolymers", Macromolecules, 33 (11), 4039-4047.

[54] McCormick C. L., Sumerlin B. S., Lokitz B. S., Stempka J. E., (2008), "RAFT-synthesized diblock and triblock copolymers: thermally-induced supramolecular assembly in aqueous media", Soft Matter, 4 (9), 1760-1773.

[55] Baek K. Y., (2008), "Synthesis and characterization of sulfonated block copolymers by atom transfer radical polymerization", Journal of Polymer Science Part A: Polymer Chemistry, 46 (18), 5991-5998.

[56] Lienkamp K., Ruthard C., Lieser G., Berger R., Groehn F., Wegner G., (2006), "Polymerization of styrene sulfonate ethyl ester and styrene sulfonate dodecyl ester by ATRP", Macromolecular Chemistry and Physics, 207 (22), 2050-2065.

[57] Oikonomou E. K., Pefkianakis E. K., Bokias G., Kallitsis J. K., (2008), "Direct synthesis of amphiphilic block copolymers, consisting of poly (methyl methacrylate) and poly (sodium styrene sulfonate) blocks through ATRP", European Polymer Journal, 44 (6), 1857-1864.

[58] Mitsukami Y., Donovan M. S., Lowe A. B., McCormick C. L., (2001), " Direct synthesis of hydrophilic styrenic-based homopolymers and block copolymers in aqueous solution via RAFT", Macromolecules, 34 (7), 2248-2256.

[59] Riess G., (1999), "Block copolymers as polymeric surfactants in latex and microlatex technology", Colloids and Surfaces A: Physicochemical and Engineering Aspects, 153 (1), 99-110.

[60] Hao Y., Zhang M., Xu J., Liu C., Ni P., (2010), "Synthesis and Micellization of Triblock Copolymers Containing MePEG-b-PDMAEMA and Fluoropolymer: ", Journal of Macromolecular Science, Part A, 47 (9), 941-951.

[61] Gref R., Babak V., Bouillot P., Lukina I., Bodorev M., Dellacherie E., (1998), "Interfacial and emulsion stabilising properties of amphiphilic water-soluble poly (ethylene glycol)–poly (lactic acid) copolymers ", Colloids and Surfaces A: Physicochemical and Engineering Aspects, 143 (2), 413-420.

[62] Petrov P. D., Drechsler M., Müller A. H., (2009), "Self-assembly of asymmetric poly (ethylene oxide)-block-poly (n-butyl acrylate) diblock copolymers in aqueous media to unexpected morphologies", The Journal of Physical Chemistry B, 113 (13), 4218-4225.

[63] Piogé S., Fontaine L., Gaillard C. d., Nicol E., Pascual S., (2009), "Self-assembling properties of well-defined poly (ethylene oxide)-b-poly (ethyl acrylate) diblock copolymers", Macromolecules, 42 (12), 4262-4272.

[64] Lim K. T., Lee M. Y., Moon M. J., Lee G. D., Hong S.-S., Dickson J. L., Johnston K. P., (2002), "Synthesis and properties of semifluorinated block copolymers containing poly (ethylene oxide) and poly (fluorooctyl methacrylates) via atom transfer radical polymerisation", Polymer, 43 (25), 7043-7049.

[65] Baines F., Billingham N., Armes S., (1996), "Synthesis and solution properties of water-soluble hydrophilic− hydrophobic block copolymers", Macromolecules, 29 (10), 3416-3420.

[66] Baines F. L., Armes S. P., Billingham N. C., Tuzar Z., (1996), "Micellization of poly (2-(dimethylamino) ethyl methacrylate-block-methyl methacrylate) copolymers in aqueous solution", Macromolecules, 29 (25), 8151-8159.

[67] Beadle P., Rowan L., Mykytiuk J., Billingham N. C., Armes S., (1993), "Synthesis and characterization of sterically stabilized colloidal dispersions of polypyrrole using novel tailor-made water-soluble block copolymers of narrow molecular weight distribution", Polymer, 34 (7), 1561-1563.

[68] Hadjiyannakou S. C., Vamvakaki M., Patrickios C. S., (2004), "Synthesis, characterization and evaluation of amphiphilic diblock copolymer emulsifiers based on methoxy hexa (ethylene glycol) methacrylate and benzyl methacrylate", Polymer, 45 (11), 3681-3692.

[69] Garnier S., Laschewsky A., (2005), "Synthesis of new amphiphilic diblock copolymers and their self-assembly in aqueous solution", Macromolecules, 38 (18), 7580-7592.

[70] Hadjichristidis N., Iatrou H., Pitsikalis M., Pispas S., Avgeropoulos A., (2005), "Linear and non-linear triblock terpolymers. Synthesis, self-assembly in selective solvents and in bulk", Progress in Polymer Science, 30 (7), 725-782.

[71] Iatridi Z., Tsitsilianis C., (2011), "Water-soluble stimuli responsive star-shaped segmented macromolecules", Polymers, 3 (4), 1911-1933.

[72] Khanna K., Varshney S., Kakkar A., (2010), "Miktoarm star polymers: advances in synthesis, self-assembly, and applications", Polymer Chemistry, 1 (8), 1171-1185.

[73] Peleshanko S., Jeong J., Shevchenko V., Genson K., Pikus Y., Ornatska M., Petrash S., Tsukruk V., (2004), "Synthesis and properties of asymmetric heteroarm PEO n-b-PS m star polymers with end functionalities", Macromolecules, 37 (20), 7497-7506.

[74] Peleshanko S., Jeong J., Gunawidjaja R., Tsukruk V., (2004), "Amphiphilic Heteroarm PEO-b-PS m Star Polymers at the Air− Water Interface: Aggregation and Surface Morphology", Macromolecules, 37 (17), 6511-6522.

[75] Francis R., Taton D., Logan J. L., Masse P., Gnanou Y., Duran R. S., (2003), "Synthesis and surface properties of amphiphilic star-shaped and dendrimer-like copolymers based on polystyrene core and poly (ethylene oxide) corona", Macromolecules, 36 (22), 8253-8259.

[76] Liu Z., Sun X., Nakayama-Ratchford N., Dai H., (2007), "Supramolecular chemistry on water-soluble carbon nanotubes for drug loading and delivery", ACS nano, 1 (1), 50-56.

[77] Hu C. Y., Li F. Y., Zhang R. B., Liao X. N., Hua L., (2007), "Effects of Neodymium on the Properties of Ni- B/CNTs Amorphous Alloy Catalyst", Journal of the Chinese Chemical Society, 54 (2), 559-562.

[78] Lu K., Lago R., Chen Y., Green M., Harris P., Tsang S., (1996), "Mechanical damage of carbon nanotubes by ultrasound", Carbon, 34 (6), 814-816.

[79] Dyke C. A., Tour J. M., (2004), "Overcoming the insolubility of carbon nanotubes through high degrees of sidewall functionalization", Chemistry-A European Journal, 10 (4), 812-817.

[80] Martinez-Rubi Y., Guan J., Lin S., Scriver C., Sturgeon R. E., Simard B., (2007), "Rapid and controllable covalent functionalization of single-walled carbon nanotubes at room temperature", Chemical Communications, (48), 5146-5148.

[81] Kocharova N., Ääritalo T., Leiro J., Kankare J., Lukkari J., (2007), "Aqueous dispersion, surface thiolation, and direct self-assembly of carbon nanotubes on gold", Langmuir, 23 (6), 3363-3371.

[82] Strano M. S., Moore V. C., Miller M. K., Allen M. J., Haroz E. H., Kittrell C., Hauge R. H., Smalley R., (2003), "The role of surfactant adsorption during ultrasonication in the dispersion of single-walled carbon nanotubes", Journal of Nanoscience and Nanotechnology, 3 (1-1), 81-86.

[83] Szleifer I., Yerushalmi-Rozen R., (2005), "Polymers and carbon nanotubes—dimensionality, interactions and nanotechnology", Polymer, 46 (19), 7803-7818.

[84] Priya B., Byrne H., (2008), "Investigation of sodium dodecyl benzene sulfonate assisted dispersion and debundling of single-wall carbon nanotubes", The Journal of Physical Chemistry C, 112 (2), 332-337.

[85] White B., Banerjee S., O'Brien S., Turro N. J., Herman I. P., (2007), "Zeta-potential measurements of surfactant-wrapped individual single-walled carbon nanotubes", The Journal of Physical Chemistry C, 111 (37), 13684-13690.

[86] Garnier S., Laschewsky A., (2005), "Synthesis of new amphiphilic diblock copolymers and their self-assembly in aqueous solution", Macromolecules, 38 (18), 7580-7592.

[87] O'connell M. J., Bachilo S. M., Huffman C. B., Moore V. C., Strano M. S., Haroz E. H., Rialon K. L., Boul P. J., Noon W. H., Kittrell C., (2002), "Band gap fluorescence from individual single-walled carbon nanotubes", Science, 297 (5581), 593-596.

[88] Jiang L., Gao L., Sun J., (2003), "Production of aqueous colloidal dispersions of carbon nanotubes", Journal of colloid and interface science, 260 (1), 89-94.

[89] Li L.-J., Nicholas R., Chen C.-Y., Darton R., Baker S., (2005), "Comparative study of photoluminescence of single-walled carbon nanotubes wrapped with sodium dodecyl sulfate, surfactin and polyvinylpyrrolidone", Nanotechnology, 16 (5), S202.

[90] Islam M., Rojas E., Bergey D., Johnson A., Yodh A., (2003), "High weight fraction surfactant solubilization of single-wall carbon nanotubes in water", Nano letters, 3 (2), 269-273.

[91] Wenseleers W., Vlasov I. I., Goovaerts E., Obraztsova E. D., Lobach A. S., Bouwen A., (2004), "Efficient Isolation and Solubilization of Pristine Single- Walled Nanotubes in Bile Salt Micelles", Advanced Functional Materials, 14 (11), 1105-1112.

[92] Hu C., Liao H., Li F., Xiang J., Li W., Duo S., Li M., (2008), "Noncovalent functionalization of multi-walled carbon nanotubes with siloxane polyether copolymer", Materials Letters, 62 (17), 2585-2588.

[93] O'Connell M. J., Boul P., Ericson L. M., Huffman C., Wang Y., Haroz E., Kuper C., Tour J., Ausman K. D., Smalley R. E., (2001), "Reversible water-solubilization of single-walled carbon nanotubes by polymer wrapping", Chemical physics letters, 342 (3), 265-271.

[94] Qiu Q., Lou A., Somasundaran P., Pethica B., (2002), "Intramolecular association of poly (maleic acid/octyl vinyl ether) in aqueous solution", Langmuir, 18 (15), 5921-5926.

[95] Zhang H., Li H. X., Cheng H. M., (2006), "Water-soluble multiwalled carbon nanotubes functionalized with sulfonated polyaniline", The Journal of Physical Chemistry B, 110 (18), 9095-9099.

[96] Zorbas V., Ortiz-Acevedo A., Dalton A. B., Yoshida M. M., Dieckmann G. R., Draper R. K., Baughman R. H., Jose-Yacaman M., Musselman I. H., (2004), "Preparation and characterization of individual peptide-wrapped single-walled carbon nanotubes", Journal of the American Chemical Society, 126 (23), 7222-7227.

[97] Karajanagi S. S., Yang H., Asuri P., Sellitto E., Dordick J. S., Kane R. S., (2006), "Protein-assisted solubilization of single-walled carbon nanotubes", Langmuir, 22 (4), 1392-1395.

[98] Fernando K. S., Lin Y., Wang W., Kumar S., Zhou B., Xie S.-Y., Cureton L. T., Sun Y.-P., (2004), "Diminished band-gap transitions of single-walled carbon nanotubes in complexation with aromatic molecules", Journal of the American Chemical Society, 126 (33), 10234-10235.

[99] Chen R. J., Zhang Y., Wang D., Dai H., (2001), "Noncovalent sidewall functionalization of single-walled carbon nanotubes for protein immobilization", Journal of the American Chemical Society, 123 (16), 3838-3839.

[100] Murakami H., Nomura T., Nakashima N., (2003), "Noncovalent porphyrin-functionalized single-walled carbon nanotubes in solution and the formation of porphyrin–nanotube nanocomposites", Chemical Physics Letters, 378 (5), 481-485.

[101] Majeed S., Filiz V., Shishatskiy S., Wind J., Abetz C., Abetz V., (2012), "Pyrene-POSS nanohybrid as a dispersant for carbon nanotubes in solvents of various polarities: its synthesis and application in the preparation of a composite membrane", Nanoscale research letters, 7 (1), 296.

[102] Zhang B., Chen Y., Wang J., Blau W. J., Zhuang X., He N., (2010), "Multi-walled carbon nanotubes covalently functionalized with polyhedral oligomeric silsesquioxanes for optical limiting", Carbon, 48 (6), 1738-1742.

[103] Chen G.-X., Shimizu H., (2008), "Multiwalled carbon nanotubes grafted with polyhedral oligomeric silsesquioxane and its dispersion in poly (L-lactide) matrix", Polymer, 49 (4), 943-951.

[104] Horowitz G., (1999), "Field-effect transistors based on short organic molecules", Journal of materials chemistry, 9 (9), 2021-2026.

[105] Horowitz G., Deloffre F., Garnier F., Hajlaoui R., Hmyene M., Yassar A., (1993), "All-organic field-effect transistors made of π-conjugated oligomers and polymeric insulators", Synthetic metals, 54 (1-3), 435-445.

[106] Schroeder R., Majewski L. A., Grell M., (2004), "Improving organic transistor performance with Schottky contacts", Applied physics letters, 84 (6), 1004-1006.

[107] Arias A. C., MacKenzie J. D., McCulloch I., Rivnay J., Salleo A., (2010), "Materials and applications for large area electronics: solution-based approaches", Chemical reviews, 110 (1), 3-24.

[108] Zhang W., Li J., Jiang S., Wang Z.-S., (2014), "POSS with eight imidazolium iodide arms for efficient solid-state dye-sensitized solar cells", Chemical Communications, 50 (14), 1685-1687.

[109] Kim Y., Roh J., Kim J.-H., Kang C.-m., Kang I.-N., Jung B. J., Lee C., Hwang D.-H., (2013), "Photocurable propyl-cinnamate-functionalized polyhedral oligomeric silsesquioxane as a gate dielectric for organic thin film transistors", Organic Electronics, 14 (9), 2315-2323.

[110] Tamaki R., Tanaka Y., Asuncion M. Z., Choi J., Laine R. M., (2001), "Octa (aminophenyl) silsesquioxane as a nanoconstruction site", Journal of the American Chemical Society, 123 (49), 12416-12417.

[111] Dubois P., Coulembier O., Raquez J.-M., (2009), "Handbook of ring-opening polymerization"

[112] Albertsson A.-C., Varma I. K., (2003), "Recent developments in ring opening polymerization of lactones for biomedical applications", Biomacromolecules, 4 (6), 1466-1486.

[113] Jérôme C., Lecomte P., (2008), "Recent advances in the synthesis of aliphatic polyesters by ring-opening polymerization", Advanced drug delivery reviews, 60 (9), 1056-1076.

[114] Yue K., Liu C., Guo K., Yu X., Huang M., Li Y., Wesdemiotis C., Cheng S. Z., Zhang W.-B., (2012), "Sequential "click" approach to polyhedral oligomeric silsesquioxane-based shape amphiphiles", Macromolecules, 45 (20), 8126-8134.

[115] Lin W., Fu Q., Zhang Y., Huang J., (2008), "One-pot synthesis of ABC type triblock copolymers via a combination of "click chemistry" and atom transfer nitroxide radical coupling chemistry", Macromolecules, 41 (12), 4127-4135.

[116] Doganci E., Tasdelen M. A., Yilmaz F., (2015), "Synthesis of Miktoarm Star- Shaped Polymers with POSS Core via a Combination of CuAAC Click Chemistry, ATRP, and ROP Techniques", Macromolecular Chemistry and Physics, 216 (17), 1823-1830.

[117] Ge Z., Wang D., Zhou Y., Liu H., Liu S., (2009), "Synthesis of organic/inorganic hybrid quatrefoil-shaped star-cyclic polymer containing a polyhedral oligomeric silsesquioxane core", Macromolecules, 42 (8), 2903-2910.

[118] Jiang X., Zhang G., Narain R., Liu S., (2009), "Covalently stabilized temperature and pH responsive four-layer nanoparticles fabricated from surface 'clickable'shell cross-linked micelles", Soft Matter, 5 (7), 1530-1538.

[119] Rozga-Wijas K., Stanczyk W. A., Kurjata J., Kazmierski S., (2015), "Star-shaped and linear POSS-polylactide hybrid copolymers", Materials, 8 (7), 4400-4420.

[120] He T., Hu T., Zhang X., Zhong G., Zhang H., (2009), "Synthesis and characterization of a novel liquid crystalline star- shaped polymer based on α- CD core via ATRP", Journal of Applied Polymer Science, 112 (4), 2120-2126.

[121] Uner A., Doganci E., Tasdelen M. A., Yilmaz F. and Gürek A. G., (2017), "Synthesis, characterization and surface properties of star- shaped polymeric

surfactants with polyhedral oligomeric silsesquioxane (POSS) core", Polymer International, 66 (11), 1610-1616

[122] Chang Z., Xu Y., Zhao X., Zhang Q., Chen D., (2009), "Grafting poly (methyl methacrylate) onto polyimide nanofibers via “click” reaction", ACS applied materials & interfaces, 1 (12), 2804-2811.

[123] Xu H., Yang B., Wang J., Guang S., Li C., (2007), "Preparation, Tg improvement, and thermal stability enhancement mechanism of soluble poly (methyl methacrylate) nanocomposites by incorporating octavinyl polyhedral oligomeric silsesquioxanes", Journal of Polymer Science Part A: Polymer Chemistry, 45 (22), 5308-5317.

[124] Yuan W., Li X., Gu S., Cao A., Ren J., (2011), "Amphiphilic chitosan graft copolymer via combination of ROP, ATRP and click chemistry: Synthesis, self-assembly, thermosensitivity, fluorescence, and controlled drug release", Polymer, 52 (3), 658-666.

BIOGRAPHY

Ahmet Üner was born in 1982 in İzmir, Turkey. He obtained her B.S. degree in Chemistry from Akdeniz University in 2004. Then he obtained his master degree in 2013 from Gebze Technical University (GTU), Graduate School of Natural and Applied Sciences, Department of Chemistry. He then continued his Ph.D. studies at GTU. His current research interests include controlled polymerization techniques, star polymers, click chemistry.

APPENDICES

Appendix A: Published Journals from Doctoral Thesis

Ahmet Uner, Erdinc Doganci, Mehmet Atilla Tasdelen, Faruk Yilmaz, Ayşe Gül Gürek, “Synthesis, characterization and surface properties of star-shaped polymeric surfactants with polyhedral oligomeric silsesquioxane core”, Polymer International, 2017, 66(11), 1610–1616.

Appendix B: Conference Presentations from Doctoral Thesis

A. Uner, E. Doganci, F. Yilmaz, "Synthesis and Surface Properties of PEG based Amphiphilic Star-shaped Polymers with POSS (Polyhedral Oligomeric Silsesquioxane) Core", 46th International Symposium on Macromolecules (MACRO 2016) - IUPAC World Polymer Congress, June 17-21, 2016, Istanbul.

E. Doganci, A. Uner, F. Yılmaz, “Polihedral Oligomerik Silseskuioksan Merkezli Homo ve Miktoarm Yıldız Polimerlerin Sentezi ve Karakterizasyonu”, 27. Ulusal Kimya Kongresi, 23-28 Ağustos, 2015, Çanakkale.

A. Uner, E. Doganci, F. Yilmaz, "Polihedral Oligomerik Silseskuioksan (POSS) merkezli ve Piren Uçlu Poli(ε-Kaprolakton) Yıldız Polimerlerin Klik Kimyası ve Halka Açılma Polimerizasyonu Yöntemleri ile Sentezi ve Karakterizasyonu” V. Ulusal Polimer Bilim ve Teknolojisi Kongresi, 1-4 Eylül, 2014, Tokat

A. Uner, E. Doganci, F. Yilmaz, “Synthesis of Pyrene End-capped Poly(ε-caprolactone) Star-shaped Polymers with a POSS Core and Their Noncovalent Interactions with Carbon Nanotubes”, European Polymer Federation (EPF), Dresden, 2015.

B. Canimkurbey, E. Doganci, A. Uner, S. E. San, F. Yilmaz, “Star-shaped Polyhedral Oligomeric Silsesquioxane Core (POSS) Based Organic Field-Effect Transistor” International Physics Conference at the Anatolian Peak (IPCAP), Erzurum, 2016.